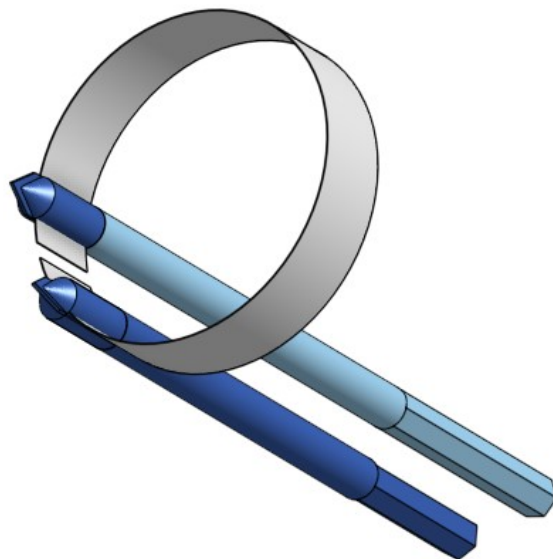


# Minimally Invasive Sentinel Lymph Node Biopsy: from surgery to out- patient procedure

L.R. Preis

Master Thesis





# Minimally Invasive Sentinel Lymph Node Biopsy: from surgery to outpatient procedure

by

L.R. Preis

to obtain the degree of Master of Science  
at the Delft University of Technology,  
to be defended publicly on Wednesday, June 29, 2022 at 09:30 AM.

Student number: 4229916  
Project duration: January 18, 2022 – June 29, 2022  
Thesis committee: Dr. ir. J. J. van den Dobbelsteen, Technical University of Delft, supervisor  
Dr. D. J. Grünhagen, Erasmus Medical Center  
Dr. E. E. A. P. Mulder, Erasmus Medical Center, supervisor



# Abstract

Every year more and more people are diagnosed with a form of skin cancer called melanoma. Chances are, in your lifetime you will meet someone or be diagnosed yourself.

Getting this diagnosis is unsettling. If you look at the numbers, it becomes even more disturbing. The patient is confronted with numbers such as: melanoma accounts for 3% of all diagnosed skin cancers, but 65% all skin cancer-related deaths.

The majority of patients with early stage melanoma are eligible for sentinel lymph node biopsy (SLNB). But that means more numbers the patient is confronted with. 2 out of 10 patients have no metastases in the lymph nodes, while 1 in 10 patients undergoing SLNB will suffer from morbidities such as wound infection and lymphedema.

You can imagine that this is not an easy decision for both the patient and the treating physician. And this is where my Master Thesis begins. I explored the possibility of designing a medical device that will reduce the strain the patients with melanoma have to undergo in order to get a better staging method and a more personalised treatment plan.

This thesis will guide you through my steps to work towards the goal of alleviating the patients with melanoma from uncertainties and giving them hope again by making the SLNB procedure minimally invasive and hence tipping the risk-reward scale in favour of the patients. As well as reducing the strain on operating room capacity and day care beds thereby reducing the pressure on health care professionals.

Throughout my work, I was inspired by a quote by Albert Einstein:

*A person who never made a  
mistake, never tried anything.*

ALBERT EINSTEIN

*L.R. Preis  
Delft, June 2022*



# Contents

<b>1</b>	<b>Introduction</b>	<b>1</b>
1.1	What is a SLNB?	1
1.2	Why is this thesis relevant?	2
1.3	Thesis' Outline	3
<b>2</b>	<b>Basic Design</b>	<b>5</b>
2.1	Requirements	5
2.2	Concepts	7
2.2.1	Spherical Excision	7
2.2.2	Wire Basket Excision	7
2.2.3	Expandable Ring	8
2.2.4	Corkscrew	9
2.2.5	Optomechanical Biopsy Tip	10
2.3	Decision Matrix	11
<b>3</b>	<b>Detailed Design</b>	<b>13</b>
3.1	Dimensions	13
3.1.1	Poles	13
3.1.2	Blade	14
3.1.3	Caps & Fixation of Blade	14
3.2	Material	15
3.3	Computer Aided Design	15
3.4	The Preis-Device	16
<b>4</b>	<b>Proof-of-Concept</b>	<b>21</b>
4.1	Device Holder	21
4.2	Test Execution	23
4.2.1	Blade Tests	23
4.2.2	Proof-of-Principal	24
4.3	Data Processing	25
4.4	Results & Analysis	26
<b>5</b>	<b>Design Evaluation &amp; Iteration</b>	<b>29</b>
5.1	Calculations	29
5.1.1	Test Validation Calculations	29
5.1.2	Pole Validation Calculations	31
5.2	Finite Element Method	33
5.2.1	Blade	33
5.2.2	Poles	37
5.3	Design Iteration	38
<b>6</b>	<b>Discussion &amp; Conclusion</b>	<b>41</b>
6.1	Limitations	41
6.2	Future Research	41
6.3	Conclusion	42
6.4	Acknowledgements	43

<b>A</b>	<b>Familiarisation</b>	<b>49</b>
A.1	What is a lymph node? . . . . .	49
A.2	What is melanoma and the treatment thereof? . . . . .	50
A.3	Previous Thesis. . . . .	52
A.3.1	Previous Thesis Design . . . . .	52
A.3.2	Previous Research Question . . . . .	52
A.3.3	Conclusions. . . . .	53
<b>B</b>	<b>Human Tissue Test</b>	<b>55</b>
B.1	Tensile Test . . . . .	55
B.1.1	Test Execution . . . . .	56
B.2	Results Tensile Test . . . . .	57
<b>C</b>	<b>Literature Study</b>	<b>61</b>
<b>D</b>	<b>Blade Test RunTables</b>	<b>77</b>
<b>E</b>	<b>Test Protocol for Prototype 1</b>	<b>81</b>
E.0.1	Goal . . . . .	81
E.0.2	Requirements. . . . .	81
E.0.3	Important . . . . .	81
E.1	Proof-of-Principal . . . . .	81
E.1.1	Execution . . . . .	82
E.1.2	Clean-up . . . . .	82
E.2	Cutting force . . . . .	82
E.2.1	Experimental Set-up . . . . .	83
E.2.2	Execution . . . . .	83
E.2.3	Clean-up . . . . .	84
E.3	Insertion force . . . . .	84
E.3.1	Experimental Det-up . . . . .	84
E.3.2	Execution . . . . .	85
E.3.3	Clean-up . . . . .	85
<b>F</b>	<b>Phantom Fabrication Prototype 1 testing</b>	<b>87</b>
F.1	Disclaimer. . . . .	87
F.2	Mixing the gelatine . . . . .	88
<b>G</b>	<b>Tensile Test Protocol</b>	<b>89</b>
G.1	Materials . . . . .	89
G.2	Experimental Set-Up . . . . .	90
G.2.1	Calibration linear stage . . . . .	90
G.3	Execution . . . . .	90
G.4	Clean-Up . . . . .	91
<b>H</b>	<b>MatLab Code</b>	<b>93</b>
<b>I</b>	<b>Medical Device Regulation &amp; Documentation</b>	<b>97</b>
I.1	Intended Purpose. . . . .	97
<b>J</b>	<b>How was the Project conceived?</b>	<b>101</b>
J.1	Idea for project . . . . .	101
J.2	Project Organisation . . . . .	101
<b>K</b>	<b>ACE Grant Proposal</b>	<b>103</b>



# Introduction

This thesis investigates the feasibility for a working principle of a minimally invasive sentinel lymph node biopsy (MISLNB) medical device designed by the author. This thesis explains the clinical background of this medical device, the design choices made as well the *proof-of-concept* tests, and the design iterations that followed due to the observations from the *proof-of-concept* tests and evaluation. First, the basics about this medical device will be presented, which include the medical background of SLNB in *Section 1.1. What is a SLNB?*, and the relevance of this medical device in *Section 1.2. Why is this thesis relevant?*

## 1.1. What is a SLNB?

A Sentinel lymph node biopsy (SLNB) is a procedure offered to patients with early stage melanoma with clinically negative lymph nodes (LNs) [5, 19, 7]. Clinically negative means that the LNs do not appear enlarged on scans and are not palpable [7]. It is important to evaluate the sentinel lymph nodes (SLNs) because 1) they are the location of the first metastases of a melanoma [4, 12, 20], and 2) their evaluation by means of *nodal staging* is an important prognostic tool and has therapeutic consequences for the patient [10, 49, 2, 14, 15, 35]. A SLNB is performed in the operating theatre (OR) under general anaesthesia [23]. Before the patient is brought into the OR, a lymphoscintigraphy is done to identify and locate the SLNs [42]. The lymphoscintigraphy is performed in the department of *nuclear medicine* because the patient is injected with a radioactive colloid (technetium 99 ( $^{99m}\text{Tc}$ )). The colloid is injected in close proximity to the melanoma or the scar from a melanoma resection [13, 12, 42].

The way  $^{99m}\text{Tc}$  identifies the SLNs is the following:  $^{99m}\text{Tc}$  targets the receptor protein CD-206 which is found in high concentrations on the surface of macrophages, which are abundant in LNs [42]. Because SLNs are the tumour draining LNs,  $^{99m}\text{Tc}$  will accumulate in these LNs first and thereby identify them as such [7, 23, 28, 30]. This is also the reason why the metastases show up first in the SLNs [7, 12].

After the nuclear scientist identifies and marks all SLNs on the patient's body, in > 20% of patients more than one SLN is identified, the patient is ready to be brought into the OR and go under general anaesthesia [23]. In the OR, the patient is injected with patent blue dye in addition to the already injected  $^{99m}\text{Tc}$  to maximise the likelihood of identifying all SLNs [39, 32]. Another advantage of administering patent blue dye is that it can be seen with the naked eye and no other detection device is needed. Then a ca. 5cm incision is made where the nuclear scientist has indicated the SLNs. A handheld gamma probe is used to identify the SLNs [23]. After identifying the SLN and checking again that they cause the spike in detected radiation, the SLN is removed. This is repeated until all SLNs identified by the nuclear scientist are removed. *Figure 1.1* shows the SLNB procedure from point of injection with  $^{99m}\text{Tc}$  until the removal of the SLNs, schematically. The removed SLNs are then sent to the pathologist who performs the *nodal staging* [10]. *Nodal staging* determines the status of the LNs, meaning whether the cancer has infiltrated the LNs, and if so, identifies the size, shape and location of the metastases [49, 21]. Determining the status of the SLNs is one of the main prognostic tools physicians have for patients with melanoma [6]. The recommended treatment after the nodal staging can range from "no further treatment needed" for node negative patients, to adjuvant treatment with immune therapy (e.g., PD-1 checkpoint inhibitor (nivolumab) or anti-CTLA-4 (ipilimumab)) or targeted therapy (a combination

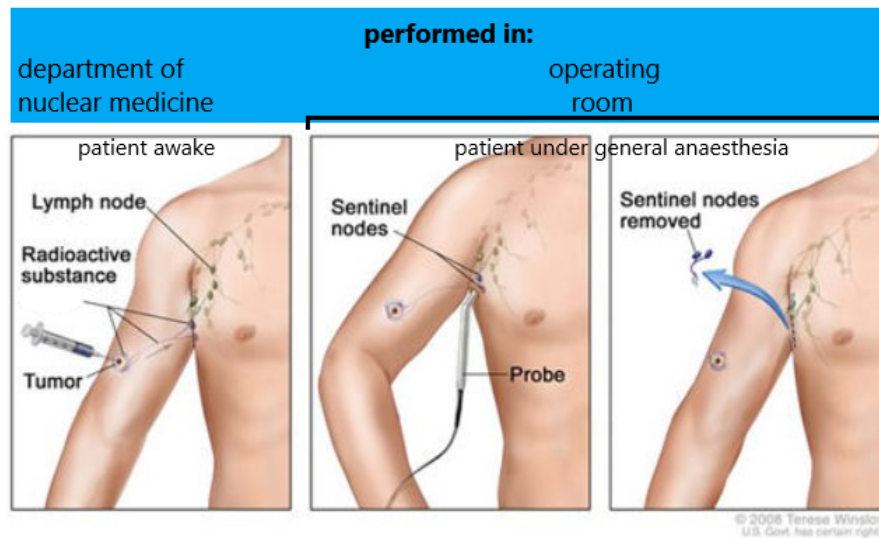


Figure 1.1: This figure depicts a schematic representation of the sentinel lymph node biopsy procedure. On the **left** the administration of  $^{99m}\text{Tc}$  close to the primary tumour site can be seen. It is also shown how the injected substances accumulate in the tumour draining LNs, the SLNs. This is done in the department of nuclear medicine. The **middle** picture shows the detection and identification of the SLN using a handheld gamma probe. This is done in the OR under general anaesthesia. The **right** picture shows the excision of the SLNs, also done in the OR. This figure was taken from: [61] and altered using 3D paint (Microsoft, Redmond, Washington, United States)

of dabrafenib plus trametinib) [2, 14]. All depending on the size of the SLN's metastasis [7, 12, 10]. Since  $\sim 80\%$  of the patients who undergo a SLNB procedure do not have metastases in the SLNs, they are not prescribed adjuvant therapy [45]. But they have a non-negligible probability of adverse events from the general anaesthesia and risk of experiencing morbidities, this is why the goal is to make SLNB, which is the most important prognostic tool for patients with early stage melanoma, more minimally invasive and thereby reduce the risks for the patients. If this device is realised, not only melanoma patients will reap the benefits, but also patients with other types of cancer (e.g. breast, colon, etc.) [20].

## 1.2. Why is this thesis relevant?

It is important to not reinvent the wheel over and over again. Therefore, the question of relevance will be answered here. Developing a device that allows SLNB to be done minimally invasive is important because it is believed to reduce the likelihood of the patients experiencing morbidities significantly [30]. Since the introduction of adjuvant systemic therapy for patients with surgically resected stage III melanoma, SLNB is performed to identify candidates with SLN metastasis who are eligible for adjuvant treatment. This led to the number of SLNBs performed on patients with melanoma within a year of diagnosis rising in the last decade.

While 40% of patients underwent SLNB within a year of diagnosis in the Netherlands in 2010, the number has risen to 65% of patients with melanoma opting for SLNB within a year of diagnosis in 2016 [11], as can be seen in *Figure 1.2*.

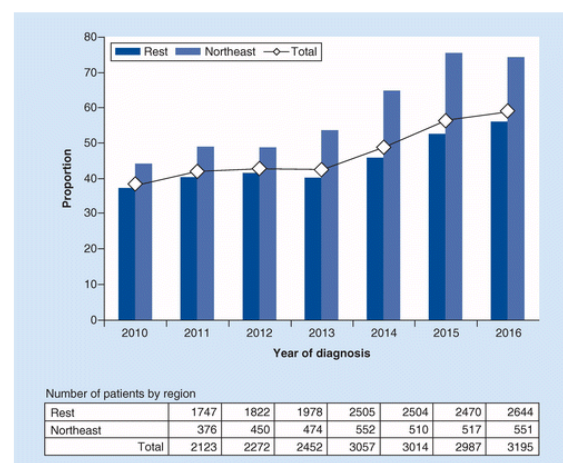


Figure 1.2: This figure depicts the trend in the proportion of SLNBs performed in the Netherlands (Northeast vs. the Rest) between 2010 and 2016 from 40% of patients with undergoing SLNB to 65% of patients with melanoma undergoing SLNB. Furthermore, the actual numbers of performed procedures can be seen in the lower half of the figure [11]

Studies have also shown that since the introduction of SLNB the quality of life of the patients treated for melanoma has improved because of a more personalised treatment approach. Thereby reducing unnecessarily harsh treatments, e.g., complete lymph node dissection (CLND), where they are not needed by up to 74% [7].

Research has furthermore shown that 10% of patients that undergo SLNB experience comorbidities [12, 62]. The most common being:

- seroma/ hematoma
- wound infection
- scar formation
- delayed wound healing
- lymphedema

While only 2 in 10 patients have pathologically proven metastases present in the SLNs [45]. Upon detection of metastases in the SLNs, the appropriate adjuvant therapy can be prescribed [2, 14].

Studies have shown that SLNB improves the recurrence-free and overall survival of patients with melanoma [12]. Therefore, the procedure itself is of great value to the treatment of melanoma patients already. Making SLNB a minimally invasive procedure done under local anaesthesia only, will improve its benefits for patient's manifold, by reducing the strain the patients experience, reducing the recovery time needed after the procedure, and make SLNB available to patients that cannot undergo general anaesthesia.

Furthermore, this device makes the use of an OR obsolete. The procedure can be done under local anaesthesia only by a radiologist who is assisted by a nurse practitioner. Not the complete OR team is needed. Which will make this procedure also available to patients during pandemics like the COVID pandemic, where surgeries had to be cancelled due to a lack of beds, as well as lower the costs of the procedure and the impact the general anaesthesia has on the human body. While simultaneously reducing the strain on OR capacity and available beds. This also has an impact on the costs of the procedure, making SLNB cheaper for the health care system. All these aspects make this project very valuable to patients, physicians and society as a whole.

Next to a relevance for the health care system, this thesis also has relevance for the technology of excision mechanisms. Because as of yet, there is not a lot of research and design done towards achieving large-volume excision systems, capable of resecting a large volume *en bloc*. From a technological point of view, this is an interesting topic because so little has been done as of yet, as well as the additional challenges this brings with it.

The idea for this project was conceived in 2019, and this is the second Master thesis on this topic. Unfortunately, a vacuum excision method designed by the previous student did not work, which was corroborated by tissue experiments done by this author, see [Appendix B Human Tissue Test, Section B.1. Tensile Test](#).

## 1.3. Thesis' Outline

This thesis starts with choosing and designing a mechanical, large-volume excision mechanism able to excise LNs *en bloc*, see [Chapter 2. Basic Design. Section 2.1. Requirements](#) explains how a set of requirements that the mechanism has to fulfil is assembled. Next, the most promising concepts are gathered and adjusted in [Section 2.2. Concepts](#). Narrowing the concept down to the most promising one by using the *decision matrix* method is explained in [Section 2.3. Decision Matrix](#).

[Chapter 3. Detailed Design](#) explains how the dimensions of the design are chosen ([Section 3.1. Dimensions](#)) and the computer aided design used to fabricate the first prototype, see [Section 3.3. Computer Aided Design](#). The chapter closes with an explanation of the working principal of the designed mechanism, see [Section 3.4. The Preis-Device](#).

[Chapter 4. Proof-of-Concept](#) concerns itself with various tests that are designed to evaluate the feasibility of the design. This chapter introduces an additional component needed for the test execution, see [Section 4.1. Device Holder](#), as well as the test set-up and executions, see [Section 4.2. Execution](#). Also included in [Chapter 4](#) is [Section 4.3. Data Processing](#) on how measurements are accumulated

and processed. The chapter closes with the test results, their analysis and interpretation, see *Section 4.4. Results & Analysis*.

*Chapter 5. Design Evaluation & Iteration* uses calculations and finite element method (FEM) to evaluate the design, see *Sections 5.1. Calculations & 5.2. Finite Element Method*, respectively, to validate the test results of the *proof-of-concept* tests. Lastly, this chapter closes with *Section 5.3. Design Iteration* combining the findings from the *proof-of-concept* tests, the calculations and the FEM analysis to iterate and improve the design of the mechanism.

Finally, *Chapter 6. Discussion & Conclusion* gives a critical view on the work done, the limitations thereof, as well as an outlook towards future research. The conclusion summarises the thesis and the most important aspects of this work.

# 2

## Basic Design

This chapter presents the design process from assembling a set of requirements in [Section 2.1. Requirements](#), via various conceptualised designs, see [Section 2.2. Concepts](#), to choosing the most promising concept in [Section 2.3. Decision Matrix](#). At the end of this chapter it will have been explained how an idea is conceptualised into various designs and the best one is chosen.

### 2.1. Requirements

A stakeholder analysis, followed by a problem analysis (not included in this thesis) derived a set of global requirements that the MISLNB medical device needs to adhere to. Based in these analyses, a set of global requirements for a MISLNB medical device includes the following problem areas: *SLN detection, Device Insertion, Navigation, Detachment, Retrieval, and After Care* is assembled.

It is agreed that the focus of this thesis lies on the *Detachment* mechanism of the MISLNB medical device. It is further chosen to incorporate the requirement areas *Insertion* together with the *Detachment*, because the requirements for *Insertion* influence the design choices for the *Detachment* mechanism. This leads to the following problem areas to be looked at in more detail: *General aspects, Safety, User Experience, and Simplicity*, see [Figure 2.1 column 2](#). Each requirement of each problem area is then defined in [column 4](#) and its importance with regards to the MISLNB medical device is explained in [column 5](#). Because there are quite a few requirements and their *priorities* vary, a number on the scale from 5 – 1 is assigned to each requirement, see [Figure 2.1 column 6](#). With 5 being a requirement of the highest priority and 1 of the lowest priority. Finally, [column 7](#) explains how it can be determined whether or not the device adheres to the requirement for the MISLNB medical device. And if it does adhere, how well. The last column holds remarks where needed.

Following this, the author commenced a literature study, see [Appendix C. Literature Study](#), to identify whether there are devices already on the market that are able to excise LNs *en bloc*, or are readily adaptable to meet the requirements listed in the table of [Figure 2.1](#). The literature search does not only include devices but is designed to also include collecting mechanisms of different areas of application, e.g., geology, aerospace, medicine (veterinarian as well as humane). The search of relevant literature includes databases and registries. The literature study, including a detailed description of the eligible concepts obtained by it and its results can be found in [Appendix C. Literature Study](#).

This study of relevant literature as well as other, previously executed literature searches performed by the author revealed five eligible concepts. These concepts are then adapted to fulfil the requirements of [Figure 2.1](#) and are presented in [Section 2.2. Concepts](#).

#	Requirement	Definition	Importance	Priority	Determination	Remark	
#1-4	GENERAL	#1 en bloc	Can an entire SLN is excised?	Important for nodal staging	5	phantom tests and ex vivo tests	
		#2 footprint	What is the diameter of the canal having to be made in order to insert the device?	Directly influence whether or not local anaesthesia can be used	4	can be determined in CAD	
		#3 accommodating	Is the device able to accommodate the different LN shapes and sizes and depths? (few mm up to 2cm in long axis; 4cm - 9cm deep)	One device can be used for several SLN in one patient. SLNs will not have the same size and/or shape	3	determined during prototype testing	for now determined with desk-top prototypes and/or 3D models
		#4 development costs	How extensive will the costs be for R&D and production?	How fast will the device be on the market and the users (physician and patient) reap the benefit?	1	literature; number of components; failure safety	
#5-7	SAFETY	#5 safe failure	What happens in case of device failure (malfunction or breakage)? Is the potential harm to the patient is nil / acceptable?	In case of device failure, the patients will not be severely harmed; no operation should be needed in order to remove device	5	extensive testing; 3D models and stress strain tests (COMSOL/ SolidWorks)	has to be done at a later stage, for now this is a determined via probability and 3D models
		#6 cauterisation	How much bleeding is caused by the detachment mechanism?	Bleeding has to be minimised in order for the procedure to be safe and good/ fast healing of the wound.	2	literature; expertise (surgeon)	
		#7 sterilisation	Can the device be sterilised?	Patient and physician safety	1	expertise (designer, sterilisationexpert) ; literature; testing (sterilisation expert)	
#8-9	USER EXPERIENCE	#8 sturdyness	Is the device prone to deformation leading to failed biopsy during use?	If the device is easily deformed during use, the biopsy is more difficult to perform. More devices might need to be used, or device will have to be repaired during procedure, leading to a bad user experience (physician and patient)	3	wires --> bend easily; desk-top prototypes; 3D models and stress strain analysis (COMSOL, SolidWorks)	
		#9 durability	How often can the device be used? Once per SLN, once per patient, one device for several patients?	Is about patient comfort. If several SLNs need to be excised, and it takes a long time to change the device and make it ready again, the patient/ physician is not going to have a good experience.	1	expertise (designer); literature; extensive testing	
#10	SIMPLICITY	simple	How intricate is the desing? How many parts etc.?	Many parts = many possible failures	2	counting number of components; looking at design	
#11		electronic components	How important are the eelectric components to the device (cauderiser etc.)?	Adds an extra layer of possible failure that needs to be accounted for	2	looking at desing	

Figure 2.1: This figure depicts the table of specific requirements that need to be fulfilled by the MISLNB medical device in order to solve the problem areas *Insertion* and *Detachment*

## 2.2. Concepts

The concepts most promising to realise large-volume excision are accumulated via various literature studies and adapted where needed to fulfil the requirements of the MISLNB medical device determined in [Section 2.1. Requirements](#). The five promising concepts are: the *Spherical Excision* system ([2.2.1](#)), the *Wire Basket Excision* system ([2.2.2](#)), the *Expandable Ring* system ([2.2.3](#)), the *Corkscrew* system ([2.2.4](#)), and the *Optomechanical Biopsy Tip* system ([2.2.5](#)). These concepts are presented in this section in their adapted form as possible MISLNB medical device LN detachment mechanisms. These are the concepts that are evaluated by the *decision matrix* in [Section 2.3. Decision Matrix](#).

### 2.2.1. Spherical Excision

The *Spherical Excision* system consists of a rigid waning crescent combined with a c-shaped cauterising knife, see [Figure 2.2](#). It is one of the systems already considered by the previous student [[26](#)]. The device is inserted through the skin via an incision and positioned so that the centre of the LNs is in the midpoint between the tips of the waning crescent, see [Figure 2.2 Step 1](#). The next step is the deployment of the c-shaped cauterising knife (depicted in red in [Figure 2.2](#)). The c-shaped cauterising knife describes a full rotation, thereby cutting the LN free from its surrounding tissue as seen in [Figure 2.2 Steps 2 - 4](#).

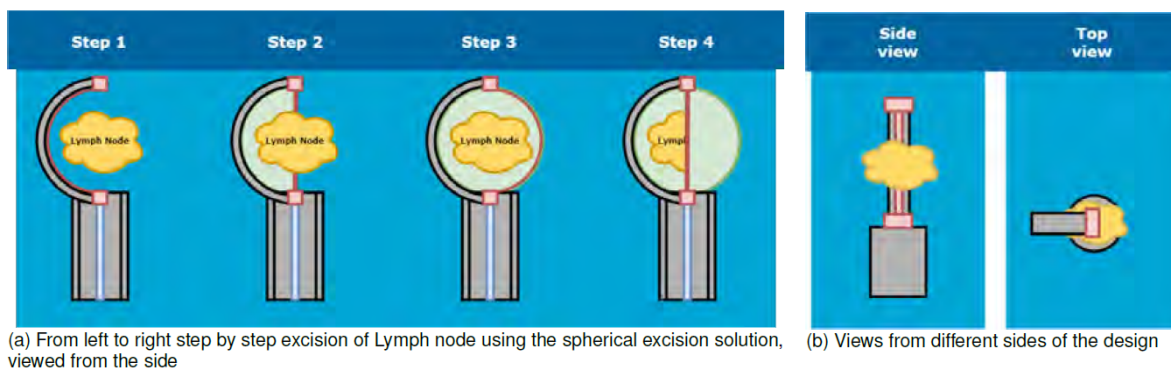


Figure 2.2: This figure depicts the working principle of the *Spherical Excision* system as described by Max Joosen [[26](#)]. **(a)** shows the working from a side view with the arch on the left, **(b)** also from a side view, but with the arch in the back (**(b) left**) as well as a top view (**(b) right**). This figure was taken from Max Joosen's master thesis [[26](#)]

While it is seemingly possible to excise a LN *en bloc* using this system, there are some apparent issues. For one, it seems to the author that positioning this device correctly will be challenging. It appears that some manoeuvring is needed inside the patient's body in order to get the device in the right position. Seen that there are no additional blades or sharp edges that could help with the positioning of the device, it is to be assumed that some force will be needed to push or tear the LN's surrounding tissue when positioning this device. Also, the device can only excise a fixed volume. LNs with twice the radius of the waned crescent will be too large for excision. Lastly, the footprint of the device is relatively large, leading to a large incision needed in order to insert the device. These aspects will be important when assigning scores to the concept in [Section 2.3. Decision Matrix](#).

### 2.2.2. Wire Basket Excision

This system is the second system taken from the previous student's thesis [[26](#)]. The *wire basket excision* system strongly resembles the B.L.E.S. (breast lesion excision system) by Medtronic Inc., see [Figure 2.3](#). The B.L.E.S. device has FDA approval [[53](#)] and is formerly known as the INTACT (Intact Medical Corporation, USA) and recently as the B.L.E.S. (Medtronic Inc., Ireland) [[27](#)]. The *wire basket excision* device consists of a pointed tip that is inserted into the patient's body via a small incision. The device is then inserted until the edge of the LN, see [Figure 2.4 Step 1](#). Once in position, a core (depicted as a white block with red outline in [Figure 2.4](#)) is pushed towards the distal tip. Attached to the core are wires (depicted in red in [Figure 2.4](#)). As the core moves towards the distal tip of the device,

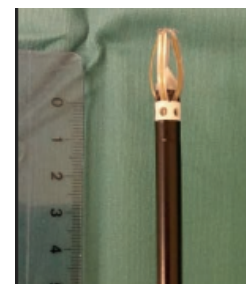


Figure 2.3: This figure depicts the B.L.E.S. device from Medtronic Inc. in closed position. This figure was taken from [[53](#)]

the wires are deployed at an angle, see *Figure 2.4 Steps 2 & 3*. The distal end of the wires can be actuated by a coagulation snare (depicted in green in *Figure 2.4*). In *Steps 1 & 2* the coagulation snare is not engaged as indicated by the open lock at the bottom of *Figure 2.4*. This means that the coagulation snare is pulled forwards while the wires expand. In *Steps 3 & 4* the coagulation snare is engaged, meaning that the coagulation snare is pulled backwards which closes the wires circumventing the LN to be excised. When the coagulation snare is fully closed, the LN is freed from its surrounding tissue by applying radio frequency, see *Figure 2.4 Step 4*. Upon this step being completed, the device is retrieved from the patient's body with the excised LN enclosed within.

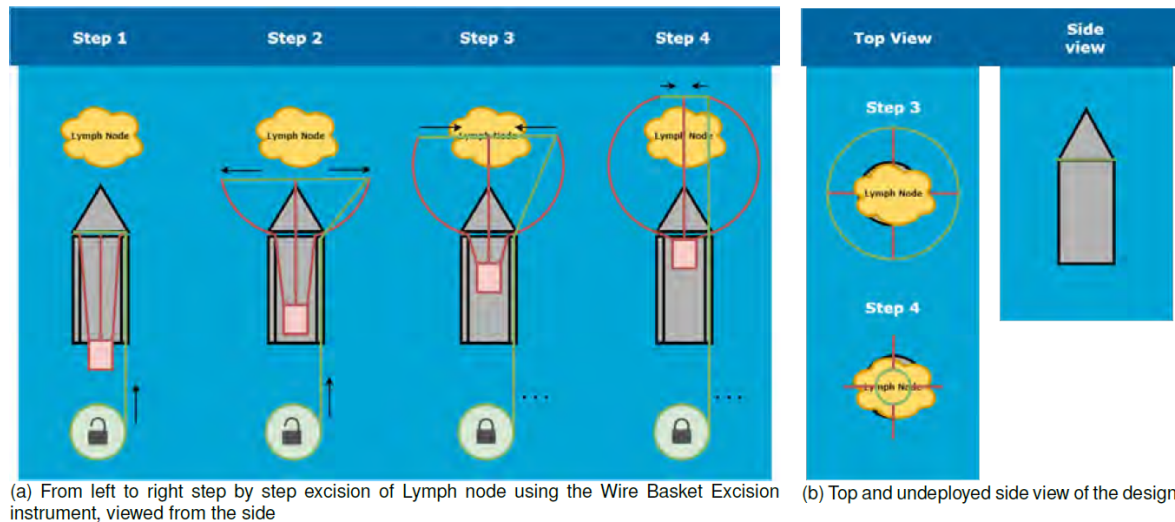


Figure 2.4: This figure depicts the working principle of the *wire basket excision* system. Depicted in yellow is the LN. The white block actuates the wires (in red) by being pushed towards the distal end of the device in *(a) Step 2*. A coagulation snare (green) closes the wires (red) in *(a) Step 3 & 4*. *(b) left* shows *Steps 3 & 4* from top view and *(b) right* shows the device in begin position from the side. This figure was taken from Max' master thesis [26]

This system has a much smaller footprint upon insertion than the *spherical excision* system. The question however is, is this device too fragile? However, troubling are the facts that the B.L.E.S. is being recalled from the market and that studies have shown that the tissue of interest is not always enclosed in the basket upon retrieval [53, 1, 52].

### 2.2.3. Expandable Ring

The *expandable ring* was designed by Fawiz et al. [17]. The author became aware of this system during the literature study, see *Appendix C. Literature Study*. The patent describes this device as a big lumen biopsy device that enables physicians to excise tumours and/ or LNs as a whole [17]. The patent for this device is part of a cohort of patents for large lumen biopsy and biopsy cavity marking devices. However, to the best of the author's knowledge, all efforts into further developing and marketing the devices

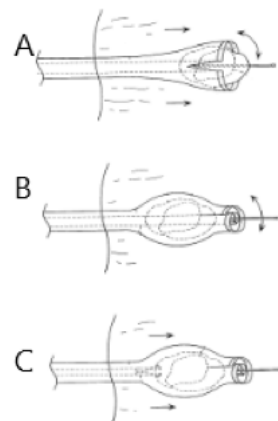


Figure 2.5: This figure depicts the working principle of the *Expandable Ring*. The expandable ring consists of two poles to actuate the cutting motion, and a cutting blade with a net attached to it. **A** shows how the LN with the expandable ring is pushed forward whilst simultaneously being unrolled. This motion cuts the LN from its surrounding tissue. **B** shows the LN fully enveloped by the net attached to the cutting blade of the expandable ring. The far end of the LN is cut by the expandable ring blade too, but rolling the blade up again after it has passed the distal tip of the LN. **C** shows the grasper that is inserted from the back inside the device in order to grasp the LN and retrieve the device together with the LN. This figure was taken from the patent of Fawiz et al. [17] and altered using 3D Paint (Microsoft, Redmond, Washington, United States)



have been disbanded since. The expandable ring system consists of a cutting blade and two actuating rods, see *Figure 2.6* [17]. The working principle of this device after alterations is the following: first the *expandable ring* is inserted through a small incision in the skin and pushed through the LN, thereby positioning the *expandable ring* in front of the LN of interest. As can be seen in *Figure 2.6 right*, where the expandable ring blade is rolled up around one of the poles. This reduces the footprint of the device considerably when compared to the fully expanded device in *Figure 2.6 left*. Next, the *expandable ring* is pushed further toward the LN whilst simultaneously unrolling and cutting the surrounding tissue [17]. The blade is unrolled by turning the right pole counterclockwise while guiding it in a circular motion around the LN, see *Figure 2.5A*. This is done until the whole LN is enveloped by the expandable ring's blade, see *Figure 2.5B*. After the blade has fully enclosed the LN, the device keeps the loose LN in place, and a grasper is inserted from the back to hold on to and guide the LN while it is retrieved from the patient's body, see *Figure 2.5C* [17].

One of the strongest properties of this device is its simplicity as well as it being able to accommodate various LN sizes. It can be folded to be very compact and fit through a small incision in the skin. However, it is questionable whether the blade is stiff enough to be guided and able to cut the tissue. And whether the actuation mechanism works.

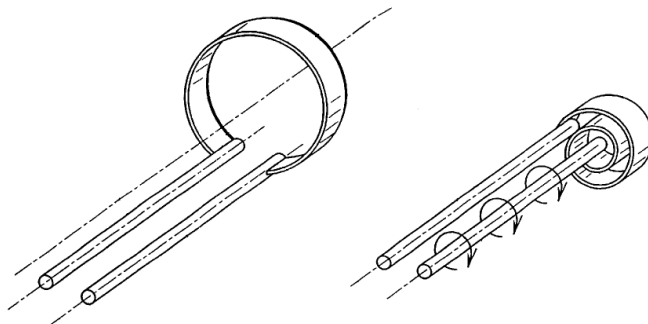


Figure 2.6: This figure shows the expandable ring in fully expanded position, on the **left**, and its rolled-up position, **right**. This figure was taken from the patent of Fawiz et al. [17] and altered using 3D Paint (Microsoft, Redmond, Washington, United States) [17]

#### 2.2.4. Corkscrew

This device too was brought to the author's attention during the literature study, see *Appendix C. Literature Study*. The device was designed by Sirimanne et al. [56] and belongs to the aforementioned cohort of patents concerning various aspects of big lumen biopsy and biopsy cavity marking. The *corkscrew* concept considered for the MISLNB medical device has nothing to do with the actual invention by Sirimanne et al. [56]. The patent of this invention describes a radiopaque marker for a biopsy cavity. However, this patent inspired the idea of a device that acts like a corkscrew that instead of cutting through the cork, cuts through the glass bottle and leaves the cork intact. The cork being the LN and the glass bottle the surrounding (adipose) tissue. This device is introduced into the body via a tube. The corkscrew is folded inside the tube and pushed towards the distal end while being rotated. Thereby the corkscrew will exit the tube and start cutting. The material properties have to be such that the corkscrew bends around the LN and cuts the surrounding tissue, meaning that the Young's modulus of the LN has to be larger than the Young's modulus of the corkscrew that in turn is larger than the Young's modulus of the surrounding tissue (Young's modulus LN > Young's modulus corkscrew > Young's modulus surrounding tissue).

This device appears to be quite simple, however, in reality it is quite complex in how it works. This is especially due to the little known material properties of the LNs. Also, the device will not be suited to retrieve the LN or keep it in place during retrieval due to the lower Young's modulus of the device's material. Upon retrieval, the device will unwind around the LN. This could be prevented by adding low melting point alloy (LMPA) segments which will be flexibly upon insertion of the device and cutting

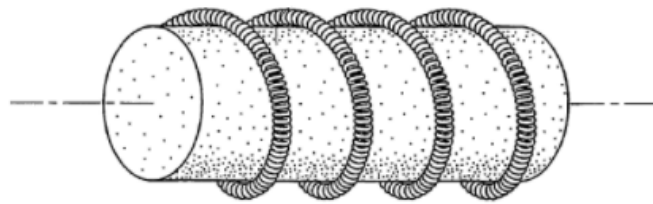


Figure 2.7: This figure was taken from the patent of Fawiz et al. [56] and altered using 3D Paint (Microsoft, Redmond, Washington, United States)

around the LN, but will be rendered stiff upon retrieval. Rendering the LMPA flexible is done by heating it and thereby creating a flexible segment. Upon cooling the LMPA segment, it takes on the shape it is in. This technology is used in *variable stiffness catheters* [8]. This will make the design of the device much more complex and add another layer of possible failures, which needs to be carefully considered when designing a medical device, especially for minimally invasive keyhole procedures such as the MISLNB. Because should the device fail inside the patient and a piece of device breaks loose, the minimally invasive procedure has to be converted into an open surgery in the operating room.

### 2.2.5. Optomechanical Biopsy Tip

This device was designed, built and tested by Jelinek et al. [24]. The author of this thesis became aware of this device through the literature study, see *Appendix C. Literature Study*. The *optomechanical biopsy tip* is designed to combine three types of biopsy devices into one, namely fine needle aspiration, core needle biopsy, and punch biopsy [24]. In addition, fibre optics are included in order to identify the tissue about to be sampled, see *Figure 2.8A*. The *optomechanical biopsy tip* consists of a tapered outer tube that houses the optical fibres (green in *Figure 2.8*), the Aristotle's Lantern (yellow in *Figure 2.8*), and a mechanical spring (purple in *Figure 2.8*). The spring is the actuation mechanism for the Aristotle's Lantern.

The working principle of this device is the following: the device is inserted via a small incision in the skin and positioned in front of the tissue of interest [24]. While Aristotle's Lantern is inside the tube, it is spring-loaded. Upon positioning the device, the spring is released, and Aristotle's Lanterns shoots out of the tube. Due to the tube's tapered end, the tips of Aristotle's Lantern are directed inward [24]. This causes them to close, cutting a conical piece of tissue [24]. The deployed device with the closed tip can then be retrieved from the patient's body and the tissue sample recovered [24].

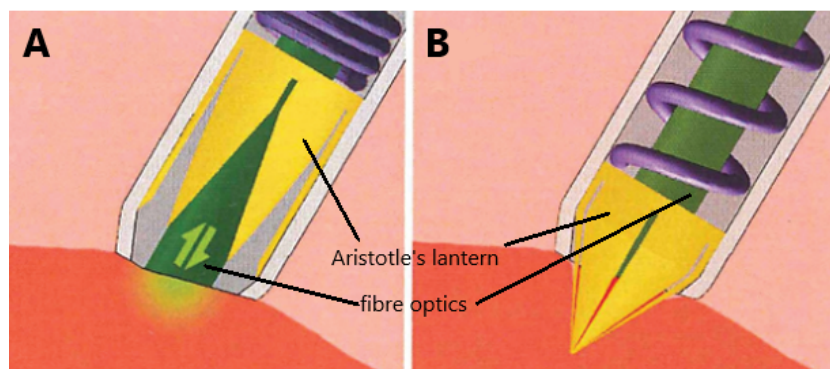


Figure 2.8: This Figure depicts the optomechanical biopsy tip designed by Jelinek et al. [24]. **A** shows the fibre optics identifying the tissue in front of the *optomechanical biopsy tip*. **B** shows the sea urchin inspired mechanical biopsy mechanism. By pushing Aristotle's lantern into the tissue, it closes and thereby cuts tissue which can be retrieved and evaluated pathologically. This picture was taken from the BITE Group site [58] and modified by the author using 3D paint (Microsoft, Redmond, Washington, United States) [24]

The altered version of the design, which is to be considered in the *decision matrix* does not include the fibre optics and is scaled with respect to the design of Jelinek et al. [24]. Furthermore, the altered design is called *Sea Urchin - Aristotle's Lantern*.

This device has no aid for insertion leading to the tube possibly being clogged with tissue upon introducing the device into the patient's body. Therefore, this device might have difficulty being inserted to a depth of  $\sim 40\text{mm}$  into the patient's body. Also, in order to be able to excise LNs *en bloc*, the device will need an inner diameter of  $> 18\text{mm}$ , which means the tissue damage upon insertion is not negligible.

This concludes *Section 2.2. Concepts*. *Section 2.3. Decision Matrix* presents the method of choosing the most promising concept for the MISLNB medical device.

## 2.3. Decision Matrix

The method of using a *decision matrix* is chosen to determine which concept is the most promising and shall be designed in more detail. Using the *decision matrix* has the advantage of assigning a priority as well as a more nuanced value to each requirement of each concept. This means that the *decision matrix* takes more detail into account when deciding on a concept than other methods like for instance the *Harris Profile* does [37].

The *Decision Matrix* in *Table 2.1* is assembled as follows: *columns 1 - 4* are the requirements and their priority which were previously presented in *Section 2.1. Requirements*. Each concept is assigned a score from 5 – 1 based in how well it fulfils each requirement. These values are recorded in *columns 5-9*, where each column represents a different concept. The scores are assigned based on the author's interpretation of how well the concept fulfils the requirement. *Column 10* shows how the author defines what qualifies for getting scored a 5 and what qualifies for a 1 for each requirement. This is done to make the allotment of scores and ultimate choice of concept more transparent and comprehensive. Also, by using several requirements, a total of 11 in this case, and assigning the weighing priority, the author of this thesis believes that the decision of choosing a concept is as unbiased as possible. When assigning the scores to each requirement for each concept the scores for the priority are not yet filled in. This shall make the assigning of scores for each concept as unbiased as possible.

The total score of a concept is calculated by multiplying the priority of each requirement with the allotted score and adding them up per concept. For example, the *spherical excision* system scored a 3 for the general requirement *en bloc* with a priority of 5, and a 1 for the requirement *footprint* with the priority 4. The score of the *spherical Excision* system for these two requirements is:  $score = 5 * 3 + 4 * 1 = 19$ . This calculation is done for all requirements per concept and noted in the last row named "SCORE", see *Table 2.1*. The concept with the highest overall score is the *expandable ring* with a score of 125, see *Table 2.1*. Therefore, this concept is deemed the most promising and is developed further.

After choosing the most promising concept, the *expandable ring*, with an overall score of 125, this design is developed further. This entails looking into the specifications such as dimensions (i.e., pole length and blade thickness) as well as assigning a biocompatible material that will also be compatible with standard sterilisation techniques. Another important aspect is, of course, how the device will be manufactured. All these aspects are explained in *Chapter 3. Detailed Design*.

Table 2.1: This table is the *decision matrix* used to evaluate which concept is the most promising out of five. *Columns 1-4* are identical to *Figure 2.1* and represent the requirements and their assigned priority. For more information concerning the requirements, please see *section 2.1*. *Columns 5 - 9* represent the different concepts and their assigned score between 5 (best) and 1 (worst). *Column 10* explains what it takes to get scored a 5 or 1, respectively. The last row shows the *score* that was achieved by each concept. The score is calculated by multiplying each score assigned to a concept per requirement with the priority of the requirement and adding the score. It can clearly be seen that the *expandable ring* scores highest in the decision matrix and was hence chosen as the most promising concept

#	Requirement	Priority	CONCEPTS					Remark	
			Spherical Excision	Wire Basket Excision	Expandable Ring	Corkscrew	Sea Urchin - Aristotle's Lantern		
#1	GENERAL	en bloc	5	3	3	5	4	3	5 = most likely to excise en bloc without damage; 1 = least likely to excise en bloc without damage
#2		footprint	4	1	3	5	5	2	5 = small cross-section upon insertion; 1 = large cross-section upon insertion
#3		accommodating	3	1	2	5	5	1	5 = one device different size LNs; 1 = for every size LN different device
#4		development costs	1	2	3	4	4	5	5 = cheap to develop; 1 = expensive
#5	SAFETY	safe failure	5	2	1	3	1	4	5 = acceptable harm during failure (no operation needed because of it to e.g., retrieve part of device) ; 1 = unacceptable harm during failure
#6		cauterising	2	4	5	5	4	2	5 = cauterisation is or can be integrated; 1 = cauterisation cannot be integrated
#7		sterilisation	1	3	3	3	3	4	5 = yes and needed AND no and not needed; 1 = no but needed
#8	USER EXPERIENCE	sturdiness	3	5	2	4	3	5	5 = very robust and unlikely to fail at excision due to deformation; 1 = very soft and possible to fail at biopsy due to it
#9		durability	1	3	1	3	2	5	5 = one device one patient; 1 = one device one LN
#10	SIMPLICITY	simple	2	1	1	5	5	4	5 = few components and straight forward working; 1 = many components and intricate working
#11		electronic components	2	2	2	4	4	5	5 = electronic components not crucial for proper working (predominantly to fully mechanical device); 1 = electrical components crucial for proper working (predominantly electrical device)
SCORE				69	67	125	104	97	

# 3

## Detailed Design

This chapter presents the design choices that are made when developing the chosen concept, the *expandable ring*, further into an executable design. For an explanation on how the *expandable ring* is chosen as the most promising concept, please see [Section 2.3. Decision Matrix](#).

During the process of *detailed design* several aspects need to be considered. For one, the *dimensions* of the medical device's detachment mechanism have to be determined, which is done in [Section 3.1. Dimensions](#). Next, [Section 3.2. Material](#) discusses the need for determining a suitable material and which choice is made. [Section 3.3. Computer Aided Design](#) presents the fabrication considerations and the final design output of the *Detailed Design* process. Lastly, [Section 3.4. The Preis-Device](#) presents the working principal of the mechanism and the fabrication of the executable design of the device in detail.

### 3.1. Dimensions

The dimensions of the *Expandable Ring* are based on the average size and location of a LN. For more information on LNs, please see [Appendix A Familiarisation, Section A.1. What is a lymph node?](#). Furthermore, it is decided to keep the incision in the skin  $\leq 15mm$ . This is an acceptable incision-size when it comes to procedures performed under local anaesthesia only. It has to be noted that the incision might have to be enlarged in order for the SLN to pass through the skin without causing additional damage to the skin by tearing it upon retrieval. The device however, shall fit within a cannula with an outer diameter of  $8mm$  when it is folded.

#### 3.1.1. Poles

In order to determine the length and diameter of the poles, the mean depth of the LNs is looked at. The mean depth of LNs in the axilla is found to be  $43mm$  [3]. The mean depth of LNs in the inguinal region is found to be  $45mm$  [38]. Therefore, the mean depth of the LNs to be considered is taken to be  $45mm$  meaning that the poles of the detachment mechanism need to be at least  $45mm$ . In order to be able to actuate the mechanism properly whilst getting information about the behaviour and translation of the actuation from the *proof-of-concept* tests the device will be subjected to, the length of the poles is chosen to be  $60mm$ , since this is deemed a realistic length also for a final device's design.

The diameter of the poles is set to  $2mm$ , which is an educated guess, because the author of this thesis does not deem the forces that will be exerted on the poles big enough to require a larger diameter to prevent plastic deformation and safe operation. However, *proof-of-concept* tests will have to conclude whether this assumption is correct. Also, calculations are made to determine whether or not the pole diameter should be increased, or the poles made hollow. The calculations are presented in [Chapter 5. Design Evaluation & Iteration, Section 5.1. Calculations](#). And will be validated by *finite element method* analyses in [Section 5.2. Finite Element Method](#). The diameter of the poles has to be optimised in terms of durability, meaning that the poles must not break or bend, and "*footprint*" of the mechanism has to be as small as possible. The "*footprint*" refers to the cross-section from a top viewpoint. This parameter determines the insertion canal that is made upon inserting the device. The "*footprint*" is a direct indication of the tissue damage that is caused by the device. Hence, the smaller

the "footprint" the smaller the tissue damage.

### 3.1.2. Blade

The average long axis of a LN is found to be  $16\text{mm}$ . By choosing the average long axis of the LN as the determining factor of the device's blade, the device is able to detach most LNs encountered in the human body. Designing the mechanism for an average sized LN is deemed the optimum in terms of the medical device accommodating most LN sizes, while keeping its "footprint" as small as possible.

By taking the long axis as the determining factor of the device's dimension, the orientation of the LN does not matter. In contrast, if the average short axis is taken to determine the dimensions, the device will have to be positioned at the tip of the LN in order to be able to detach the LN from its surrounding tissue. Taken all these aspects into account, the length of the blade is calculated as follows:

$$L = \pi * D = \pi * 16 = 50.27\text{mm} \approx 51\text{mm}, \text{ with}$$

- L = length of blade
- D = diameter of the volume to be cut

The length of the blade is set to be the circumference of a LN of average size which is simplified to be a sphere in order to eliminate orientation dependence of the device's detachment mechanism. Because the pole diameter is  $2\text{mm}$ ,  $4\text{mm}$  are added to the blade's length, which increases the it to  $L = 55\text{mm}$ .

The height of the blade is set to be  $5\text{mm}$  which is an educated guess by the author and discussed with Jan van Frankenhuyzen (TUD) and Mario van der Wel (Demo) whose expertise and experience is valued greatly. The reasoning behind choosing a non-arbitrary height for the blade is that the height will give the blade a certain amount of stiffness and stability against bending in unwanted direction. This is important for the blade to be steered accurately and easily by the poles and have some resistance against the pressures and forces exerted on it by the adipose tissue. The thickness of the blade is determined by available spring-leaf thicknesses, these are  $0.04\text{mm}$ ,  $0.05\text{mm}$ ,  $0.7\text{mm}$ , and  $0.1\text{mm}$ .

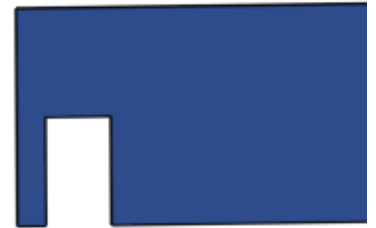


Figure 3.1: This figure depicts one end of the designed blade. The rectangular cut out can clearly be seen. Its function is to prevent the blade from slipping through the pole. The material of the blade is stainless steel. Both ends of the blade are fabricated the same. This figure was created using Onshape (Onshape Inc., Massachusetts, USA)

### 3.1.3. Caps & Fixation of Blade

It is chosen to connect the blade and the poles primarily with the use of cut outs and caps.



Figure 3.2: This figure depicts the distal end of the pole. It shows the  $0.1\text{mm}$  slit the blade cut out fits into. It can also be seen that the milled down end of the pole,  $1\text{mm}$  in diameter, which accommodates the cap. Both poles are fabricated the same. This figure was created using Onshape (Onshape Inc., Massachusetts, USA)

Figure 3.1 shows the cut out in the blade in order to connect the blade to the pole. This cut out is designed to fit into a slit made into the pole, see Figure 3.2. The slit's width is  $0.1\text{mm}$ , which is determined by the fabrication mechanisms which is wire-EDM. The cut out prevents the blade from slipping through the pole laterally. In order to prevent the blade from slipping off the pole in an upwards direction, caps are designed. The outer diameter of the caps is the same as the outer diameter of the poles. The tips of the poles are milled down to measure a diameter of  $1\text{mm}$  in order to accommodate the caps, see Figure 3.2. The caps have the same slit of  $0.1\text{mm}$  as the poles. These slits are to accommodate for the

blade protruding from the pole on both sides. *Figure 3.3* shows the blade connected to the pole as well as the cap, which is pulled off to allow viewing the blade fixation method. The cap has a tapered tip in order to ease insertion into the adipose tissue as well as cutting it. Whether a welding or other (semi-)permanent fixation mechanism needs to be implemented will have to be seen during testing such as the *proof-of-concept* tests in *Chapter 4. Proof-of-Concept*.

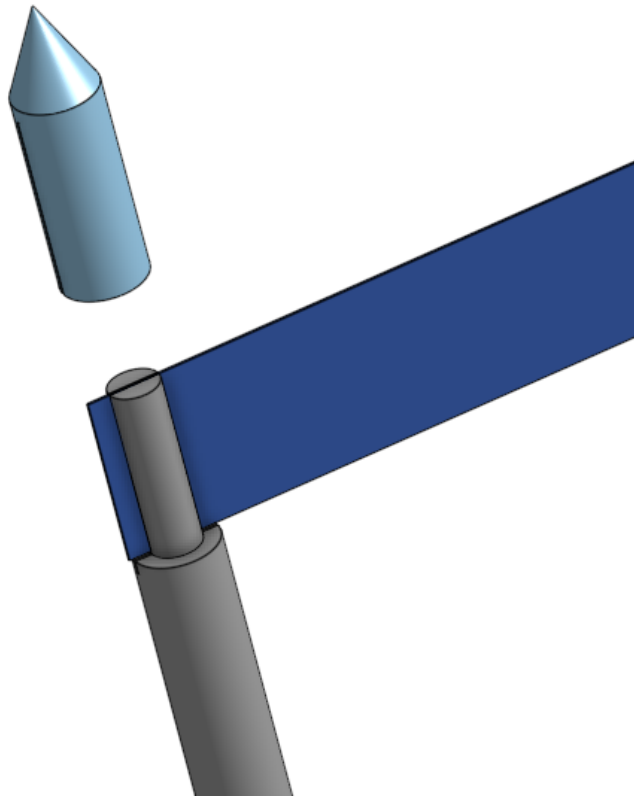


Figure 3.3: This figure shows how the blade is fixed in the pole. The cap is pulled off in order to show the fixation method. Furthermore, the layout of the cap is shown with an outer diameter of  $2\text{mm}$  to match the diameter of the pole and a tapered tip in order to facilitate insertion into and cutting of the tissue. This figure was created using Onshape (Onshape Inc., Massachusetts, USA)

## 3.2. Material

The material chosen to fabricate the detachment mechanism is stainless steel. This material can be manufactured using various methods, i.e., milling, wire-EDM, drilling, and is biocompatible. Also several stainless steel alloys have been approved according to the MDR 2017/745 [22, 57]. Some more information of the MDR with regards to this project can be found in *Appendix I Medical Device Regulation & Documentation*.

Another advantage of using stainless steel, next to it already conforming to the MDR, is that it can be sterilised. This is an important factor pertaining to developing and designing a medical device. Stainless steel also has electrical properties suitable for implementing a cauterisation mechanism in a later design-step, which will in turn aid cutting the surrounding tissue.

## 3.3. Computer Aided Design

With all the information and dimensions determined in *Sections 3.1. Dimensions & 3.2. Material*, the MISLNB medical device's detachment mechanism can be implemented in a 3D computer aided design (CAD) program. The CAD program Onshape (Onshape Inc., Massachusetts, USA) is used, which is available to students online. This program is used to generate *Figures 3.1-3.4*. The implementation of the design is shown in *Figure 3.4*. The device is implemented in the configuration seen in *Figure 3.4*

(instead of how the device is used, namely rolled up) in order to generate the drawings that Mario van der Wel needs to fabricate the device's prototype. After the parts are fabricated and assembled, the *proof-of-concept* tests can commence, see [Chapter 4. Proof-of-Concept](#). But first, [Section 3.4. The Preis-Device](#) explains how the device is designed to be used.

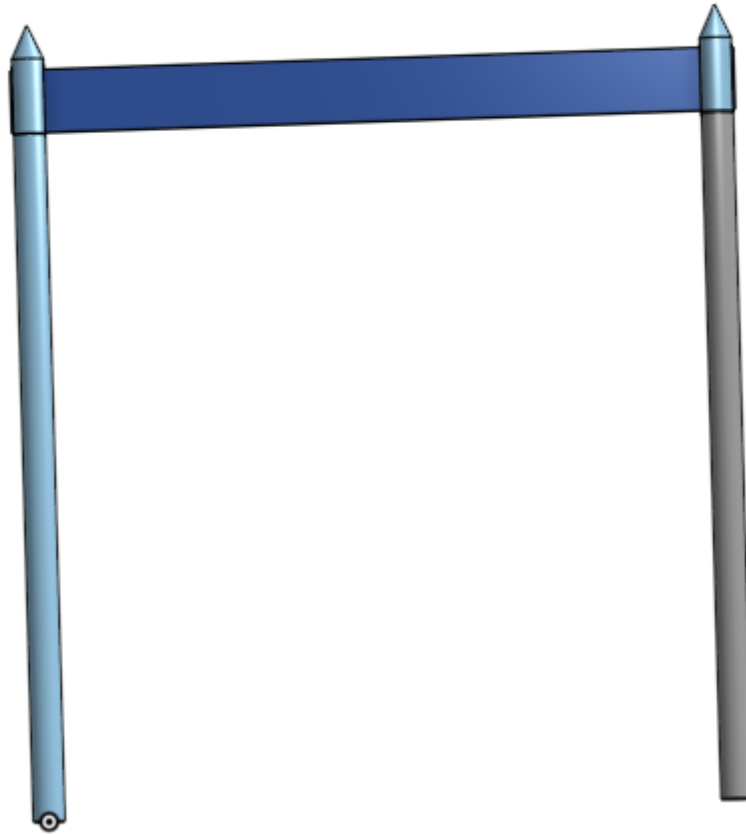


Figure 3.4: This figure shows an Assembly of all device parts as they are supposed to interact with each other. This assembly is used to create the drawings that are sent to Mario van der Wel for fabrication of the prototype that is subsequently used for the *proof-of-concept* tests. This figure was created using Onshape (Onshape Inc., Massachusetts, USA)

### 3.4. The Preis-Device

The device is named the *Preis-Device*, also because *MISLNB medical device* or *intact sentinel lymph node biopsy medical device* are a mouthful. The *Preis-Device* consists of the following parts:

- detachment mechanism, see [Figure 3.4](#)
- a cannula, see [Figure 3.5](#)
- a sharp cannula insert, see [Figure 3.5](#)
- actuation mechanism (either electrical or mechanical)
- a cauterisation mechanism (to be implemented)
- a handle (to be implemented)

The author of this thesis deems it prudent to keep the working principal of the *Preis-Device* as simple as possible in order to assure save failure, but also to make the experience for the patient as uneventful



as possible since the patient is awake during the entire procedure. Furthermore, the complexity of a system is not correlated to its performance!

The *Preis-Device* is designed to work as follows: The radiologist makes an incision in the skin where the device is to be inserted. Then the sharp, tipped insert positioned inside the cannula, see [Figure 3.5](#), is introduced into the patient's body via the small incision in the patient's skin. The SLNs have previously been identified either by *lymphoscintigraphy* or preferably using a method not using a radioactive colloid, for instance the method described by Ophuis et al. [46]. The cannula with the sharp, tipped insert is positioned in front of the SLN using ultrasound guidance. As the author experienced, identifying and locating LNs using ultrasound is easily done when performed by an experienced radiologist. The author saw this when dr. Cécile de Monyé, a radiologist at the Erasmus MC, helped identify and mark LNs using an ultrasound and needles in the dissecting room. For more information please see [Appendix B Human Tissue Test, Section B.1. Tensile Test](#). When the cannula with insert is positioned, the insert is retracted while the cannula stays in place. Now the folded *Preis-Device* is inserted through the cannula and pushed into the tissue to the side of the SLN. Now the excision of the SLN can begin. The actuation mechanism is engaged and the *Preis-Device* starts cutting the SLN's surrounding tissue whilst simultaneously protruding further from the cannula. The pole without the blade wrapped around it describes a spiral motion around the SLN, thereby cutting it free. At the same time, the pole with the blade wrapped around slowly unwinds the blade in order to enlarge the radius of the spiral whilst also moving forward towards the distal end of the LN. How fast and far the second pole unwinds the blade depends on the size of the SLN and can be controlled by the radiologist. The *Preis-Device* can be wound up again in order to shorten the radius of the spiral. At the end, when the poles are next to each other, the device is twisted in order to ensure that all the surrounding tissue is cut.



Figure 3.5: This figure depicts the cannula and the sharp, pointed insert. The cannula and the insert are introduced into the body and positioned in front of the LN. The insert can be removed from the cannula. This figure was created using Onshape (Onshape Inc., Massachusetts, USA)



Figure 3.6: This picture shows various configurations of a disposable stone excision basket as produced by JiuHong Med. The Stone Excision Basket is used as a retrieval mechanism for the detached SLN. The collapsed Stone Excision Basket is pushed past the SLN and then deployed, enveloping the detached SLN. Then, the Stone Excision Basket, the *Preis-Device*, the cannula, and the SLN can all be retrieved from the patient's body. This picture was taken from their website [40]

In order to retrieve the SLN, the device can be used in combination with for instance a *Stone Extraction Basket*, see [Figure 3.6](#) as produced by JiuHong Med [40]. The *Stone Excision Basket* is inserted through the cannula. In the beginning it is flat, like a guide wire of a catheter for instance. In this state it is pushed past the detached SLN. When the *Stone Excision Basket* is pushed sufficiently past the SLN, it is deployed, enveloping the SLN without damaging it. Another way of retrieving the free SLN is using the *Pull-and-Harvest* method designed by the previous Master student Max Joosen, which has been validated with respect to retrieving loose LNs through suction undamaged. For more information on the *Pull-and-Harvest* method please see [Appendix A Familiarisation, Section A.3. Previous Thesis](#).

After the SLN is retrieved it is prepared to be sent to the pathologist for *nodal staging* [14]. In case of the patient having more than one SLN, which is the case in > 20% of patients [23], the device is reused, and the procedure starts anew until every SLN is excised. However, the device is not designed to be used on different patients. This is also described in the *Intended Purpose* statement in *Appendix I Medical Device Regulation & Documentation, Section I.1. Intended Purpose*.

Now that the *Preis-Device* is designed and implemented in Onshape (Onshape Inc., Massachusetts, USA), the technical drawings are sent to Mario van der Wel (Demo) to be manufactured using wire-EDM and milling. The manufactured *Prototype 1* is shown in *Figures 3.7 & 3.8*. It was chosen to manufacture several blades in the different thicknesses (0.04mm, 0.05mm, 0.07mm, and 0.1mm) and test them in order to determine which works the best. See *Chapter 4. Proof-of-Concept* for a detailed introduction to the test set-up, execution, and test results and interpretation thereof.

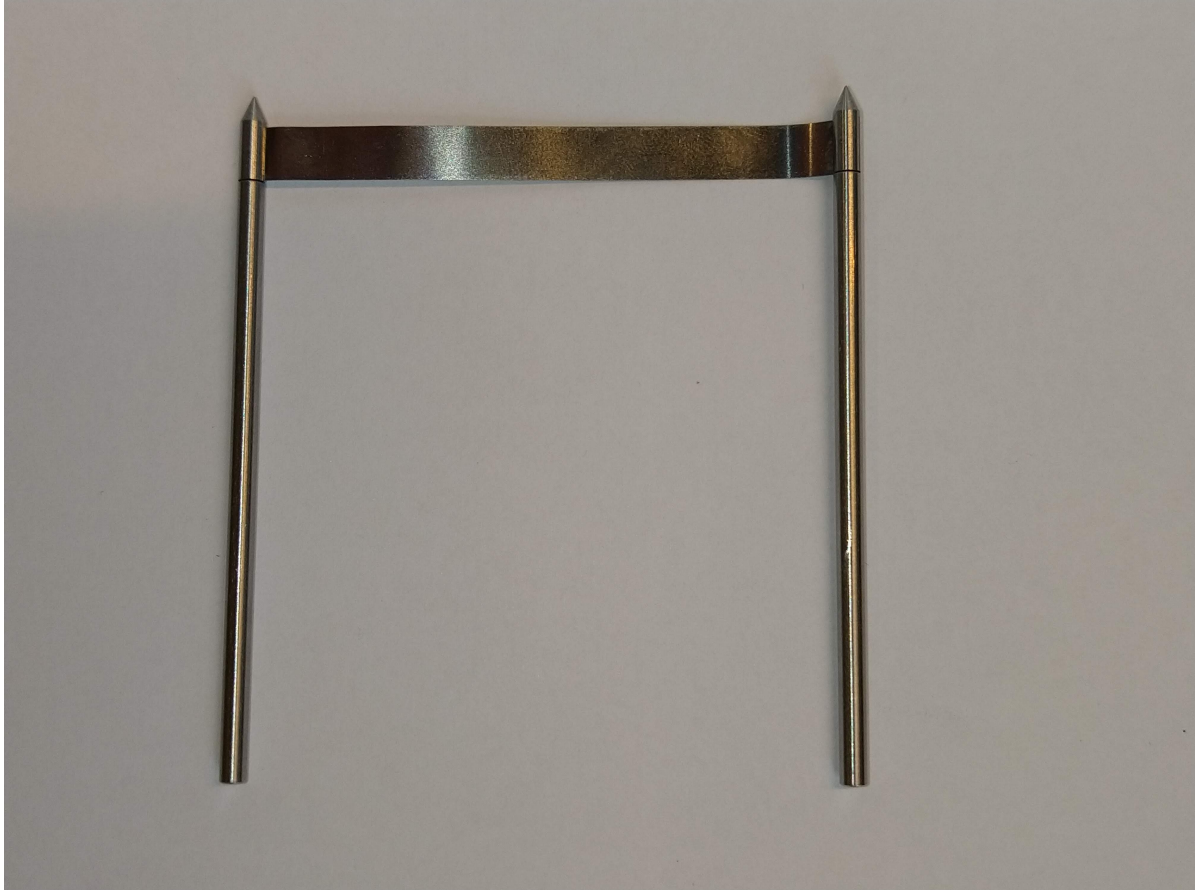


Figure 3.7: This photo shows the manufactured prototype when first assembled. The caps sit snugly on the rods and keep the blade well in place. This is the same position as the CAD picture from *Figure 3.4*. This photo was taken by the author

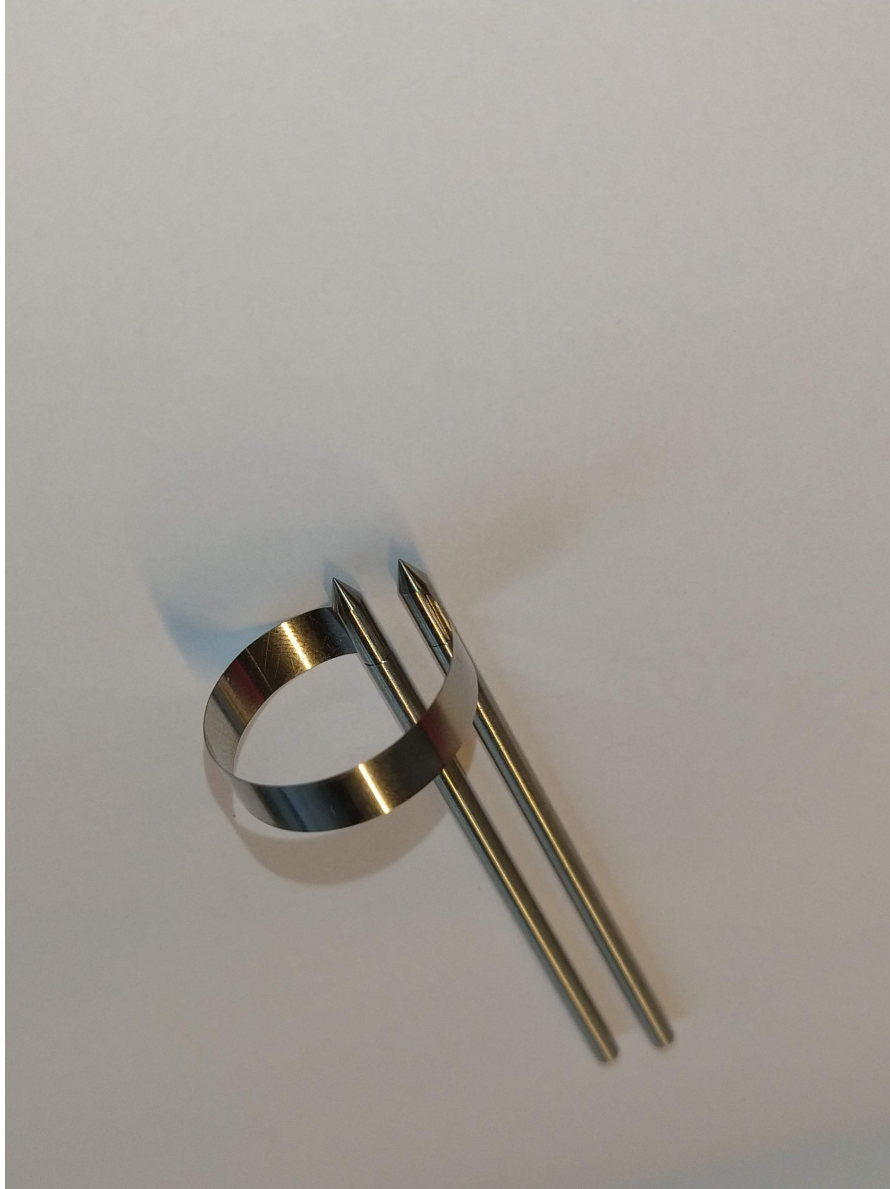
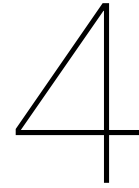


Figure 3.8: This photo depicts the prototype in "*cutting*" mode, aka the blade fully extended to form a circle. This is the same position as the CAD picture on the cover of this thesis. This photo was taken by the author





# Proof-of-Concept

This chapter presents the *proof-of-concept* tests' design, execution and evaluation. [Section 4.1. Device Holder](#) introduces the *device holder* that is designed and 3D printed in order to make the tests reproducible and reliable. [Section 4.2. Test Execution](#) discusses how the blades are tested, see [Section 4.2.1. Blade Tests](#), and the *Proof-of-Principal* test, see [Section 4.2.2. Proof-of-Principal](#). How the measurements from the *blade tests* is analysed is explained in [Section 4.3. Data Processing](#). The goal of the *proof-of-Concept* tests is to answer the following hypothesis:

## **Can the Preis-Device excise LNs minimally invasive and en bloc?**

In order to answer this hypothesis, several questions are contrived that needed to be answered to conclusively prove or disprove the hypothesis, namely:

1. Is the *Preis-Device* able to cut through adipose tissue? (see [Section 4.2.1. Blade Tests](#))
2. What are the cutting forces of the *Preis-Device*? (see [Section 4.2.1. Blade Tests](#))
3. Does the *Preis-Device* fulfil the requirements of a MISLNB medical device? (see [Section 4.2.2. Proof-of-Principal](#))

This chapter ends with [Section 4.4. Results & Analysis](#) explaining and interpreting the results as well as answering these questions definitively.

## 4.1. Device Holder

It is worth mentioning the device holder that is designed to execute the *proof-of-concept* blade tests because it gives the tests more reliability and reproducibility. The goal of the *device holder* is to connect the device to the sensor tightly, to prevent deflection of the device in different directions and to achieve reliable force measurements. [Figure 4.1](#) depicts an isometric view of the *device holder* with the device inserted, showing how it is used during test execution.

The *device holder* is a 35mm by 20mm 3D printed block. It has a slit through roughly 2/3s of its length, see [Figure 4.1](#). The slit squeezes the device's poles, thereby holding them in place. Securing the poles is enhanced by two M3 bolts and nuts that pass through the entire thickness of the *device holder*, see [Figure 4.1](#), and squeeze the two slabs tighter, to hold the device even more tightly. During the *proof-of-concept* tests it is evident that the device is secured tightly against deflection as well as translation in vertical direction.

At the back of the *device holder* a hexagon-shaped gap can be seen that fits the nut and head of the bolt interchangeably, see [Figure 4.2](#). The rectangular gap in the top half of the backside of the *device holder* is the attachment point of the *device holder* to the linear stage sensor, see [Figure 4.2](#). For a more detailed overview of the used apparatuses (e.g., the linear stage, the force sensor) and a description thereof, please see [Appendix B Human Tissue Test, Section B.1. Tensile Test](#).

The holes for the device's poles pass through the whole height of the device, see [Figure 4.3](#), in order to ease post-fabrication cleaning of support structures. The support structures are needed because

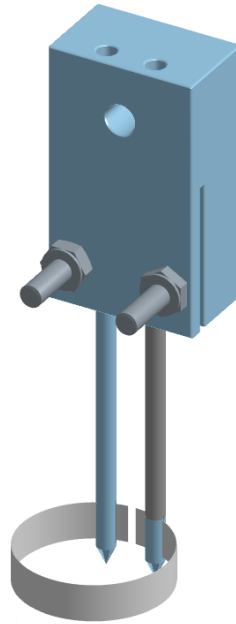


Figure 4.1: This figure shows an **isometric** view of the device holder with the device attached. The device holder is attached from the front through the hole in the upper half of this figure to the sensor of the linear stage. M3 bolts can be seen protruding from the device holder. These bolts and nuts securely fasten the device into the device holder. A slit through the bottom 2/3s of the device holder clamps the device' poles. It can furthermore be seen that the holes for the device' poles run through the entire height of the device holder. It was chosen to do so in order to facilitate post-processing of the print. The poles are marked during testing to indicate the insertion depth of the poles into the device holder. This ensures that the device is always inserted to the same depth. The device holder was manufactured using 3D printing. This figure was created using Onshape (Onshape Inc., Massachusetts, USA)

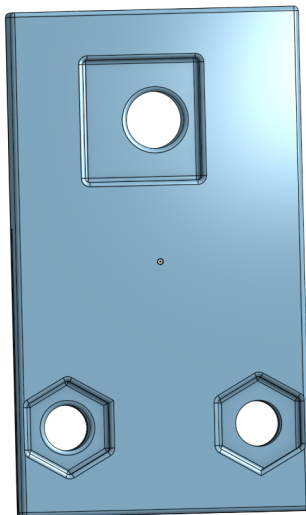


Figure 4.2: This figure shows the **back** of the device holder. In the top half the attachment to the force sensor of the linear stage can be seen. In the bottom half the hexagon-shaped gaps are shown. These gaps enable for either the nut or the bolt's head to be submerged to ease tightening of the bolt-nut configuration. This figure was created using Onshape (Onshape Inc., Massachusetts, USA)

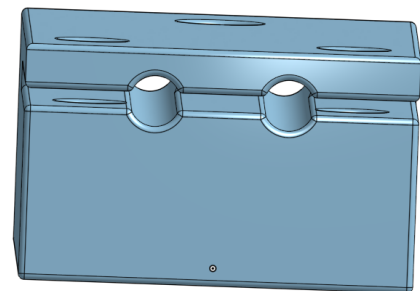


Figure 4.3: The figure shows a **bottom**-view of the device holder. The slit as well as the holes for the poles can clearly be seen. The poles are stuck into the holes and clamped by the two parts of the device holder separated by the slit. The M3 bolts are used to fasten the grip of the device holder on the poles of the device. This figure was created using Onshape (Onshape Inc., Massachusetts, USA)

of the slit that holds the poles in place, and the hexagon-shaped gaps. No matter how the device is oriented while printing, there is a need for a support structure. During the tests the poles would be marked with a line in order to insert the poles the same distance every time, for more information on the test execution please see [Section 4.2. Test Execution](#) or [Appendix E Test Protocol for Prototype 1](#).

## 4.2. Test Execution

This section explains the execution of the various tests, namely the *Blade Tests* ([Section 4.2.1](#)), and the *proof-of-principal* test ([Section 4.2.2](#)). The goal of these tests is to extract as much information as possible from the first prototype of the *Preis-Device*, therefore, *blade tests* as well as a *proof-of-concept* test are set up. All tests are executed on phantoms made from gelatine that resembles the Young's modulus of adipose tissue [25]. Because the *blade tests* concern the cutting forces of adipose tissue, no artificial LNs (ALNs) are incorporated in the phantoms. The *proof-of-principal* test on the other hand aims at proving that the concept works, which means that ALNs have to be incorporated in the phantoms for those tests. For a detailed protocol on how the phantoms are made, please see [Appendix F Phantom Fabrication Prototype 1 testing](#).

### 4.2.1. Blade Tests

The *blade tests* are executed to get an insight into the forces encountered when cutting adipose tissue. These tests measure force being applied on the phantom in a downwards direction when the blade is cutting the phantom.

To execute these tests, the *device holder*, see [Section 4.1. Device Holder](#), the *Preis-Device* is attached to the force sensor on the linear stage and a phantom is positioned underneath the device. The phantom is positioned in such a way that the *Preis-Device* almost completely cuts through the phantom, which is  $\sim 3\text{cm}$  in height. The linear stage is then moved to its initial position and the test can be executed. When the test is run, the linear stage moves the *Preis-Device* downwards into the phantom, thereby cutting it. The force sensor measures and records the forces exerted by the *Preis-Device* onto the phantom. For a more detailed description of the linear stage and the force sensor please see [Appendix B Human Tissue Test, Section B.1. Tensile Test](#). For a more detailed description of the execution of the blade tests please see [Appendix E Test Protocol for Prototype 1](#).

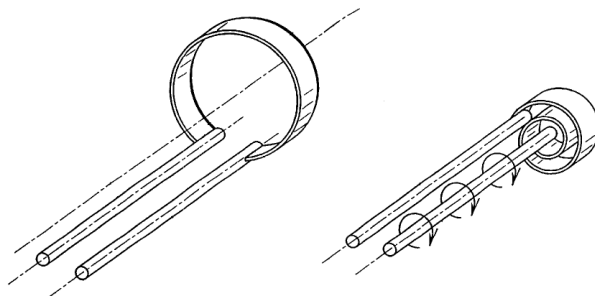


Figure 4.4: This figure depicts the two per-defined "modes" of the device during the *blade tests*. **LEFT** shows the device in "cutting" mode. **RIGHT** shows the device in "insertion" mode. During the latter mode, the device has the smallest "footprint".

It is important to note that the *blade tests* are executed in two variations. The first being with the blade in "cutting" mode, the blade being fully unrolled and forming a circle, see [Figure 4.4, LEFT](#). The second variation is executing the *blade tests* with the device in "insertion" mode, where the blade is completely rolled up around one pole, see [Figure 4.4, RIGHT](#). The latter mode is called "insertion" mode, because the device, is designed to be inserted into the patient's body in this mode. When rolled up, the device has the smallest "footprint" possible, meaning that the cross-sectional area orthogonal to the direction of movement (insertion) is minimal.

By reducing the "footprint" of the device upon insertion the least amount of tissue is damaged.

Furthermore, when in "insertion" mode, the device can be introduced into the body through a cannula with a diameter of  $< 10\text{mm}$ , which suffices to the agreed upon dimension of the incision being  $< 15\text{mm}$ , see [Chapter 3. Detailed Design, Section 3.1. Dimensions](#). For more information on the cannula and the *Preis-Device's* working principle please see [Chapter 3. Detailed Design, Section 3.4. The Preis-Device](#).

These *blade tests* are also executed for different blade-thicknesses, a  $0.04\text{mm}$ -blade and a  $0.05\text{mm}$ -blade. The observations as well the maximum forces that are recorded in the respective *RunTables*, see [Appendix D Blade Test Runtables, Figures D.1 & D.2](#). Previously executed tests with the blade thicknesses of  $0.07\text{mm}$  and  $0.1\text{mm}$  (not included in this thesis) revealed that these blade thicknesses are unsuitable for the device. The *blade tests* described in this section do not only measure the force needed to cut the phantom, but also show that the cap-pole-design for attaching the blade to the poles is a sturdy design that keeps the blade securely in place.

The main limitations of these tests are that no connective tissue is integrated into the phantoms and that the phantoms are homogeneous. However, by making the phantoms homogeneous, valuable input for the finite element method (FEM) analysis in [Chapter 5. Design Evaluation & Iteration, Section 5.2. Finite Element Method](#) is gathered.

#### 4.2.2. Proof-of-Principal

The *proof-of-principal* test is designed to test whether the detachment mechanism of the *Preis-Device* works. For this test, special phantoms are used that include ALNs, see [Appendices E Test Protocol for Prototype 1 & F Phantom Fabrication Prototype 1 testing](#). The size of the ALNs is recorded in order to determine whether the *Preis-Device* can in fact accommodate average sized LNs ( $\sim 16\text{mm}$ ), see [Chapter 3. Detailed Design, Section 3.1.2. Blade](#). The size of the LN as well as the blade thickness and whether the test is successful or not is recorded in the *RunTable*, see [Figure 4.5](#).

The long and (LA) short axis (SA) of the ALNs is measured according to the same guidelines used on human LNs. For further explanation on how the LA and SA is measured please see [Appendix B Human Tissue Tests, Section B.1 Tensile Test](#).

The *proof-of-principal* tests are executed by placing the phantom on a sturdy surface. The *Preis-Device* is brought into "insertion" mode manually. Next, the *Preis-Device's* detachment mechanism is inserted into the phantom to one side of the ALN. Like described in [Chapter 3. Detailed Design, Section 3.4. The Preis-Device](#). Then, the poles are actuated manually, meaning that the pole the blade is wound around is kept in place and only rotates around its own vertical axis. Whereas the second pole, with no blade wound around, begins cutting the phantom around the ALN in a spiral motion until it describes a full circle. When the two poles are situated next to each other, the device is twisted to make sure the ALN is cut free. Then the device is pulled from the phantom. In some cases, this leads to the ALN being retrieved from the phantom at the same time as the device.

Besides testing the *Preis-Device's* detachment mechanism, the *proof-of-principal* test also gives valuable information on the sturdiness of the device and the attachment of the blade by the cap-pole-design. Which turns out to be very sturdy and the caps have never slipped off. Therefore, no soldering or welding of the caps is deemed necessary at this point.

It is chosen to actuate the *Preis-Device's* detachment mechanism manually. By actuating the mechanism manually more degrees of freedom are kept, giving the author more information about the working of the mechanism and how to design an optimal actuation mechanism. Grapes were originally considered as suitable ALNs, however, after measuring, they turned out to be much larger than  $16\text{mm}$ .

The biggest limitation of the *proof-of-principal* test is the gelatine, which lets the author see what is happening with the device without needing ultrasound. Another limitation is the limited size of the phantom, which leads to the author having to hold the phantom while executing the *proof-of-principal* test. A phantom holder or bigger phantoms should be design for future tests. Also, the phantoms have to reach room temperature before testing, and it was noticed that the commonly stated *30minutes* is not enough time for the phantoms to reach room temperature. Only at room temperature does the Young's modulus of the phantom resembles that of adipose tissue. Also, each phantom can only be used once!



#	color cupcake form*	blade thickness [mm]	successful? Yes (Y)/ No (N)	Remark	Video? Yes (Y)/ No (N)	ALN size	
						SA [cm]	LA [cm]
1	raisin	0.05	Y	*gelatine still a bit *cold to the touch	Y	1.1	1.6
2	raisin	0.05	Y	*ALN came out too	Y	1.3	1.7
3	cranberry	0.05	Y	*two cranberries stuck together *ALN came out as well	Y	1.9	2.1
4	cranberry	0.04	Y	*ALN came out on second try	Y	1.2	2.2
5	raisin	0.05	Y	*deep *measured after test	Y	1.00	1.40
6	raisin	0.05	Y	*deep *measured after test	Y	1.40	1.60
7	cranberry	0.05	Y	*very superficial *measured after test	Y	1.50	1.80
<b>AVERAGE SIZE</b>						1.342857	1.77

Figure 4.5: This figure shows the *RunTable* of the proof-of-principal tests. These tests are executed in phantoms with embedded ALNs. The type of ALN (raisin or cranberry) used is recorded in *column 2*. The blade thickness is recorded in *column 3* and whether the test was successful or not is recorded in *column 4*. *Column 5* contains all observations that are made during the tests. *Columns 7 & 8* contain the measured short and long axis of the respective ALNs, SA and LA respectively. The averages of the SAs and LAs are calculated and shown in the last row. This figure is a screen-capture of the actual *RunTable* made in Microsoft Excel (Microsoft, Redmond, Washington, United States)

### 4.3. Data Processing

The experimental data recorded by the force sensor (LSB200-FSH00104, FUTEK Advanced Sensor Technology Inc., Irvine, CA, USA) is saved in a Matlab .m-file. Each experiment took 306800 measurements of position and force in *mm* and *Volt*, respectively. Appropriate data processing was necessary in order to 1) convert the force measured in *Volt* to force in *Newton* and 2) to analyse the data in order to obtain insight into the problem and forces at hand.

To achieve those goals, a Matlab code is written that converts and analyses all recorded data points, see [Appendix H Matlab Code](#).

In order to set up an equation to convert the measured force in *Volt* to force in *Newton*, the relation between *Volt* and *Newton* has to be determined. Six calibration weights of

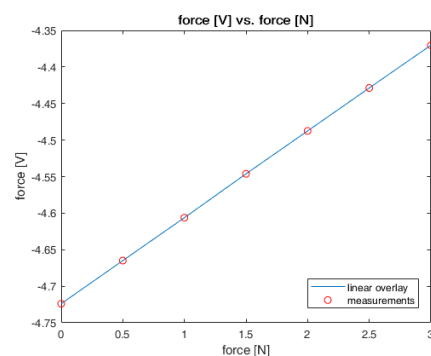


Figure 4.6: This graph shows that the relation between Volts and Newton measured with the experimental set-up is indeed linear. This picture was created using the Matlab plot function and subsequently saving the picture in .png format

each 50g are available, totalling up to 300g. An attachment-block is connected to the sensor and the sensor, linear stage and attachment-block are seen as one. Then the first calibration test is run with 0g, or nothing attached to the sensor. For the next run, 50g are attached and for each consecutive run an additional 50g are added.

Since the weights used are calibration weights, the force the sensor should measure is: 0N for 0g, 0.5N for 50g and so on. Each calibration run is analysed and averaged using Matlab, and the results saved in a vector. Another vector is set up for the force in *Newton* and the two are plotted against each other, see *Figure 4.6*. As can be seen in *Figure 4.6* the relation between *Volt* and *Newton* is linear. What the graph also shows is a certain offset that needs to be taken into account. The offset can be seen where at 0[N] the measured *Volt* does not equal 0[V] but instead  $\sim -4.725[V]$ .

However, since the relation is linear, a simple correlation formula can be set up:

$$F[N] = A * F[V] - B \quad (4.1)$$

Where variable *A* is a multiplication factor and equals  $-8.48176[N/V]$ . *F[V]* is the force measured in *Volt*, which in this case is a 1x306800 vector. Variable *B* represents the offset that can be seen in *Figure 4.6*. *B* is determined to be 38.41, which is done by averaging a 0g-calibration test. How these parameters are determined in detail can be seen in *Appendix H Matlab Code*. However, the value of *B* has to be determined for every set of tests, because the offset measured by the sensor depends on environmental factors (e.g., humidity, temperature). Therefore, before each set of experiments, a new 0g-calibration test is run in order to increase the accuracy of the data analysis.

The measured maximum force values are saved in vectors and recorded in the *RunTables*, see *Appendix D Blade Test RunTables*, *Figures D.1 & D.2*. Furthermore, the force vectors with the converted force in [N] are saved as well. For more information on the documentation of this project, please see *Appendix I Medical Device Regulation & Documentation*.

#### 4.4. Results & Analysis

This section presents the results, analysis and interpretation of all *proof-of-concept* tests. Data on these tests is collected in two manners: 1) by measuring the forces, by means of the load cell force sensor (LSB200-FSH00104, FUTEK Advanced Sensor Technology Inc., Irvine, CA, USA); 2) by observations made by the author and test executioner.

During the *blade tests*, see *Section 4.2.1. Blade Tests*, force measurements are taken for every test executed. The maximum measured force is evaluated using Matlab and recorded in a respective *RunTable* for the blade thickness (either 0.04mm or 0.05mm), see *Appendix D Blade Test RunTables*, *Figures D.1* (for the *RunTable* of the 0.04mm-blade) & *D.2* (for the *RunTable* of the 0.05mm-blade). Furthermore, all graphs of the tests are plotted in *Figures 4.8-4.11*. These graphs show that the behaviour of the measured forces is the same for the "cutting" mode using the 0.04mm-, or the 0.05mm-blade, see *Figures 4.8 & 4.10*. Also, the force behaviour for the "insertion" mode tests is the same independent of the blade-thickness, as can be seen in *Figures 4.9 & 4.11*. Because of the behaviour of the graphs of each test variation being so similar, reliability and reproducibility of the tests is assumed. However, as can be seen in *Table 4.1*, the average values for the maximum forces measured vary.

Table 4.1: This table lists the average maximum forces evaluated with Matlab and recorded during the respective *blade tests*. The averages are determined using Microsoft Excel (Microsoft, Redmond, Washington, United States)

	0.04 [mm]	0.05 [mm]
Fmax - cutting	7.16 [N]	8.63 [N]
Fmax - insertion	2.72 [N]	2.14 [N]

As can be seen in *Table 4.1*, the maximum cutting force of the 0.05mm-blade is 1.47N greater than that of the 0.04mm-blade. However, in insertion mode, the maximum insertion force of the 0.05mm-blade is 0.58N lower than that of the 0.04mm-blade. Which is counter intuitive because a thicker blade has more area which will need a greater force to exert the same amount of pressure on the phantom in order to cut it. The most probable explanation is that the 0.05mm-blade is more tightly wound during the "insertion" mode tests than the 0.04mm-blade.

Another important finding from the collected data is the fact that the *Preis-Device* is indeed able to excise ALNs of average LN size, as can be seen in *Figure 4.5*, last row.

In terms of observations, it can be seen that the  $0.04\text{mm}$ -blade breaks more easily than the  $0.05\text{mm}$ -blade. This can also be seen in the *remark*-section of the *RunTable* in *Appendix D Blade Test RunTables*, *Figure D.1*, Test #1.2, #4 & #9. The  $0.04\text{mm}$ -blade comes loose and has to be changed before the set of "cutting" mode tests is concluded. Two more  $0.04\text{mm}$ -blades are used due to the blade tearing and small pieces breaking off. In general, it is noticed that the blades experienced permanent plastic deformation, however, the  $0.05\text{mm}$ -blades experiences no unexpected deformations or failures, unlike the  $0.04\text{mm}$ -blades.

Because of the  $0.04\text{mm}$ -blade failing, and in order to rule out that the blades are getting blunt and distort the force measurements, new blades are used for the "insertion" mode tests regardless of the state the blade is in after the "cutting" mode tests. After looking at the forces listed in the respective *RunTables* in *Appendix D Blade Test RunTables*, *Figures D.1 & D.2*, it cannot be concluded that the test results indicate the blades getting blunt. A considerable increase in force would be seen if a blade becomes blunt. This can neither be seen in *Figure D.1* nor when looking at the maximum measured force in *Figure D.2* where only one blade was used for all "cutting" mode tests. It has to be noted that the number of the test indicated in the first column in both *Figures (D.1 & D.2)* is the order in which the tests are executed, beginning with test # 1.

Another important observation made during testing was that the insertion cannal is  $< 5\text{mm}$  in diameter for the  $0.04\text{mm}$ -blade, see *Figure 4.7*.

Now the research questions asked the beginning of this chapter, which were:

1. Is the *expandable ring* able to cut through adipose tissue?
2. What are the cutting forces of the *expandable ring*-blade? And do they suffice?
3. Does the *expandable ring* fulfil the requirements of a MISLNB medical device?

can be answered.

1. Yes, the "insertion" and "cutting" tests, see *Section 4.2.1. Blade Tests*, have shown that the device can cut through the phantom resembling adipose tissue, see *Section 4.4. Results & Analysis*.
2. The cutting forces of the blades are  $7.16\text{N}$  and  $8.63\text{N}$  for the  $0.04\text{mm}$ - and the  $0.05\text{mm}$ -blades, respectively, see *Table 4.1*.
3. Yes, the *Preis-Device* fulfils the requirements, because it is able to excise average sized ALNs *en bloc*, as was shown in *Section 4.2.2. Proof-of-Principal*, *Figure 4.5* and it causes acceptable tissue damage with an insertion cannal  $< 5\text{mm}$ , see *Section 4.4. Results & Analysis*, *Figure 4.7*.

**Therefore, it can be concluded that the hypothesis: *Can the Preis-Device excise LNs minimally invasive and en bloc?*, is proven true.**

This concludes *Chapter 4. Proof-of-Concept* on testing the first prototype of the *Preis-Device*. *Chapter 5. Design Evaluations & Iteration* tevaluates and translates the test results and designs into actionable design optimisations where needed.



Figure 4.7: This figure shows the insertion cannal (inside the black circle). The blade is held for reference, showing that the insertion cannal is less than  $5\text{mm}$  in diameter. This cannal was made with a  $0.04\text{mm}$  blade. The picture was taken by the author

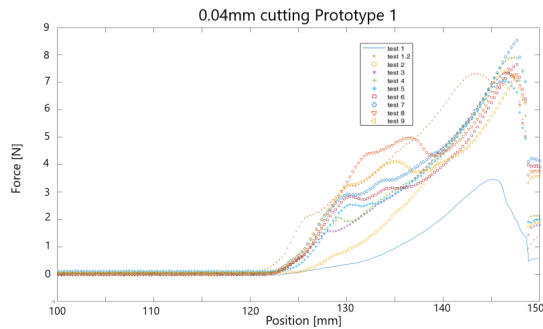


Figure 4.8: This graph shows the force measurements of the cutting test graphs executed with a  $0.04\text{mm}$  blade. The average maximum cutting force of the  $0.04\text{mm}$  -blade was  $7.16\text{N}$ . This was evaluated using the entries from [Figure D.1](#) for the cutting tests and averaging them using Microsoft Excel (Microsoft, Redmond, Washington, United States). This picture was created using the Matlab plot-function and subsequently saving the picture in .png format.

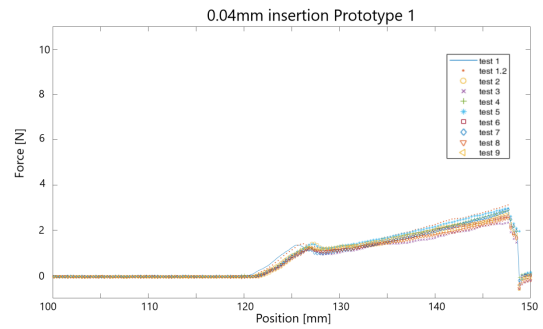


Figure 4.9: This graph shows the force measurements of the insertion test graphs executed with a  $0.04\text{mm}$  blade. The average maximum cutting force of the  $0.04\text{mm}$  -blade was  $2.72\text{N}$ . This was evaluated using the entries from [Figure D.1](#) for the cutting tests and averaging them using Microsoft Excel (Microsoft, Redmond, Washington, United States). This picture was created using the Matlab plot-function and subsequently saving the picture in .png format.

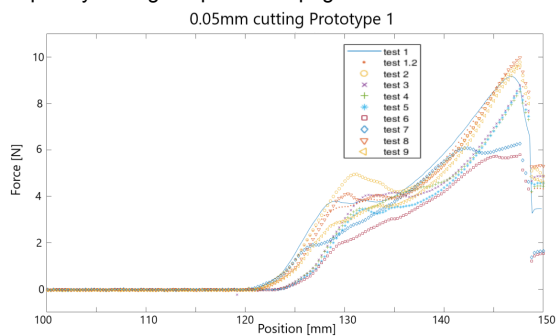


Figure 4.10: This graph shows the force measurements of the cutting test graphs executed with a  $0.05\text{mm}$  blade. The average maximum cutting force of the  $0.05\text{mm}$  -blade was  $8.63\text{N}$ . This was evaluated using the entries from [Figure D.1](#) for the cutting tests and averaging them using Microsoft Excel (Microsoft, Redmond, Washington, United States). This picture was created using the Matlab plot-function and subsequently saving the picture in .png format.

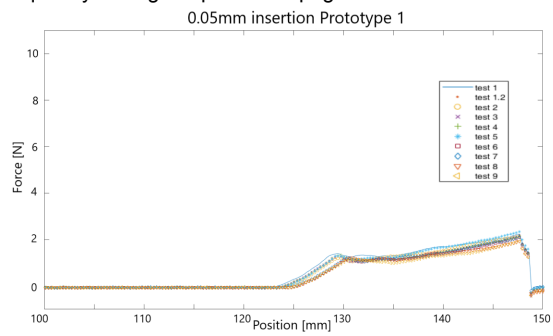


Figure 4.11: This graph shows the force measurements of the insertion test graphs executed with a  $0.05\text{mm}$  blade. The average maximum cutting force of the  $0.05\text{mm}$  -blade was  $2.14\text{N}$ . This was evaluated using the entries from [Figure D.1](#) for the cutting tests and averaging them using Microsoft Excel (Microsoft, Redmond, Washington, United States). This picture was created using the Matlab plot-function and subsequently saving the picture in .png format.

# 5

## Design Evaluation & Iteration

This chapter evaluates the design of the *Preis-Device*'s first prototype based on test results and observations from [Chapter 4. Proof-of-Principal, Section 4.4. Results & Analysis](#). The evaluation is done by means of calculations, see [Section 5.1. Calculations](#) and *finite element method* (FEM) analyses, see [Section 5.2. Finite Element Method](#). In [Section 5.3. Design Iteration](#) the results from the evaluations are implemented into the *Preis-Device*'s second prototype.

### 5.1. Calculations

This section presents calculations to check and validate tests, see [Section 5.1.1. Test Validation Calculations](#). The calculations are also used to check design options in terms of feasibility, see [Section 5.1.2. Pole Validation Calculations](#). Each calculation includes an explicit goal, a section about the assumptions made as well as the calculations and an analysis and interpretation of the results in terms of the tests and design.

#### 5.1.1. Test Validation Calculations

This section explains the calculations performed in order to validate the *blade tests* from [Chapter 4. Proof-of-Concept, Section 4.2.1. Blade Tests](#). The calculations in this section are done to investigate whether the results of the *blade tests* agree with the mechanical theory of materials. The goal of these tests and calculations is also to determine whether the blades can cut adipose tissue sufficiently in order to be able to function without relying on a cauterisation mechanism to cut the surrounding tissue. However, for coagulation purposes a cauterisation mechanism will still be considered.

##### Goal

The goal of these calculations is to interpret the results from the *blade tests*, see [Chapter 4. Proof-of-Principal, Sections 4.2.1. Blade Tests & 4.4. Results & Analysis](#) for more information, by comparing them to the theory of material mechanics. This is done by finding the relation between the forces needed to cut the phantom theoretically and compare the theoretical value to the measured forces obtained from the test.

##### Assumptions

- 1) The force needed to cut the phantom can be expressed in the pressure (or stress) applied to the phantom by the *Preis-Device*'s blade until the phantom's structure fails.
- 2) Because the phantom is the same for all tests, as it is made from one batch and randomly selected to be cut with the 0.04mm- or the 0.05mm-blade, the pressure, and hence the force needed to cut the phantom is the same:

$$P_{0.04} = P_{0.05} \quad (5.1)$$

##### Calculations

The following expression for the *pressure* is used

$$P = \frac{F}{A} \quad (5.2)$$

The calculations are done for the "cutting" mode tests and the "insertion" mode tests separately because:

- 1) the measured forces for "cutting" mode tests and for "insertion" mode tests are different
- 2) determining the area ( $A$ ) is different for "cutting" mode tests than for "insertion" mode tests.
- 3) the behaviour of the measured force curves in *Figures 4.8 & 4.10* are similar as are the measured force curves in *Figures 4.9 & 4.11*. Which indicates that the forces can be compared to each other using a ratio.

Substituting *Equation (5.2)* in *(5.1)* gives the ratios:

$$\frac{F_{0.04}}{F_{0.05}} = \frac{A_{0.04}}{A_{0.05}} \quad (5.3)$$

The area for the "cutting" mode tests is calculated as follows:

$$A_{0.04} = h_{0.04} * L_{effective} = 0.04mm * 51mm = 2.04mm^2 \quad (5.4)$$

$$A_{0.05} = h_{0.05} * L_{effective} = 0.05mm * 51mm = 2.55mm^2 \quad (5.5)$$

, with

- $h_{0.04} = 0.04mm$ , the thickness of the 0.04mm-blade
- $h_{0.05} = 0.05mm$ , the thickness of the 0.05mm-blade
- $L_{effective} = 51mm$ , the length of the blade as designed, see *Chapter 3 Detailed Design, Section 3.1.2. Blade*

It has to be added that during the "cutting" mode blade tests the poles were not inserted into the phantom but only the blade, see the test protocol in *Appendix E Test Protocol for Prototype 1*.

Substituting the values from *Equations (5.4) & (5.5)* into *Equation (5.3)* gives an expected ratio of 0.8, see *Table 5.1*.

Next, the areas for the "insertion" mode tests are evaluated from drawings that are made with the *Preis-Device* in "insertion" mode securely fastened in the *device holder*, but not yet attached to the force sensor. Therefore, the drawing is of the device as it was used during the tests. The drawing is made by tracing the outside of the *Preis-Device* and can be seen in *Figure 5.1*. See *Appendix E Test Protocol for Prototype 1* for more information on how the drawings are made.

The area of the *Preis-Device* orthogonal to the phantom and the device's movement is estimated based on the drawings. The grid on the paper is 5mm x 5mm. Upon close inspection, the areas are determined to be:

$$A_{0.04} = 0.75 * 5mm * 5mm = 0.75 * 25mm^2 = 18.75mm^2 \quad (5.6)$$

$$A_{0.05} = 0.6 * 5mm * 5mm = 0.6 * 25mm^2 = 15mm^2 \quad (5.7)$$

It has to be noted that it is counter intuitive to assign the 0.04mm-blade in "insertion" mode a larger area, however, the author felt that this is the correct value and it is later confirmed that this might have been the case since the average maximum force of the 0.04mm-blade "insertion" mode tests is larger than the average maximum

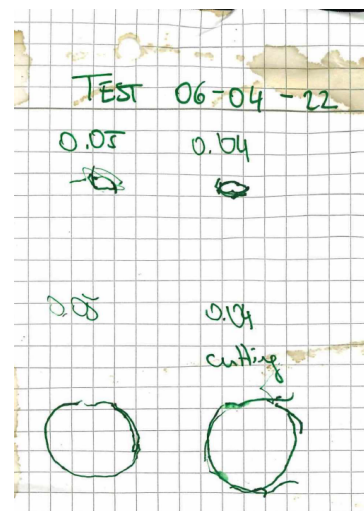


Figure 5.1: This is a scan of the drawings made by tracing the circumference of the blade in "insertion" mode (top half), and "cutting" mode (bottom half). The drawings of the area in "insertion" mode are used to calculate the ratio in *Table 5.1*

force of the 0.05mm-blade "insertion" mode tests. This highlights the fact that these tests are prone to human error.

Further substituting the values from *Equations (5.6) & (5.7)* into *Equation (5.3)* gives an *expected ratio* of 1.25, see *Table 5.1*.

Table 5.1: This table lists the maximum forces evaluated with Matlab and recorded during the respective *blade tests*

	0.04 [mm]	0.05 [mm]	Ratio	expected ratio
cutting - Fmax	7.16 [N]	8.63 [N]	0.83	0.8
insertion - Fmax	2.72 [N]	2.14 [N]	1.27	1.25

After executing these calculations and recording the values in *Table 5.1*, it has to be concluded that the tests, despite some inconsistencies and human error, seem to resemble the theory quite well. The difference between the expected ratio and the measured ratio is most likely caused by friction and resistance forces that are not taken into account in the theoretical approximation of the test. This leads to the author to the conclusion that the tests are representative of the theory and that the device can cut the surrounding tissue without relying on a cauterisation mechanism. These calculations also prove that simplicity does not necessarily mean that the (test-) result is unreliable.

In terms of limitations of these calculations it has to be noted that the author chose to guesstimate the area instead of writing a Matlab script or using another program to determine the exact area because because it would have been to far outside the scope of this thesis. Also, putting that much effort into determining the exact area of a traced footprint of the device is contradictory. A more accurate approach of determining the are is by taking pictures orthogonal to the insertion direction and calculating the exact area using Matlab. This method has to be used to determine the area of the blades in "insertion" mode as well as in "cutting" mode. The question however stands, if following this approach will deliver more accurate results. And whether these results will grant the extra work going into the determination of these values.

### 5.1.2. Pole Validation Calculations

This section investigates whether the poles can be made hollow or thinner by means of calculating the strain the poles will experience and comparing the result to the *shear yield stress* (SYS) of the material (stainless steel 316). Thereby determining whether the poles will fail or not. This is valuable also to corroborate or disprove the author's educated guess of choosing to design the poles of being 2mm in diameter in *Chapter 3. Detailed Design, Section 3.1.1. Poles*.

#### Goal

The goal is to optimise the design of the *Preis-Device's* poles with respect to the following two questions:

- 1) Can the poles be made hollow?
- 2) Can the poles be made thinner?

As well as corroborating that a diameter of 2mm is sufficient for the poles.

#### Assumptions

The *force – per – mm<sup>2</sup>* measured needed to cut the phantom in vertical direction is the same force that exerts torque onto the poles while cutting the phantom in horizontal direction. This assumption is valid due to the phantom being homogeneous.

#### Calculations

First, the maximum shear stress,  $\tau_{max}$  is calculated using  $F = 10N$  which was the maximum force measured in *Test #9* of the 0.05mm-blade, during "cutting" mode tests, see *Appendix D Blade Test RunTables, Figure D.2*. In order to calculate the *maximum shear stress* the following formula is used:

$$\tau_{max} = \frac{T * r}{J} = 6.366Nmm^{-2} = 6.366MPa, \text{ with} \quad (5.8)$$

- $T = F * r = 10Nmm$ , the torque
- $r = 1mm$ , the radius of the pole
- $J = \frac{\pi * (2*r)^4}{32} = 1.57mm^4$ , the polar moment of inertia

When considering that the SYS of stainless steel (316) equals  $0.58 * 290MPa = 168.2MPa$ , these poles should have no problem with the forces applied. Which is also the impression the author got during the execution of the tests.

The next question is: 1) can the poles be made hollow?. To answer this question, *Equation 5.8* is used again, but rearranged to read as follows:

$$d_{inner}^4 = \frac{16 * T * d}{\pi \tau_{max}} = \frac{16 * F * d * d}{\pi \tau_{max}} = 24, with \quad (5.9)$$

- $d = 3mm$ , the outer diameter of the new poles
- $F = 10N$ , the measured force
- $\tau_{max} = 6.366MPa$ , the calculated maximum shear stress

The outer diameter was chosen to be  $3mm$  because this is a realistic diameter, meaning that the device will still fit in the cannula of  $< 10mm$ . Therefore,  $d_{inner} = 2.45mm$ , meaning that the poles can be made hollow with an outer diameter  $d_{outer} = 3mm$ , an inner diameter  $d_{inner} = 2.45mm$ , and a wall thickness of  $t_{pole} = 0.55mm$ . Which means; *YES, the poles can be made hollow*. However, these poles are more difficult to fabricate hollow because of the tapered end where the blade is fastened. The tapered shape is needed in order to fit the cap onto the poles which holds the blade in place. Furthermore, in case of material defects, these will weigh more heavily on hollow poles, making them more likely to fail and thereby increasing the risk for device failure. Device failure can have a negative effect on the patient, and in a worst case scenario can lead to the patient having to undergo surgery to remove a piece of device that broke off in their body.

In terms of 2) can the poles be thinner?, *Equation (5.8)* can be used. When using a radius of  $r_{new} = 0.5mm$ , the calculated  $\tau_{max-new} = 50.93MPa$  which is considerably higher than  $\tau_{max}$  of *Equation (5.8)* which was  $6.366MPa$ . At this point, the blade will probably fail before the poles experience this shear stress. Therefore, the answer to this question is: *NO, the poles should not be made thinner*. Although from a purely material mechanics point of view of the poles they can be made thinner without failing.

In conclusion, the calculations show that the *blade tests* are representative of the theory and the poles are sufficiently well designed with a diameter of  $2mm$ .



## 5.2. Finite Element Method

Doing a FEM analysis gives insight into the stresses the device experiences. FEM analyses also give indications on where the device has to be improved. The analysis is done by implementing the design in COMSOL Multiphysics (COMSOL®) and applying a so-called mesh, see *Figure 5.2*. The mesh divides the structure into small pieces that are each analysed by the program. This gives a more accurate picture of the loads and forces the device experiences. If one were to calculate these stresses by hand, it would take much longer than running an analysis using COMSOL Multiphysics (COMSOL®) or any similar program.

For the FEM analyses in this thesis the program *COMSOL Multiphysics (COMSOL®)* is used with an Academic Class Kit License. This unfortunately means that the 3D CAD models from *Chapter 3. Detailed Design, Section 3.3. Computer Aided Design* cannot be imported. Instead, the device has to be implemented again in this program. In the implementation in COMSOL Multiphysics (COMSOL®), one simplification has been made namely the caps are not implemented in COMSOL Multiphysics (COMSOL®), since the tests of interest are the *first principal stresses* of the blade, see *Section 5.2.1. Blade* and the *first principal stresses* in the various pole configurations (massive 2mm diameter pole, hollow pole, massive 1mm diameter pole), see *Section 5.2.2. Poles*.

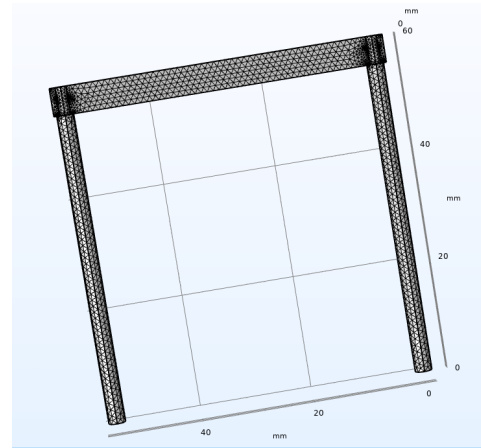


Figure 5.2: This figure shows the *Preis-Device* implemented in COMSOL Multiphysics (COMSOL®)

### 5.2.1. Blade

The blade is implemented according to the parameters defined in *Chapter 3. Detailed Design, Section 3.1.2. Blade*, see *Figure 5.3*. This study concerns itself with the cutting forces around the LN. Therefore, one end is set to be fixed, since the blade is rolled around the pole and is not able to move or exert any cutting forces. The other end of the blade is cutting around the LN and, hence exerting force. The force the simulation uses is the maximum force obtained from the "cutting" mode tests, see *Appendix D Blade Test Run Tables, Figure D.1, Test #7* which is rounded up to whole *Newtons* which then equals 9N.

This force is used to apply a *boundary load* in a *stationary study* which is set to display the *first principal stress* in [MPa]. The result of this study is then represented in a *contour plot* and can be seen in *Figure 5.4*. Where a clear stress hot-spot can be seen in the left corner of the blade's cut-out. A *minimum-maximum* analysis shows the maximum stress to be 6.6MPa, which lies in the ballpark of the calculated value of 6.36MPa, see *Section 5.1. Calculations, Equation (5.8)*. This simulation also shows the exact spot where the 0.04mm-blade broke during the *proof-of-concept* tests and the other was permanently deformed in an up-and-outward-twisted manner, see *Figure 5.5*. The red circles show the two 0.04mm-blades that failed. The 0.04mm-blade in the middle failed during a *proof-of-principal* test, the one on the left bottom during a "cutting" mode test. It can be seen that both blades failed in the spot that is shown to experience the stress-hot-spot in *Figure 5.4*. Therefore, the author believes these sim-

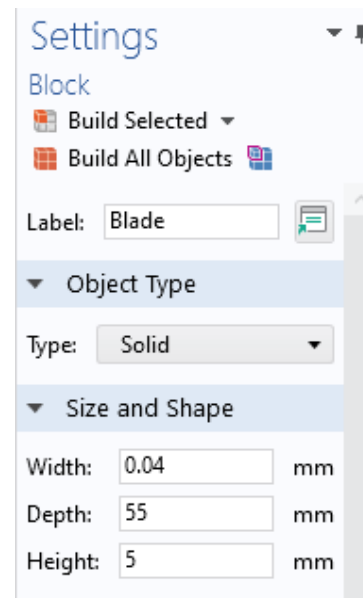


Figure 5.3: This figure shows the geometric settings used to implement the 0.04mm-blade in COMSOL Multiphysics (COMSOL®). This picture was created using COMSOL Multiphysics (COMSOL®)

ulations to be representative and accurate.

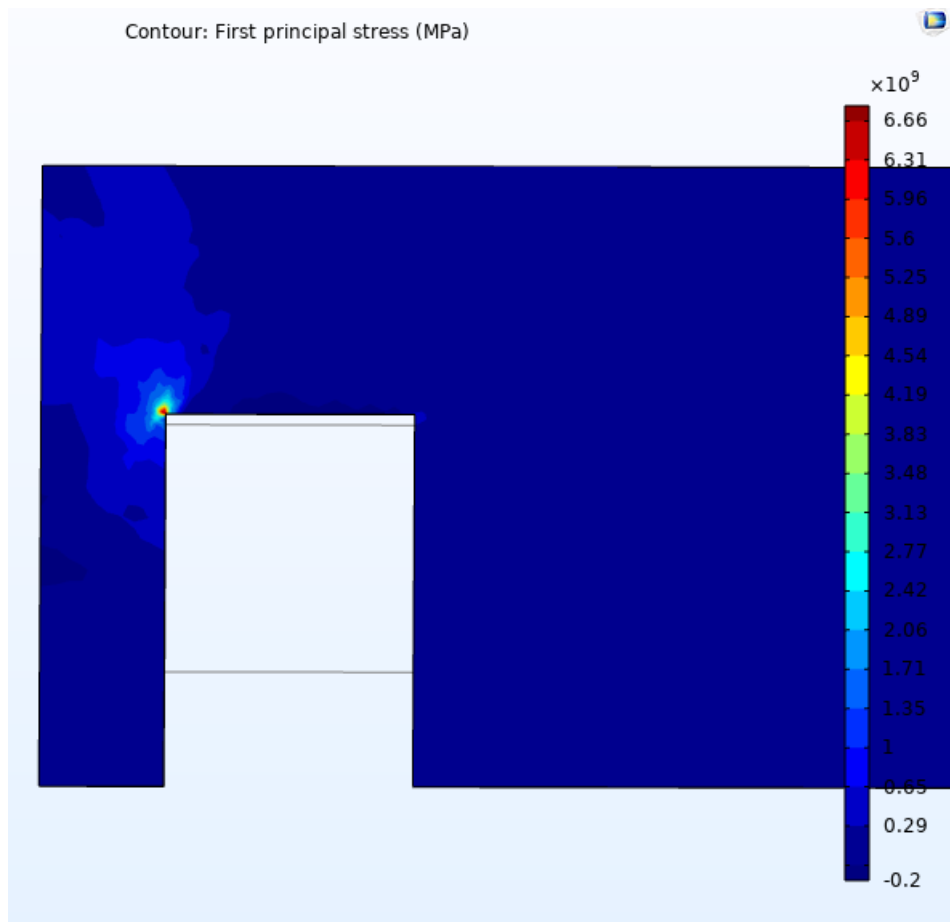


Figure 5.4: This figure shows the study performed on the  $0.04\text{mm}$ -blade. A stress-hot-spot can be seen in the top left corner of the blade's cut out. This explains why the  $0.04\text{mm}$ -blade failed during testing. This test is simulated using a the maximum measured force from the "cutting" mode tests of the  $0.04\text{mm}$ -blade tests performed in [Chapter 4. Proof-of-Principal, Section 4.4. Results & Analysis, Figure D.1, Test #7](#) rounded up to  $9\text{N}$ . This picture was created using COMSOL Multiphysics (COMSOL®)

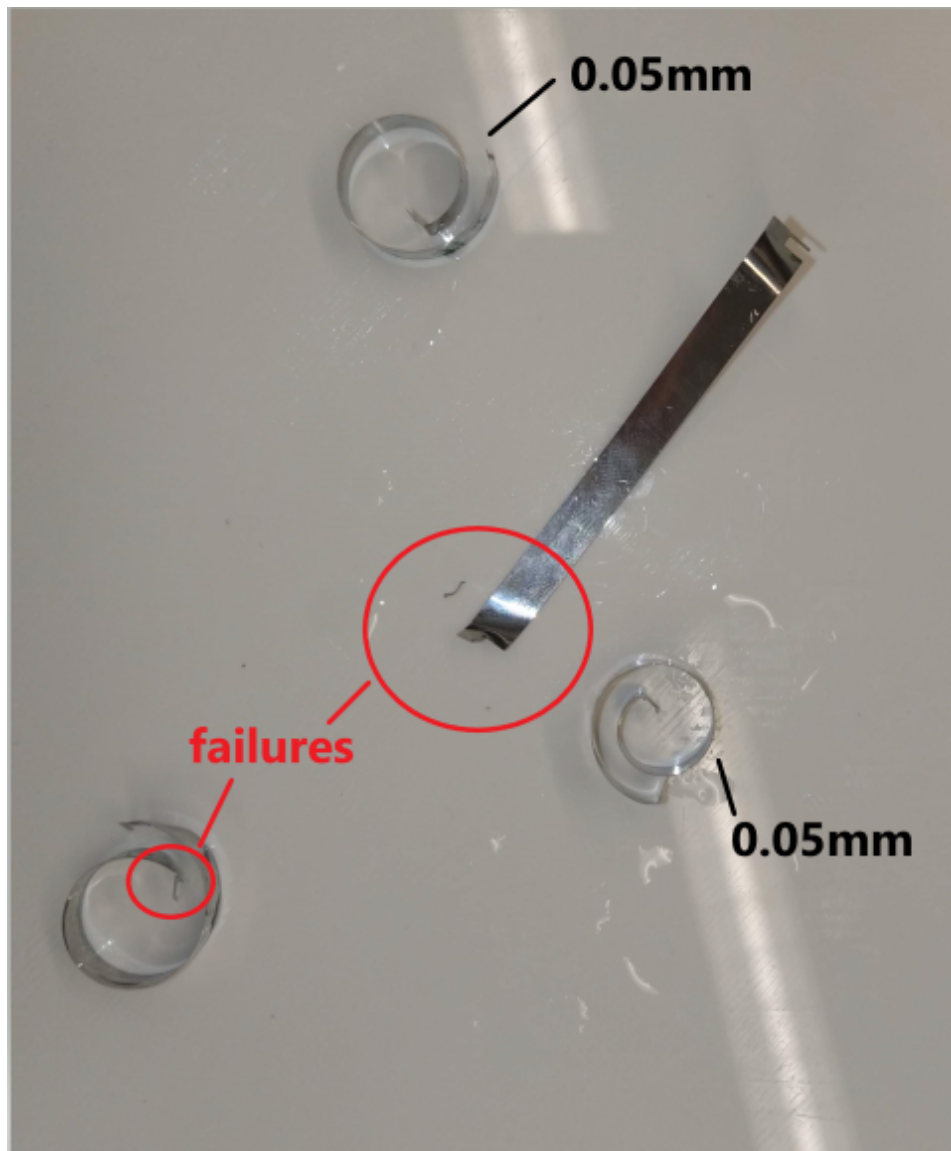


Figure 5.5: This figure shows the *failures* of the  $0.04\text{mm}$ -blade as marked in red. One can see that one end of the  $0.04\text{mm}$ -blade has been twisted outward and permanently been deformed. The extended blade in the middle even experiences the end being torn off. This happened during *proof-of-principal* testing. The  $0.05\text{mm}$ -blades however, did not experience any unintended plastic deformation. This picture was taken by the author

Next, the geometry settings are changed in order to simulate the 0.05mm-blade, see [Figure 5.6](#). Only the blade width is altered, the other geometric parameters remain the same, see [Figures 5.3 & 5.6](#). Also, the force is changed from 9N to 10N, which is the highest force measured during the "cutting" mode tests of the 0.05mm-blade, see [Appendix D Blade Test Run Tables, Figure D.2, test #9](#).

The *fixed constraints* remain the same, as does the location of the *boundary load*. Then the same *stationary study* is run, and the results are shown in a contour plot with the *first principal stresses* in [MPa]. The contour plot of the study can be seen in [Figure 5.7](#), where again a stress-hot-spot is visible in the upper left corner of the blade's cut out. However, the depicted stresses are lower than in the simulation of the 0.04mm-blade, see [Figures 5.4 & 5.7](#).

This simulation again corroborates the findings from the physical tests as well as the calculations in [Chapter 4. Proof-of-Concept, Section 4.4. Results & Analysis](#) and [Chapter 5. Design Evaluation & Iterations, Section 5.1. Calculations, Equation \(5.8\)](#), respectively. During the tests, the 0.05mm-blade exhibited some plastic deformations, however, only as expected by being wound up. No failure or functionality-damaging deformation is experienced, as can be seen in [Figure 5.5](#), all 0.05mm-blades are wound up in a spiral motion and not twisted or broken.

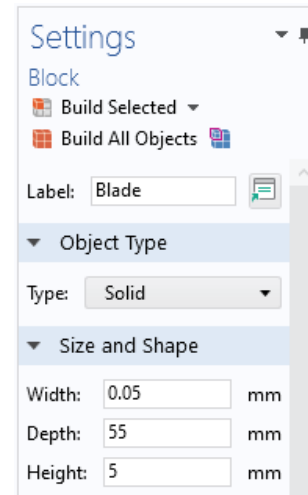


Figure 5.6: This figure shows the geometric settings of the 0.05mm-blade implemented in COMSOL Multiphysics (COMSOL®) for FEM simulations. This figure was created using COMSOL Multiphysics (COMSOL®)

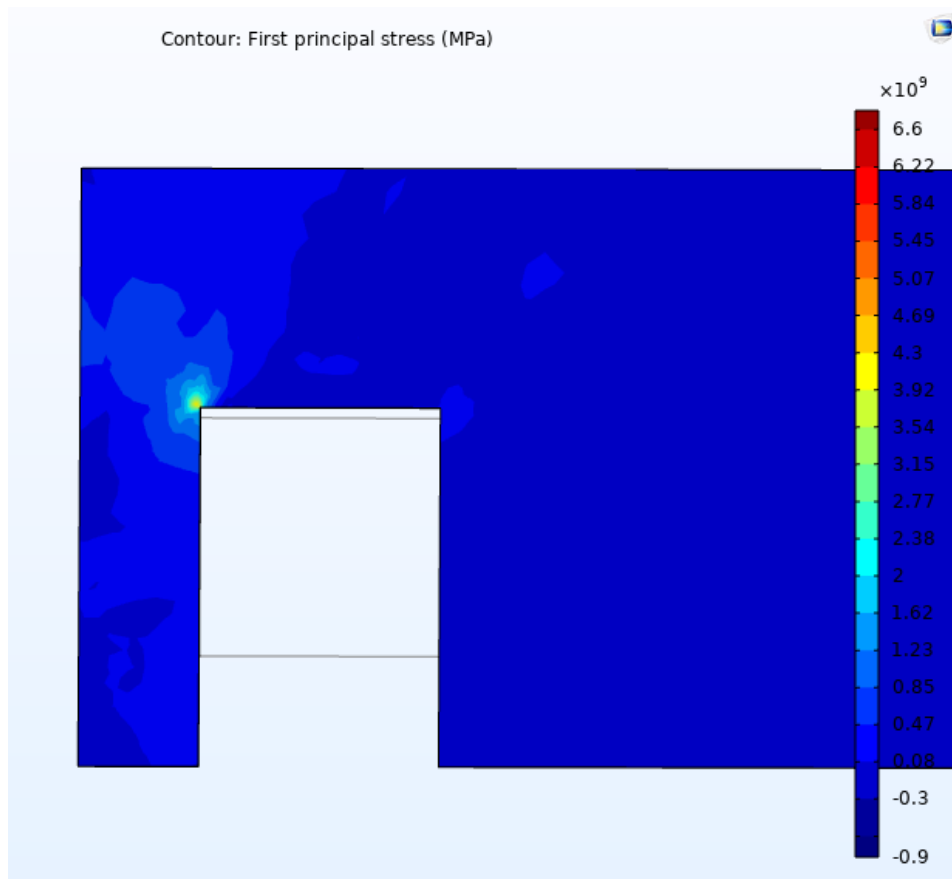


Figure 5.7: This figure shows the study performed on the  $0.05\text{mm}$ -blade. A stress-hot-spot can be seen in the top left corner of the blade's cut out. However, when compared to the stress-hot-spot of the  $0.04\text{mm}$ -blade's cut out in the same spot, see Figure 5.4, the stresses are lower. This explains why the  $0.04\text{mm}$ -blade failed during testing whereas the  $0.05\text{mm}$ -blade only experiences plastic deformations as is to be expected. This test is simulated using the maximum measured force from the "cutting" mode tests of the  $0.05\text{mm}$ -blade tests performed in Appendix D Blade Test Run Tables, Figure D.2, Test #9 rounded up to  $10\text{N}$ . This picture was created using COMSOL Multiphysics (COMSOL®)

### 5.2.2. Poles

Besides the blade, also the poles are studied using COMSOL Multiphysics Class Kit License (COMSOL®). The poles are implemented without the caps and without the tapered tip, see Figures 3.3 & 5.2 for comparison. The first simulation is of a  $2\text{mm}$  in diameter, massive pole, as the one used in the prototype, see Figure 5.8. Figure 5.9 shows the simulations of a hollow,  $3\text{mm}$  in diameter pole with an inner diameter of  $2.45\text{mm}$ , and Figure 5.10 shows the simulation of the  $1\text{mm}$  in diameter, massive pole. The applied boundary loads as well as the fixed constraints are the same for all studies.

These simulations show that a thinner pole indeed experiences significantly higher first principal stresses. As was calculated in Section 5.1. Calculations. For comparison see Figure 5.10. The simulations also shows that it is feasible to use a hollow pole, as was calculated in Section 5.1. Calculations. This can be seen in Figure 5.9. The simulation of the  $2\text{mm}$  in diameter massive pole's first principal stresses are higher than the stresses experienced by the hollow pole and lower than the stresses by the thinner pole. Therefore it can be concluded that the calculations and the interpretations thereof are indeed corroborated by the FEM analysis, and the assumptions made have been accurate. Therefore, the design process can continue as planned.

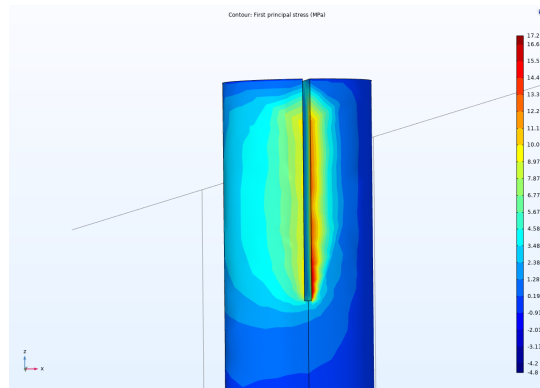


Figure 5.8: This figure shows the simulation of the 2mm in diameter, massive pole. This picture was created using COMSOL Multiphysics (COMSOL®)

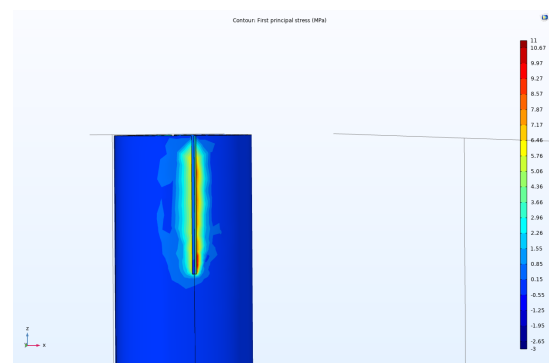


Figure 5.9: This figure shows the simulations of the 3mm in diameter, hollow pole with an inner diameter of 2.45mm. This picture was created using COMSOL Multiphysics (COMSOL®)

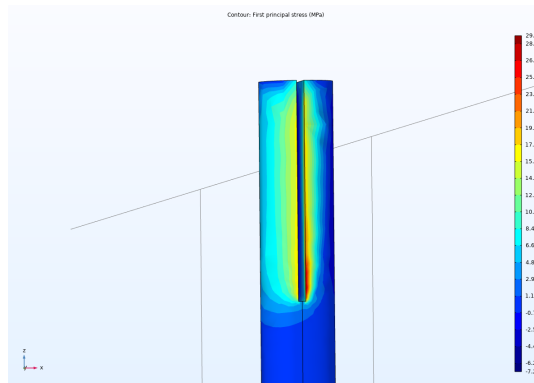


Figure 5.10: This figure shows the simulation of the 1mm in diameter, massive pole. This picture was created using COMSOL Multiphysics (COMSOL®)

### 5.3. Design Iteration

This section presents the design iterations of the *Preis-Device*'s prototype 2. The iterations are based on the observations from the *proof-of-concept* tests, see [Section 4. Proof-of-Concept](#), the calculations, see [Section 5.1. Calculations](#), and simulations, see [Sections 5.2. Finite Element Method](#).

The main design iteration made is the discontinuation of the 0.04mm-blade. Because the 0.04mm-blade failed during the *proof-of-concept* tests, see [Chapter 4. Proof-of-Concept, Section 4.4. Results & Analysis](#), which is also corroborated by the *FEM* analyses in [Section 5.2. Finite Element Method, Figures 5.4 & 5.7](#).

Another important design iteration is the protruding blade through the poles, see [Figure 5.11](#). This is done to create a blade that can cut the surrounding tissue more easily by means of creating an edge which reduces the area over which the force is applied. The blade protrudes from both poles, in order to be able to design and test the actuation mechanism freely.

At a later stage it will suffice for the blade to protrude only from the pole that cuts the tissue in a spiralling motion around the SLN. It has previously been discussed with Mario van der Wel that the blade can additionally be sharpened. Which further facilitates the cutting process of the *Preis-Device*. There is no clear indication from the *proof-of-concept* tests that the blade has to be sharpened, therefore, if implemented, this iteration is for optimisation purposes of the *Preis-Device* only.

The poles of prototype 2 have different lengths and exhibit a hexagonal shape towards the end, as shown in [Figure 5.11](#). These changes are made to facilitate the implementation and testing of an actuation mechanism. The idea for the actuation mechanism is to use gears that can slide onto the poles and actuate the poles without slip due to their hexagonal shape. The reason for the poles to have different lengths is to create the possibility of a turning knob for actuating the mechanism, which can be made bigger without hindering the movement of the other pole due to the other pole being shorter.



Figure 5.11: This figure shows the *Preis-Device 2* with all the design iterations. It can be seen that the blade protrudes through both poles. The poles are changed as well, one is longer, and the other is shorter. This is to create space for the actuation mechanism being used manually and not hinder the movement of the other pole. Another iteration concerning the poles is the hexagonal shape towards the end of the poles. This is done in order to fasten the actuation mechanism to the poles in an easy manner. The last iteration that can be seen is the tip of the caps. Instead of the caps being tapered, a blade-like ridge has been incorporated in order to facilitate cutting and insertion of the device. This figure was created using Onshape (Onshape Inc., Massachusetts, USA)

There is no need to change the diameter of the poles, as shown in [Section 5.1. Calculations](#), a thinner pole experiencing the same amount of force will exert more force onto the blade, which will break the blade. Also, the pole is to stay massive, because it is the author's belief that what is gained in terms of reduced stresses within the pole, see [Figure 5.9](#), does not outweigh the more intricate fabrication of a  $0.55\text{mm}$ -walled pole with a tapered tip. And hence, making the poles hollow will not enhance the *Preis-Device's* design. The wall thickness was determined in [Section 5.1. Calculations](#) to be  $0.55\text{mm}$  which is possible to produce. Another reason to not opt for hollow poles is that in case of device failure the patient's safety is at risk because of possible debris from the failed pole. And patient safety is of the utmost importance when designing a medical device, even at this stage of the design process.

Furthermore, the cap design has changed from a tapered tip, to a blade-like ridge on top of the tapered tip, see [Figures 5.12 & 5.13](#). This is done in order to facilitate cutting the surrounding tissue as well as inserting the device. The blade-like ridge reduces the surface area over which the force is exerted by the device onto the tissue, thereby enhancing its ability to cut the LN's surrounding tissue. The changes of the blade and the caps are shown in [Figure 5.14](#). Comparing [Figure 5.14](#) to [Figure 5.15](#) depicts these changes clearly.

This concludes [Chapter 5. Design Evaluation & Iteration](#) and the gathering and evaluation of data pertaining to the design. [Chapter 6. Discussion & Conclusion](#) will show the limitations of this thesis, give recommendations for future research and present a comprehensive conclusion.

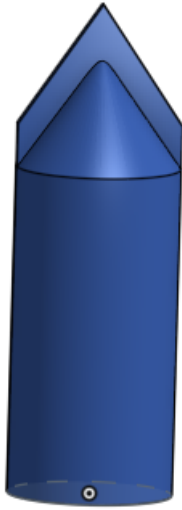


Figure 5.12: This figure depicts the blade-like ridge iteration of the cap. This design change was implemented in order to facilitate cutting the surrounding tissue and reduce the insertion forces. This figure is turned 90° with respect to the depiction of the cap in *Figure 5.13*. This figure was created using Onshape (Onshape Inc., Massachusetts, USA)

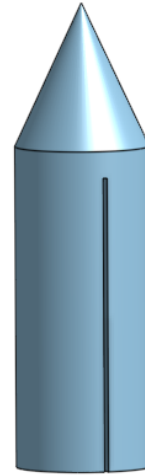


Figure 5.13: This figure shows the cap design of prototype 1 with a tapered top of the cap. The depiction of the cap is turned 90° with respect to the depiction of the new cap design depicted in *Figure 5.12*. This figure was created using Onshape (Onshape Inc., Massachusetts, USA)

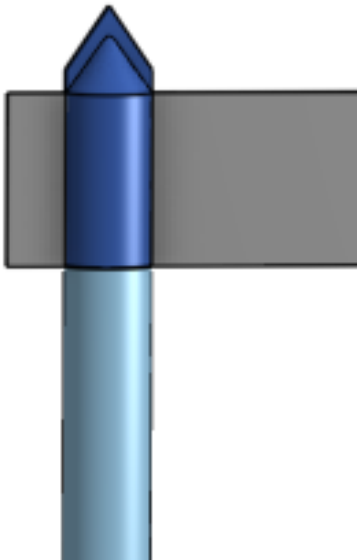


Figure 5.14: This figure depicts the design iteration of the blade and the cap. This figure was created using Onshape (Onshape Inc., Massachusetts, USA)

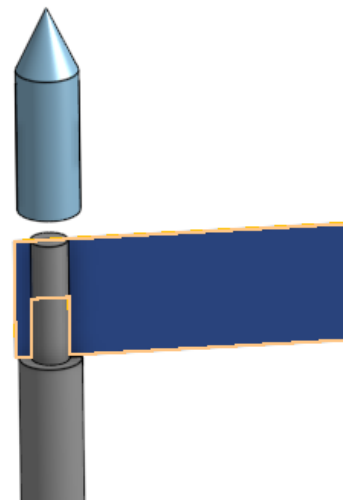


Figure 5.15: This figure depicts the assembly of blade, pole and cap of prototype 1. This figure was created using Onshape (Onshape Inc., Massachusetts, USA)



# 6

## Discussion & Conclusion

This chapter discusses what has already been achieved with this thesis and what still needs to be done in the future. *Section 6.1. Limitations* discusses the limitations and shortcomings of this thesis and possible solutions thereof. And *Section 6.2. Future Research* highlights some points of interest with regard to the *Preis-Device* that should be investigated further in the future. *Section 6.3. Conclusion* summarises the thesis and its findings in broad strokes. Finally, this chapter closes with *Section 6.4. Acknowledgements* which names all the people without whom this project would not have been possible.

### 6.1. Limitations

This thesis has its limitations. Although the tests are representative, only 10 tests were executed per mode (*"cutting"* or *"insertion"*) per blade, leading to 40 tests overall. Executing more tests will be beneficial when going further with the design of the *Preis-Device*, as they will give more information on the working of the device as well as its safety.

The biggest limitation of all is that the device has only been tested on phantoms. The phantoms were produced according to a study that investigated the fabrication of phantoms resembling breast tissue. Although the phantoms seemed to resemble adipose tissue well, a phantom is still a phantom and not the actual tissue. Therefore, it is suggested to test the next prototype on actual tissue if possible.

Another limitation is the size of the phantoms. Cupcake forms that measured *7cm* in diameter were used to make the phantoms. During the tests the author had to hold the phantoms as well as actuate the device. Bigger phantoms or even a phantom holder will make the tests more reproducible as well as facilitate the execution of the *proof-of-principal* tests. If a phantom holder is designed, it is the authors suggestion to make it transparent for evaluation and filming purposes. This can be done at the workplace of the TU Delft. Also, using the cupcake forms led to the phantoms having ridges on the sides. This distorted the view when filming. A suggesting is to use the disposable Erasmus MC coffee cups as moulds to fabricate phantoms without ridges and hence a clear view of the ALN during testing.

Another limitation of this thesis is that the consequences of reducing the blade height which is currently *5mm*, was not investigated.

### 6.2. Future Research

There is still a lot of research that needs to be done, for instance, the knowledge on LNs and their material, mechanical and electrical properties is very limited. Therefore, more research into these properties of LNs will aid the design process of the *Preis-Device* as well as making more representative phantoms for future testing. This will speed up the design of the *Preis-Device* and identify problem areas early. Which in turn will save money and time.

Research should also be done on the implementation of a cauterisation mechanism which will aid cutting the surrounding tissue, as well as seal cut blood vessels and lymph ducts. This mechanism also

needs to be evaluated with respect to damage caused to the LN to make sure the cauterisation mechanism does not impair nodal staging. This cauterisation mechanism will also be important because it will prevent the patient from bleeding, as well as post-operative formation of blood-pools in the biopsy cavity and lymphoedema.

A third important field for future research is the navigation towards the SLN and the identification of the SLN. At the moment radioactive colloid  $^{99m}\text{Tc}$  and patent blue dye are used to identify the SLNs. Not having to use the radioactive colloid will eradicate the need for a nuclear scientist. If being able to substitute patent blue dye for another medium, for instance indocyanine green (ICG), would eradicate the risk of the patient being tattooed by the patent blue dye. Therefore, this is also a very important field for future research.

A fourth area worth looking into in the near future is the retrieval of the SLNs. Although, the *proof-of-principal* tests, see [Section 4.2.2. Proof-of-Principal](#), have shown that the ALNs are more often than not retrieved with this mechanism, it is worth looking into the retrieval of the SLNs. As already discussed, a possible solution is the application of a *Stone Excision Basket*, see [Section 3.4. The Preis-Device](#). Another possible application for retrieving the loose SLNs is the *Pull-and-Harvest* method designed by the previous student Max Joosen, see [Appendix A, Section A.3 Previous Thesis](#).

Lastly, another important area to be considered on the way of bringn the *Preis-Device* to the patients will be the design input of physicians and patients. This will have influence on the design of the actuation mechanism as well as the handle of the design. When talking to the physicians on how they will want to perform the MISLNB, with the patient sitting or lying etc., important design characteristics are collected that need to be taken into account when further designing the device.

In order to create more traction for this project to build off of promising first results the decision was made to apply for the ACE IT-TI grant which supports the collaboration between Erasmus MC and TU Delft. The proposal can be found in [Appendix K Grant Proposal](#). The hope is to get the grant of 2.5k awarded which will go towards further testing the *Preis-Device* and implement the cauterisation mechanism. With the results from these tests and the further research, other grants can be applied for. And the *Preis-Device* will soon benefit the patients.

### 6.3. Conclusion

This thesis shows that the SLNB is an important prognostic tool for early-stage melanoma patients. The results of the SLNB lead to personalised treatment for the patients. However, as this thesis has also shown, due to the relatively high risk of experiencing morbidities when undergoing this procedure, as well as a difficulty scheduling surgeries that have to take place in an OR during pandemics like the COVID pandemic, and the chronically understaffed and overworked healthcare professionals, it is crucial to transform the SLNB surgery into the MISLNB procedure.

This is exactly what this thesis tackles by developing a medical device able to excise LNs *en bloc* requiring only a small incision and local anaesthesia. The benefits of which are the decrease in workload on hospital staff because these patients do not need a bed or a complete OR and OR team. The costs of the procedure will reduce, making this procedure more affordable. But most importantly, the risk of experiencing morbidities will decrease and more patients will be able to undergo this procedure and get the right treatment.

The solution this thesis proposes to achieve this transformation is the *Preis-Device*. This thesis shows how the excision mechanism of the *Preis-Device* is chosen and designed, following a *literature study* that revealed that no large-volume excision device exists capable of excising LNs *en bloc*. Various promising concepts were introduced and a *decision matrix* was used to determine the most promising concept according to a previously assembled set of requirements. The design was worked out further in more detail to realise the first prototype. Which was then tested in various *proof-of-concept* tests. The tests were validated towards how well they represent the theory using calculations and FEM analyses. The test and validation results were interpreted in order to improve upon the design and answer the hypothesis and questions. Especially, the *proof-of-principal* test was important, because it shows that the mechanism works. The FEM analyses corroborated the finding that the 0.04mm-blade fails during normal device use. Which was a valuable insight and the decision was made to discontinue the 0.04mm-blade. Furthermore, the *blade tests* showed that the device can cut phantoms resembling

the adipose tissue. And that the insertion cannal is  $< 5mm$  which is fantastic when trying to perform a minimally invasive procedure. And is well within the requirement set for the device. Therefore, the hypothesis of whether the *Preis-Device* is suitable for a MISLNB medical device was proven true and the design was improved according to the validation results as well as observations made by the author during the tests.

Therefore, it can be concluded that the detachment mechanism designed, evaluated and verified in this thesis is a promising mechanism for a MISLNB medical device, the *Preis-Device*. This thesis lays the foundation in terms of documentation as well as design to be built on when further developing the *Preis-Device*. The author hopes that soon, the *Preis-Device* will be further developed and start helping the patients and medical professionals in their fight against melanoma.

## 6.4. Acknowledgements

First of all, I want to thank my wonderful team of supervisors Dr. ir. van den Dobbelen and Dr. Mulder. They gave me all the freedom to go wild with my ideas and were ready to help whenever I hit a snag. I want to specially thank Dr. Ev for being a better supervisor than I could have dreamed of. Always ready to answer questions about the procedure and reading countless pages of my reports and papers, always giving formidable feedback.

Apropos feedback, I want to thank Teun Schurink for his! Whenever I thought about taking a shortcut, he was there to suggest I take another look at things. He caught me every time! And I thank him for it, because these results would not have been possible without him, or the late nights in de dissecting room with him, Yvonne Steinvooort and Sjoerd van de Weerd. Who helped locating LNs and preparing tissue samples for the tests. Yvonne was also the one who came up with the name for the device, and what a name it is!

However, I did not only meet the lovely people from the dissecting room, but also the Micro-Lab Ladies Manja Muijtjens and Esther Fijneman, who were so kind as to let me put the linear stage and my big box with cupcake making utensils in their lab.

Although I felt fully immersed in the Erasmus MC culture, I could not have gotten this far with the *Preis-Device* without Jan van Frankenhuyzen, Mario van der Wel and the entire IWS team of the TU Delft. Their combined experience and knowledge about mechanisms, research test set-ups and fabrication of small devices, as well as their readiness to hear me out and help, was a great asset to have and I am grateful to have had their input.

Last but not least I want to thank all the PhD candidate of Na21! You have made my time at the Erasmus MC unforgettable!

A list of all the people involved and their affiliation:

- Dr. Dirk Grünhagen (Erasmus MC)
- Prof. dr. Gert-Jan Kleinrensink (Erasmus MC)
- Yvonne Steinvooort (Erasmus MC)
- Cécile de Monyé (Erasmus MC)
- Teun Schurink (Erasmus MC)
- Sjoerd van de Weerd (Erasmus MC)
- Manja Muijtjens (Erasmus MC)
- Esther Fijneman (Erasmus MC)
- Giesela Ambagtsheer (Erasmus MC)
- Kelly van der Geest (Erasmus MC)
- Jan van Frankenhuyzen (TU Delft)
- Mario van der Wel (TU Delft)

- Jos Driel (TU Delft)
- Damian de Nijs (TU Delft)
- Ellen de Vries (TU Delft)

# Bibliography

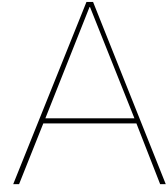
- [1] Steven D Allen, Ashish Nerurkar, and Guidabaldo U Querci Della Rovere. “The breast lesion excision system (BLES): a novel technique in the diagnostic and therapeutic management of small indeterminate breast lesions?” In: *European radiology* 21.5 (2011), pp. 919–924.
- [2] Paolo A Ascierto et al. “Adjuvant nivolumab versus ipilimumab in resected stage IIIB–C and stage IV melanoma (CheckMate 238): 4-year results from a multicentre, double-blind, randomised, controlled, phase 3 trial”. In: *The Lancet Oncology* 21.11 (2020), pp. 1465–1477.
- [3] Gunilla C Bentel et al. “Variability of the depth of supraclavicular and axillary lymph nodes in patients with breast cancer: is a posterior axillary boost field necessary?” In: *International Journal of Radiation Oncology\* Biology\* Physics* 47.3 (2000), pp. 755–758.
- [4] AR Bodenham and SJ Howell. *General anaesthesia vs local anaesthesia: an ongoing story*. 2009.
- [5] Genevieve M Boland and Jeffrey E Gershenwald. “Principles of melanoma staging”. In: *Melanoma* (2016), pp. 131–148.
- [6] Silvia Cabrera et al. “Technetium-99m-indocyanine green versus technetium-99m-methylene blue for sentinel lymph node biopsy in early-stage endometrial cancer”. In: *International Journal of Gynecologic Cancer* 30.3 (2020).
- [7] Jung Min Chang et al. “Axillary nodal evaluation in breast cancer: state of the art”. In: *Radiology* 295.3 (2020), pp. 500–515.
- [8] Christophe Chautems et al. “A variable stiffness catheter controlled with an external magnetic field”. In: *2017 IEEE/RSJ International Conference on Intelligent Robots and Systems (IROS)*. IEEE. 2017, pp. 181–186.
- [9] ChemTalk. *Percent by Weight Calculation*. <https://chemistrytalk.org/percent-by-weight-calculation/>.
- [10] Martin G Cook et al. “An updated European Organisation for Research and Treatment of Cancer (EORTC) protocol for pathological evaluation of sentinel lymph nodes for melanoma”. In: *European Journal of Cancer* 114 (2019), pp. 1–7.
- [11] Eric A Deckers et al. “Increase of sentinel lymph node melanoma staging in The Netherlands; still room and need for further improvement”. In: *Melanoma management* 7.1 (2020), MMT38.
- [12] Alberto Falk Delgado, Sayid Zommodi, and Anna Falk Delgado. “Sentinel lymph node biopsy and complete lymph node dissection for melanoma”. In: *Current oncology reports* 21.6 (2019), pp. 1–7.
- [13] Nasuh Utku Dogan et al. “The basics of sentinel lymph node biopsy: anatomical and pathophysiological considerations and clinical aspects”. In: *Journal of oncology* 2019 (2019).
- [14] Reinhard Dummer et al. “Five-year analysis of adjuvant dabrafenib plus trametinib in stage III melanoma”. In: *New England Journal of Medicine* 383.12 (2020), pp. 1139–1148.
- [15] Alexander MM Eggermont et al. “Adjuvant pembrolizumab versus placebo in resected stage III melanoma (EORTC 1325-MG/KEYNOTE-054): distant metastasis-free survival results from a double-blind, randomised, controlled, phase 3 trial”. In: *The Lancet Oncology* 22.5 (2021), pp. 643–654.
- [16] EU. *Regulation (EU) 2017/745 of the European Parliament and of the Council of 5 April 2017 on medical devices, amending Directive 2001/83/EC, Regulation (EC) No 178/2002 and Regulation (EC) No 1223/2009 and repealing Council Directives 90/385/EEC and 93/42/EEC (Text with EEA relevance) Text with EEA relevance*. <https://eur-lex.europa.eu/legal-content/EN/TXT/?uri=CELEX:02017R0745-20200424>. 2017.

- [17] Natalie V. Fawiz et al. *EXPANDABLE RING PERCUTANEOUS TISSUE REMOVAL DEVICE*. <https://patentimages.storage.googleapis.com/aa/24/f9/f21625df78b3a7/US6471709.pdf>. US 6,471,709 B1, Oct. 2002.
- [18] Angela Filoni and Mauro Alaibac. “Reflectance Confocal Microscopy in Evaluating Skin Cancer: A Clinicians’s Perspective”. In: *Frontiers in Oncology* (2019), p. 1457.
- [19] David P Frishberg et al. “Protocol for the examination of specimens from patients with melanoma of the skin”. In: *Archives of pathology & laboratory medicine* 133.10 (2009), pp. 1560–1567.
- [20] Michael Frumovitz and Alessandro Buda. “Encouraging worldwide adoption of sentinel lymph node biopsies for gynecologic malignancies”. In: *International Journal of Gynecological Cancer* 30.3 (2020), pp. 281–282.
- [21] Skandadas Ganeshalingam and Dow-Mu Koh. “Nodal staging”. In: *Cancer Imaging* 9.1 (2009), p. 104.
- [22] Victor Geanta et al. “Stainless steels with biocompatible properties for medical devices”. In: *Key Engineering Materials*. Vol. 583. Trans Tech Publ. 2014, pp. 9–15.
- [23] M Gherghe, C Bordea, and A Blidaru. “Sentinel lymph node biopsy (SLNB) vs. axillary lymph node dissection (ALND) in the current surgical treatment of early stage breast cancer”. In: *Journal of medicine and life* 8.2 (2015), p. 176.
- [24] Filip Jelínek, Gerwin Smit, and Paul Breedveld. “Bioinspired spring-loaded biopsy harvester—experimental prototype design and feasibility tests”. In: *Journal of Medical Devices* 8.1 (2014).
- [25] Yu-Chen Jheng and Chi-Lun Lin. “Fabrication and testing of breast tissue-mimicking phantom for needle biopsy cutting: a pilot study”. In: *Frontiers in Biomedical Devices*. Vol. 40672. American Society of Mechanical Engineers. 2017, V001T08A022.
- [26] Max Joosen. “Minimally Invasive Sentinel Lymph Node Biopsy”. Masterthesis. 2021.
- [27] Hakki Muammer Karakas and Gulsah Yildirim. “Minimally Invasive Excision of Breast Masses under Ultrasound Guidance: A Single Center’s Five-Year Experience on the Breast Lesion Excision System”. In: *The Breast Journal* 2022 (2022).
- [28] Emily Z Keung and Jeffrey E Gershenwald. “The eighth edition American Joint Committee on Cancer (AJCC) melanoma staging system: implications for melanoma treatment and care”. In: *Expert review of anticancer therapy* 18.8 (2018), pp. 775–784.
- [29] Sujeet Vinayak Khiste, V Ranganath, and Ashish Sham Nichani. “Evaluation of tensile strength of surgical synthetic absorbable suture materials: an in vitro study”. In: *Journal of periodontal & implant science* 43.3 (2013), pp. 130–135.
- [30] Theodore Kim, Armando E Giuliano, and Gary H Lyman. “Lymphatic mapping and sentinel lymph node biopsy in early-stage breast carcinoma: a metaanalysis”. In: *Cancer* 106.1 (2006), pp. 4–16.
- [31] David Lebovitz. *How to Use Gelatin*. <https://www.davidlebovitz.com/how-to-use-gelatin/>. (Accessed on 11/28/2021). Apr. 2009.
- [32] Kevin M Lin et al. “Intradermal radioisotope is superior to peritumoral blue dye or radioisotope in identifying breast cancer sentinel nodes”. In: *Journal of the American College of Surgeons* 199.4 (2004), pp. 561–566.
- [33] GI Lobov and MN Pan’kova. “Mechanical properties of lymph node capsule”. In: *Bulletin of experimental biology and medicine* 151.1 (2011), pp. 5–8.
- [34] GI Lobov et al. “Characteristic of the active and passive mechanical properties of the lymph node capsule”. In: *Doklady Biological Sciences*. Vol. 434. 1. Springer Nature BV. 2010, p. 310.
- [35] Georgina V Long et al. “Adjuvant dabrafenib plus trametinib in stage III BRAF-mutated melanoma”. In: *New England Journal of Medicine* 377.19 (2017), pp. 1813–1823.
- [36] *LYMPH NODE*. [https://smart.servier.com/smart\\_image/lymph-node-2/](https://smart.servier.com/smart_image/lymph-node-2/). (Accessed on 11/04/2021).
- [37] Julia Martins. “7 quick and easy steps to creating a decision matrix, with examples”. In: *asana* (2021).

- [38] Anne R McCall, Mary C Olson, and Ronald K Potkul. "The variation of inguinal lymph node depth in adult women and its importance in planning elective irradiation for vulvar cancer". In: *Cancer* 75.9 (1995), pp. 2286–2288.
- [39] Kelly M McMasters et al. "Sentinel lymph node biopsy for melanoma: controversy despite widespread agreement". In: *Journal of Clinical Oncology* 19.11 (2001), pp. 2851–2855.
- [40] JiuHong Med. *Disposable Foreign Body Removal Diamond Shape Basket*. <https://jiuhongmed.en.made-in-china.com/productimage/RXjQThcuhNkG-2f1j00eFrtVpqrJokU/China-Disposable-Foreign-Body-Removal-Diamond-Shape-Basket.html>.
- [41] Kagami Miyaji et al. "The stiffness of lymph nodes containing lung carcinoma metastases: a new diagnostic parameter measured by a tactile sensor". In: *Cancer: Interdisciplinary International Journal of the American Cancer Society* 80.10 (1997), pp. 1920–1925.
- [42] Valeria M Moncayo, John N Aarsvold, and Naomi P Alazraki. "Lymphoscintigraphy and sentinel nodes". In: *Journal of Nuclear Medicine* 56.6 (2015), pp. 901–907.
- [43] Toshio Ohhashi. "Lymphodynamic properties governing sentinel lymph nodes". In: *Annals of Surgical Oncology* 11.3 (2004), 275S–278S.
- [44] D Olmedo et al. "Valor de la ecografía ganglionar previa a la biopsia del ganglio centinela en 384 pacientes con melanoma: análisis de coste-efectividad." In: *Actas Dermo-Sifiliográficas (English Edition)* 108.10 (2017), pp. 931–938.
- [45] Charlotte MC Oude Ophuis et al. "Effects of time interval between primary melanoma excision and sentinel node biopsy on positivity rate and survival". In: *European Journal of Cancer* 67 (2016), pp. 164–173.
- [46] Charlotte MC Oude Ophuis et al. "Gamma probe and ultrasound guided fine needle aspiration cytology of the sentinel node (GULF) trial-overview of the literature, pilot and study protocol". In: *BMC cancer* 17.1 (2017), pp. 1–9.
- [47] Sabrina N Pavri et al. "Malignant melanoma: beyond the basics". In: *Plastic and reconstructive surgery* 138.2 (2016), 330e–340e.
- [48] Fausto Petrelli, Veronica Lonati, and Sandro Barni. "Axillary dissection compared to sentinel node biopsy for the treatment of pathologically node-negative breast cancer: a meta-analysis of four randomized trials with long-term follow up". In: *Oncology reviews* 6.2 (2012).
- [49] Augustinus PT van der Ploeg et al. "The prognostic significance of sentinel node tumour burden in melanoma patients: an international, multicenter study of 1539 sentinel node-positive melanoma patients". In: *European journal of cancer* 50.1 (2014), pp. 111–120.
- [50] Marco Rastrelli et al. "Melanoma: epidemiology, risk factors, pathogenesis, diagnosis and classification". In: *In vivo* 28.6 (2014), pp. 1005–1011.
- [51] Piotr Rutkowski. "Neoadjuvant and Adjuvant Therapies of Melanoma". In: *New Therapies in Advanced Cutaneous Malignancies*. Springer, 2021, pp. 401–415.
- [52] WBG Sanderink. "Detection and minimally invasive treatment of small breast cancers". PhD thesis. [SI: sn], 2021.
- [53] WBG Sanderink et al. "Minimally invasive breast cancer excision using the breast lesion excision system under ultrasound guidance". In: *Breast Cancer Research and Treatment* 184.1 (2020), pp. 37–43.
- [54] Matteo Savazzi et al. "Development of an anthropomorphic phantom of the axillary region for microwave imaging assessment". In: *Sensors* 20.17 (2020), p. 4968.
- [55] *Sentinel node biopsy - Mayo Clinic*. <https://www.mayoclinic.org/tests-procedures/sentinel-node-biopsy/about/pac-20385264>. (Accessed on 11/04/2021). 2018.
- [56] D. Laksen Sirimanne, D. Fawiz Natalie V., and Sutton. *Device and method for safe location and marking of a biopsy cavity*. [https://patentscope.wipo.int/search/en/detail.jsf?docId=US43358722&\\_cid=P21-KY04HS-00209-1](https://patentscope.wipo.int/search/en/detail.jsf?docId=US43358722&_cid=P21-KY04HS-00209-1). US 20100234726, May 2010.
- [57] Carpenter Technology. *STAINLESS STEEL ALLOYS TO COMPLY WITH EU MDR 2017/745 UPDATES*. <https://www.carpentertechnology.com/blog/seu-mdr-2017/745>. 2021.

- [58] BITE Group TuDelft. *BIOPSY HARVESTER – HIGH-SPEED TISSUE CUTTING*. <https://www.bitegroup.nl/interventional-devices/biopsy-harvester/biopsy-harvester/>. Jan. 2013.
- [59] Daniëlle Verver et al. “Gamma probe and ultrasound-guided fine needle aspiration cytology of the sentinel node (GULF) trial”. In: *European journal of nuclear medicine and molecular imaging* 45.11 (2018), pp. 1926–1933.
- [60] Lyn M Wancket. “Regional draining lymph nodes: considerations for medical device studies”. In: *Toxicologic Pathology* 47.3 (2019), pp. 339–343.
- [61] Teresa Winstow. *Sentinel Lymph Node Biopsy - National Cancer Institute*. <https://www.cancer.gov/about-cancer/diagnosis-staging/staging/sentinel-node-biopsy-fact-sheet>. (Accessed on 12/16/2021). June 2019.
- [62] Sandra L Wong et al. “Sentinel lymph node biopsy and management of regional lymph nodes in melanoma: American Society of Clinical Oncology and Society of Surgical Oncology Clinical Practice Guideline Update”. In: *Annals of surgical oncology* 25.2 (2018), pp. 356–377.
- [63] Queeny Wing-Han Yuen et al. “In-vitro strain and modulus measurements in porcine cervical lymph nodes”. In: *The open biomedical engineering journal* 5 (2011), p. 39.





## Familiarisation

This chapter concerns the familiarisation with the topics of lymph nodes in *section A.1*, melanoma and the treatment thereof in *section A.2*, as well as the previous student's thesis in *section A.3*. In order to be able to evaluate and design a medical device, its application and purpose need to be understood. Some important questions that need answering are: *What is the device going to be designed for? Is there a need for this device? Does a device already exist that can do what is asked?* In this case, it was also crucial to get familiar with the work done towards answering these questions by previous student Max Joosen, see *section A.3*.

### A.1. What is a lymph node?

LNs are part of the lymphatic system which is part of the body's immune system. They filter extracellular fluid and lymph to maintain the tissue-fluid balance and detect tissue injury [60]. The lymphatic system is a vascular system that runs throughout the whole body connecting different organs (e.g., liver, kidneys, bone marrow, thymus) and transporting fluid and proteins [43]. A schematic drawing of the lymphatic system can be seen in *Figure A.1*.

Lymph flows through the lymphatic vessels due to rhythmic contractions of lymphatic vessels, most likely caused by the contraction of lymphatic smooth muscle cells, the exact working is however not yet known [34, 43].

LNs are not round but bean shaped (oval), and are dispersed along the lymphatic system, with increased population in certain areas (e.g., inguinal, axilla, head neck) [42, 21]. The basic building blocks of a LN are the capsule, afferent and efferent lymphatic vessels and lymphoid tissue [34] and can be seen in *Figure A.2*. Connective tissue together with numerous smooth muscle cells form the LN capsule [34]. Also, a LN is not a hollow reservoir, but filled with lymphoid tissue, as can be seen in *Figure A.2* [34]. Lymph flows to the LN via afferent lymphatic vessels and is transported away from the LN via an efferent lymphatic vessel, see *Figure A.2*. It is important to note that there are valve structures within the different types of lymphatic vessels which prevent back-flow of lymph, see *Figure A.2*. Whilst there is one efferent lymphatic vessel, there are several afferent lymphatic vessels per LN, see *Figure A.2* [33]. A LN is also connected to the blood circulation via an artery and a vein, see *Figure A.2*.

For several cancers (e.g., melanoma and breast cancer) the LNs are the first stop when spreading throughout the body [7, 23, 28]. The LN that receives direct lymphatic drainage from the primary tumour is the first to be infiltrated by metastases and is known as the SLN [30, 23, 7, 48]. >20% of

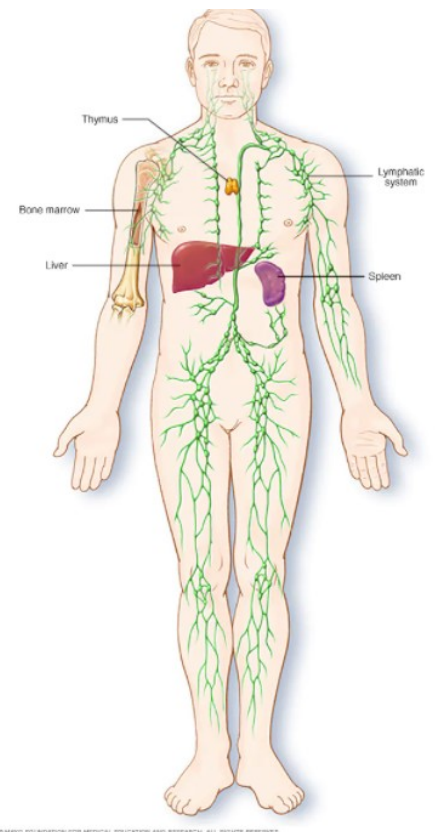


Figure A.1: This Figure depicts the lymphatic system. It can be seen that the lymphatic system is connected to bone as well as major organs and spans the whole body [55].

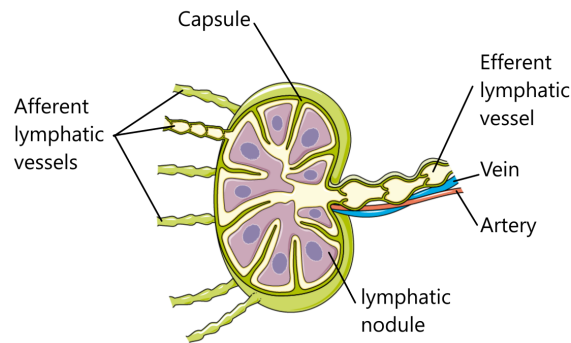


Figure A.2: This figure was taken from [https://smart.servier.com/smart\\_image/lymph-node-2/](https://smart.servier.com/smart_image/lymph-node-2/) and modified using 3D Paint (Microsoft, Redmond, Washington, United States) [36]

patients have more than one SLN [23]. Metastases of a primary melanoma can be present in the form of satellites, microsattellites, perforating the LN capsule, the metastases can be micro-scale or bigger, clustered or spread throughout the SLN [28, 49]. This is why nodal staging is performed in order to determine the patient's cancer status by evaluating the presence, shape and location of metastases [21]. Which in turn determines the prognosis as well as the next treatment steps [7].

## A.2. What is melanoma and the treatment thereof?

Melanoma is a form of skin cancer that accounts for 3% of all diagnosed skin cancers, but 65% all skin cancer-related deaths [47]. Melanomas have a high probability to metastasise even in an early stage [44, 35]. The incidence and mortality of melanoma has been increasing over the last decades [44, 50]. Which increases the socio-economic problem melanoma poses [50].

The most important risk factors according to Rastrelli et al. [50] are:

- the number of melanocytic nevi, which are congenital or acquired benign accumulations of melanocytes or nevus cells
- family history
- genetic susceptibility

In terms of diagnosis, the pathological examination remains the gold standard, and steps can be taken beforehand to catch the disease in an early stage [50]. One of these steps is the *skin self-examination* according to the "ABCD" method [50]. *A* stands for Asymmetry, *B* for Border irregularity, *C* for Colour variegation, and *D* for a Diameter of  $>6$  mm [50]. Later this method was extended to "ABCD(E)", with *E* standing for Evolving [50]. The *skin self-examination* is reported to be sensitive for melanoma detection, also when done by non-dermatologists [50]. *Figure A.3* depicts a schematic representation of examples to watch out for when conducting the "ABCD(E)" method.

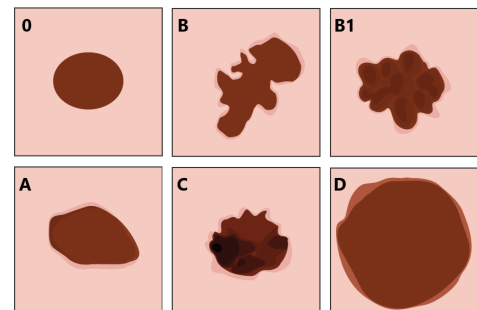


Figure A.3: This Figure represents the ABCD(E) method criteria. **0** depicts a normal beauty mark. **A** shows Asymmetry. **B** and **B1** depict irregular borders. **C** depicts colour variegation and **D** depicts an enlarged diameter of  $< 6$ mm. This figure was made using 3D Paint (Microsoft, Redmond, Washington, United States) and pictures from <https://smart.servier.com/?s=melanoma>

Another frequently used method for melanoma diagnosis is *dermatoscopy*. This method uses assistive optical devices including high-resolution optical handheld devices [50]. It is a non-invasive diagnostic technique for *in vivo* observation of the skin and works by optic magnification of morphological

structures that are not visible otherwise [50]. Dermatoscopy has increased the accuracy of melanoma detection because it renders early signs of disease visible before clinical changes appear [50].

A valuable imaging tool used for diagnosis of malignant melanocytic lesions is *Reflectance Confocal Microscopy* (RCM) [50, 18]. This tool is a non-invasive examination of skin in real-time [50]. It works by emitting a near-infrared, coherent laser beam to illuminate the skin [50]. The laser beam is partly backscattered due to microanatomical structures while passing through the upper skin layers [50]. The backscattered light is analysed by a computer and delivers black and white RCM images that reveal skin changes at a cellular level [50]. When combined with clinical examination and dermatoscopy, it has a high accuracy differentiating between benign and malignant skin neoplasms [18]. Although RCM is a valuable technique for early melanoma detection, as of now, it is only used in academic medical centers [18]. RCM's limited use is due to the costs and knowledge gap amongst dermatologists [18].

However, this shows that there are a lot of approaches taken to make melanoma detection and treatment less invasive for the patient, from diagnosing melanoma [50, 18], identifying SLNs [59, 46], to excising SLNs [45]. And finally, also this thesis, where a minimally invasive device is proposed.

When a patient is thought to have a cutaneous melanoma, the suspicious lesion is excised and pathologically examined [33, 50]. The pathologist determines the Breslow thickness of the tumour and whether it is ulcerated [28, 49]. Based on this information, the patient's disease can be staged according to the *American Joint Committee on Cancer* (AJCC) guidelines [28].

Nowadays, if the patient is staged as T1b and lower the patient is considered for SLNB [5, 19]. Before, and for patients staged higher than T1b, a complete lymph node dissection (CLND) was recommended [12]. The reason that CLND is no longer standard of care for patients with melanoma is that there is no added survival when compared to SLNB [12]. There are ongoing studies to investigate the added survival as well as recurrence risk after SLNB for patients with stage II and III melanoma [51, 14].

After the patient undergoes SLNB or CLND, which are both procedures where LNs are removed, with the difference that SLNB only removes the tumour draining LNs whereas CLND removes all LNs in the region of the tumour (either axilla or inguinal), the excised LNs are examined by the pathologist who performs *nodal staging* [12, 10]. During the nodal staging, the pathologist examines the excised LNs for the presence of metastasis. If metastases are detected, they are evaluated by their size and location [10, 49]. Various forms of LN metastases can be seen in *Figure A.4*. The nodal staging further specifies the stage of the cancer [28]. This determines the prognosis and treatment plan for the patient [7].

Based on the nodal staging the recommended treatment of the patient can be determined. For patients with no metastasis in the LNs, no further treatment is needed, for patients with detectable metastases in the LNs adjacent therapies like isolated limb perfusion or isolated limb infusion with

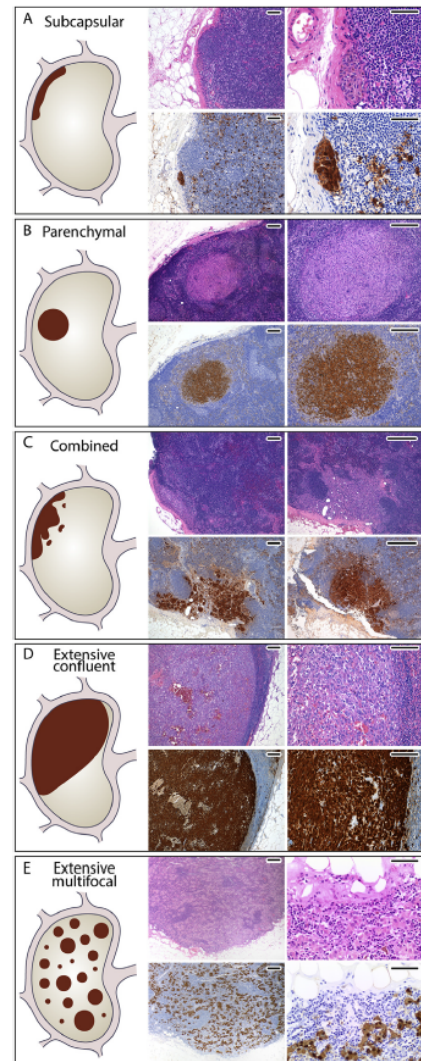


Figure A.4: This Figure depicts the vastly varying topography of metastatic deposits in SLNs, schematically drawn on the left and as found in tissue during nodal staging on the right. **A** shows subcapsular metastasis; **B** shows parenchymal metastasis; **C** shows a combination of subcapsular and parenchymal metastases; **D** shows extensive confluent metastases and **E** shows extensive multifocal metastases. It was adjusted from a publication of Cook et al. [10]

immune therapy (e.g., PD-1 checkpoint inhibitor (nivolumab) or anti-CTLA-4 (ipilimumab)) or targeted therapy (a combination of dabrafenib plus trametinib) [7, 12, 2, 14] are prescribed.

The author of this thesis deemed it important to be familiar with the topic of melanoma and its treatment in order to be able to design a MISLNB medical device. Another important manner in which the author got acquainted with the topic was shadowing physicians and attending live operations as well as training in the dissecting room. More information about these experiences can be found in the internship report, since this was part of the authors internship at the Erasmus Medical Center (Erasmus MC). All these impressions were useful information for the *stakeholder analysis* and the project as a whole.

### A.3. Previous Thesis

Another important part of the familiarisation that was done at the start of this project was the Master Thesis of Max Joosen. Max was the first student to tackle this problem and graduated in January 2021. He started this project by investigating the Young's Modulus of LNs and designing and testing a vacuum excision mechanism called the *Pull-and-Harvest* method [26]. In this section his work will be summarised as it presented the starting point of this follow-up project. This will be done by presenting the previous thesis design A.3.1, the previous research question A.3.2, and his conclusions A.3.3.

#### A.3.1. Previous Thesis Design

Max designed a vacuum gripper to manipulate LNs and excise them by pulling them into a tube to be cut [26]. This mechanism is called the *Pull-and-Harvest* method, see Figure A.5 [26]. The method works as follows: A tube with a pointed-tip-insert is introduced into the patient's body via a small incision and positioned in front of the LN, see Figure A.5(a) "Step 1". Next, the vacuum gripper is inserted through the tube, see Figure A.5(a) "Step 2".

Upon making contact with the LN, the vacuum pump is engaged in order to grip the LN and starts pulling the LN into the lumen of the tube, see Figure A.5(a) "Step 3". After pulling the LN into the lumen of the tube completely, a snare will close and resect the LN utilising radio frequency energy, see Figure A.5(a) Step 4. A top view of Step 4 and the closure of the snare are depicted in Figure A.5(b).

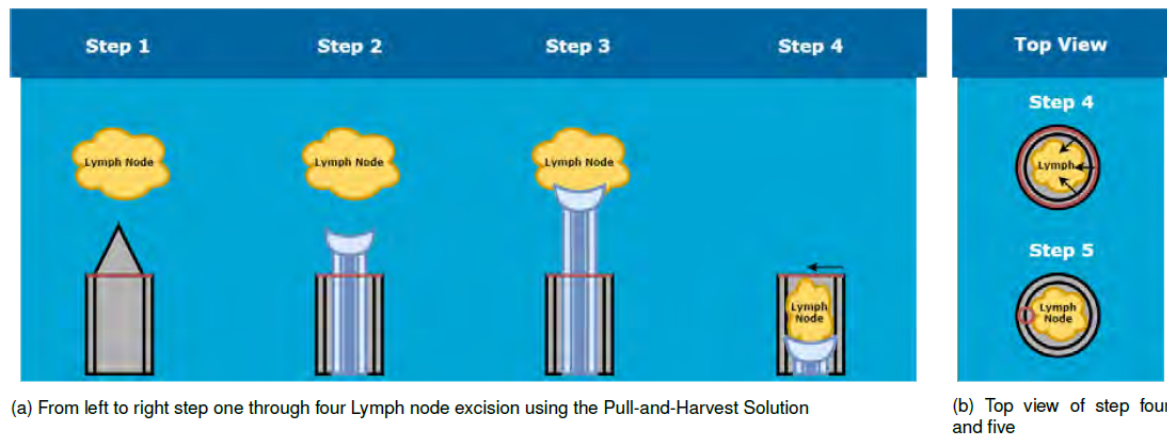


Figure A.5: This figure depicts the working principle of the *Pull-and-Harvest method* designed by Max Joosen. (a) shows the main steps in a side view. **Step 1** shows the insertion of the tube that is later used in order to insert the device. **Step 2** depicts the vacuum gripper being inserted through the tube and positioned in front of the LN. **Step 3** shows the vacuum gripper engaging the LN. At this point the vacuum pump is activated and the LN is starting to be pulled into the lumen of the tube. **Step 4** depicts the LN fully enveloped by the tube and the snare, in red, being closed in order to resect the LN. (b) depicts "Step 4" and the snare (in red) being closed from a top view. This figure was taken from the Master thesis of Max Joosen [26]

#### A.3.2. Previous Research Question

In order to evaluate his design, Max formulated a number of questions which will be presented now. Max' main question was: **"Can lymph nodes be harvested minimally invasive utilising a vacuum sucker without hindering nodal staging?"** [26].

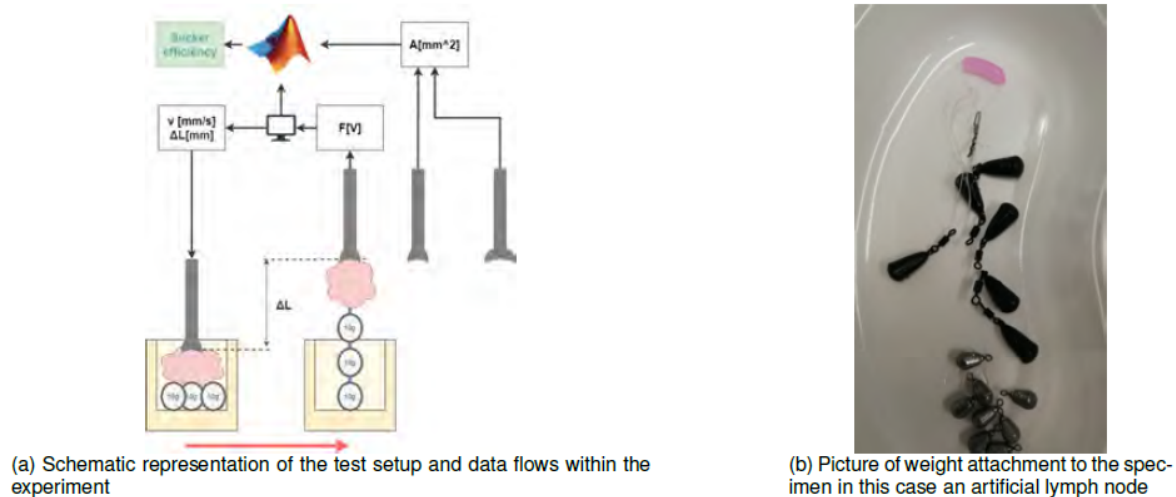


Figure A.6: This figure depicts a schematic drawing of the experimental set-up for the vacuum suction maximum force test in (a) and a picture of the phantom LN with attached weights in (b). This figure was taken from Max Joosen's Master thesis [26]

In order to answer this question Max divided this question into three subquestions:

1. What forces are required to separate the lymph node from the surrounding tissue?
2. Is vacuum suction an effective gripper for lymph node manipulation?
3. Can a lymph node be stashed inside a cylindrical volume without impairing nodal staging, to prevent spillage and enable safe extraction?

In order to answer these questions, three corresponding tests were devised:

1. mechanical test
2. vacuum suction maximum force test
3. LN stashing experiment

These tests will now be presented in short.

**1. mechanical test** This test was set up to derive material properties in order to be able to evaluate the feasibility of the *Pull-and-Harvest* method. A stress-strain test was done in order to evaluate the susceptibility of LNs to compression.

**2. vacuum suction maximum force test** This test utilised two different vacuum suction cups (  $4\text{mm}$  and  $6\text{mm}$  ) in order to determine their gripping efficacy. Weights were used in order to determine the peak force of the suction cups. Weights were attached to the phantom of an LN and the suction cup would exert an upward force, lifting one weight after the other. The experiment was deemed successful upon spontaneous detachment of phantom LN and weights, see *Figure A.6* [26].

**3. LN stashing experiment** This test was designed to evaluate the concept of stashing a LN in a tube and whether it would limit the ability for nodal staging. A tapered tube (start diameter  $14\text{mm}$  tapered to  $8.5\text{mm}$ ) that the LN had to be pulled through by the vacuum gripper [26]. In order to evaluate whether LNs that had passed through the tapered tube were still suited for nodal staging, one LN was pulled through and subsequently evaluated by the pathologist [26].

### A.3.3. Conclusions

The conclusions from these tests were the following: In terms of *mechanical tests* no Young's modulus could be determined due to the non-linearity of the stress-strain curves [26]. In terms of *vacuum suction maximum force* a peak force of  $0.116\text{N}$  was determined for the  $4\text{mm}$  suction cup and a peak force of  $0.253\text{N}$  for the  $6\text{mm}$  suction cup [26]. Max also calculated the theoretical force the *Pull-and-Harvest* method could deliver to be  $2.547\text{N}$  for the  $6\text{mm}$  suction cup, which he described as the one that could achieve maximum force [26]. The *LN stashing experiment* revealed that the histological architecture

had not been disturbed by the vacuum test, and the stashing method was suitable [26].  
This concludes the chapter on familiarisation.

# B

## Human Tissue Test

After the *Familiarisation* with the relevant topics and the previous Master Thesis in *Appendix A Familiarisation* was concluded, a plan was made to test the tensile strength of the tissue surrounding human LNs. Since Max had shown that using suction is a viable option for manipulating already cut loose LNs by showing the *Pull-and-Harvest* method is able to pick LNs up and pull them through a tube without damaging their integrity [26], a logical first step was to evaluate the force needed to pull LNs from the surrounding tissue. This test would evaluate whether the *Pull-and-Harvest* method would be developed further, or another working principle had to be chosen. The test was coined the *Tensile Test*, see *section B.1 Tensile Test*, since its purpose was to measure the tensile strength that is needed to be overcome in order to detach a LN from its surrounding tissue by means of pulling on it.

### B.1. Tensile Test

The goal of the *tensile test* was to determine the force needed to pull a LN free of its surrounding tissue. Because no conclusive information could be found to estimate the force one could expect, due to a lack of information on LNs' mechanical, electrical, and material properties [34, 63, 33, 41, 54] in scientific literature. Therefore, it was decided to design a test set-up utilising human tissue obtained from the dissecting room.

Besides human tissue, a mechanical measurement set-up was needed. The measurement set-up can be seen in *Figure B.2*. The set-up uses a linear stage (EGSL-BS-45-200-3P, Festo BV, Delft, The Netherlands), a S-beam load cell sensor (LSB200-FSH00104, FUTEK Advanced Sensor Technology Inc., Irvine, CA, USA) (indicated in bright red in *Figure B.2*), a Lab Jack T7 (Lab Jack Measurement & Automation, Lakewood, USA), an aluminium block with a hook for tissue attachment (indicated in dark red in *Figure B.2*), a tissue holder (white and transparent plates in *Figure B.2*), as well as a laptop with Matlab interface in order to actuate the linear stage and record the force sensor measurements, see *Figure B.2*.

The sensor measures forces from  $0.1N$  to  $45N$  and the linear stage can displace the attachment block and hook up and down over  $150mm$  with the following velocities:  $1mm/s$ ,  $5mm/s$ ,  $10mm/s$ ,  $20mm/s$ . Before testing could commence, several protocols had to be written. One for the tensile test itself, including setting the experiment up, executing it and cleaning up afterwards, see *Appendix G Tensile Test Protocol*.

Phantoms were used to perform a *proof-of-principal* test of the stage as well as to get familiar with handling the stage and troubleshooting it. There is no protocol over the detection of the LNs in the tissue, because this was not done by the author herself. The detection was done by radiologist dr.

For privacy reasons this picture cannot be shared publicly

Figure B.1: This figure depicts the marked LN embedded in adipose tissue. The sutures (black) not only indicate the position of the LN, but also serve as an attachment point to the linear stage. This picture was included with the permission of dr. Kleinrensink

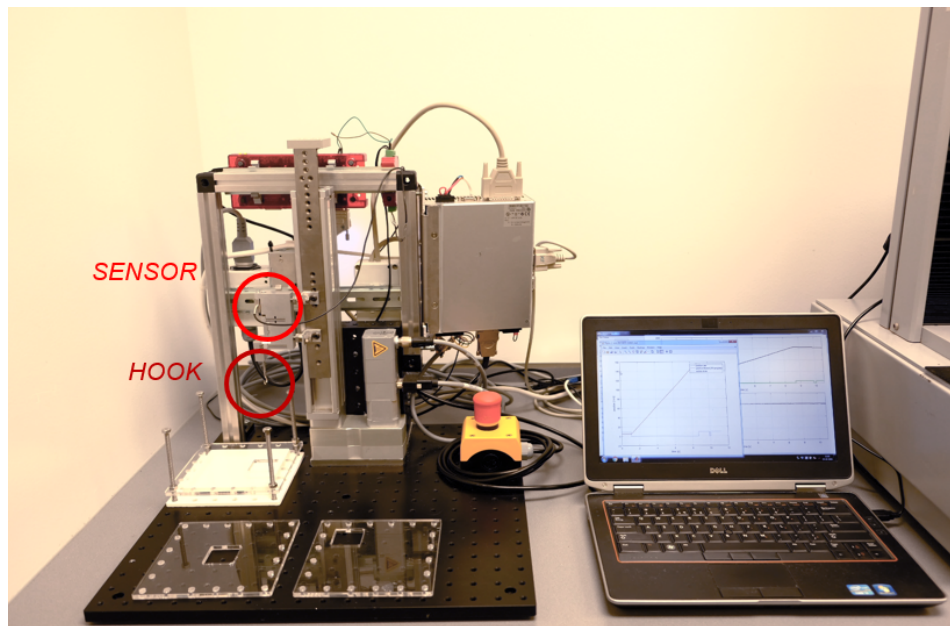


Figure B.2: This picture depicts the experimental set-up with the tissue holder (white and transparent plates), the laptop with the Matlab interface, the linear stage (EGSL-BS-45-200-3P, Festo BV, Delft, The Netherlands)(EGSL-BS-45-200-3P, Festo BV, Delft, The Netherlands), the S-Beam Load Cell sensor (LSB200-FSH00104, FUTEK Advanced Sensor Technology Inc., Irvine, CA, USA) (indicated in bright red), the tissue attachment hook (indicated in dark red), and the Lab Jack T7 (Lab Jack Measurement & Automation, Lakewood, USA) (red rectangle at the back of the top part of set-up). This picture was taken by Ellen de Vries and used with her permission

Cécile de Monyé (Erasmus MC) who was so kind as to come to the dissecting room and explain the working of an ultrasound machine, the detection of LNs as well as marking the LNs.

Afterwards, Sjoerd van de Weerd (Erasmus MC) and Teun Schurink (Erasmus MC) helped with the preparation of the LNs by cutting away tissue until the LN could be identified visually and placing sutures to mark the LNs as well as create an attachment point for the linear stage, see [Figure B.1](#). Sutures were chosen, because its tensile strength was expected to withstand the expected forces of a couple of Newtons [29].

But more importantly, using sutures, the tissue surrounding the LN would stay as intact as much as possible while creating a strong attachment to the linear stage with little chance of the LN slipping out and the experiment failing. This gave representative measures of the forces one can expect *in vivo*. When marking the LNs with the sutures, the goal was to not penetrate the LN, but lay the suture around it. This was almost always successful.

Lastly, the tissue was prepared to measure about  $10\text{cm} \times 10\text{cm}$ . After the preparation of the tissue was completed, the tensile tests could commence.

### B.1.1. Test Execution


A short description of the execution of the *tensile test* will follow now, for a more extensive description please see [Appendix G Tensile Test Protocol](#). The tensile test was executed as follows: The ground plate (black with holes in [Figure B.2](#)) and the electronics were covered with an absorbent cloth in order to prevent tissue and fluid to contaminate the measurement apparatus as well as provide a blank backdrop for documentation. The tissue with the embedded and marked LN was placed in the tissue holder (white and transparent plates in [Figure B.2](#)) and fixated on the ground plate using bolts and nuts, see [Figure B.2](#). It was made sure that the sutures were protruding through the window in the top plate.

The stage was then brought into starting position, which was the farthest point down ( at  $150\text{mm}$ ), see [Figure B.2](#). Next, the sutures were securely fastened to the hook. The parameters in the Matlab interface were set so that the linear stage would move upwards for  $150\text{mm}$  at a constant velocity of  $1\text{mm/s}$  and the file name the experiment would be saved under was adjusted. Then the experiment was run. This resulted for all LNs to be completely pulled from the tissue. A total of 4 LNs were tested



in this manner. The findings of these tests will be presented in section [B.2 Results Tensile Test](#).

After the LN had been pulled from the tissue, it was cleaned from lymph ducts, blood vessels and adipose tissue. Measurements of weight, dimensions and volume ensued. It was decided to do these measurements because very little is known about the LN's properties, and as much information as possible was set out to be gathered. The weight was measured using a *mg*-scale, see [Appendix G](#). For the dimensions, the short axis and the long axis were measured at the widest point each. A calliper was used to achieve a more accurate measurement. In order to determine the volume, a water displacement test was chosen, because this is the most efficient method to evaluate an accurate estimate of the LNs volume. A water displacement test is shown in [Figure B.3](#). The results from these measurements as well as the evaluation of the recorded sensor measurements were noted in the *RunTable*, who will be discussed in [Section B.2 Results Tensile Test](#).



For privacy reasons this picture cannot be shared publicly

Figure B.3: This figure depicts a water displacement test executed in order to determine the volume of the tested LN. This picture was included with the permission of dr. Kleinrensink

## B.2. Results Tensile Test

The *proof-of-concept* tests revealed that the gelatine fabricated according to findings from Jheng et al. [25] did resemble adipose tissue. This was confirmed by Sjoerd van de Weerd, an employee of the dissecting room and medical student. It was also observed that olives were too soft and tore easily. Furthermore, their density was too low, and they were floating on the gelatine instead of sinking. Olives were deemed unsuitable for ALNs. Other observations were that grapes start fermenting after two days in the refrigerator and that the gelatine shrinks considerably after an extra day in the refrigerator, changing the Young's modulus of the gelatine.

The results of the data analysis of the *tensile tests* can be seen in [Figures B.4, B.5, B.6, and B.7](#). And the maximum forces measured are displayed in the *RunTable Table B.1*. Some observations that have to be made are the following:

1. [Figure B.4](#) shows a plateau. This does not mean that a constant force was exerted onto the LN. It actually depicts the sensor's safety mechanism engaging due to excessive force ( $> 45N$ ).
2. There is no force measurement of LN #2. As can be seen in the *remark* section of [Table B.1](#). During the first test of LN #2 the tissue sample was pulled through the window. During test number two no data was recorded. The recorded data of test one of LN #2 was looked at, but an insufficient number of data points (only 22400) were collected. Upon inspection, the graph did not look representative.
3. Also, LN #3 was completely pulled through the window in test one. However, all data points were collected and upon inspection the graph seemed to be representative, see [Figure B.5](#).
4. It has to be noted that the recorded maximum force recorded in test two of LN #3 is 41% lower than the maximum force recorded in test one of LN #3. One explanation is that the tissue had partly been torn already, therefore less force was required to pull LN #3 free of the adipose tissue.

Generally speaking, the graphs look as one would expect. During the observations of the tests, it was seen that at first, the movement of the linear stage was continuous and at a certain point the tissue tore irregularly, which can be seen in all graphs where at the beginning the force smoothly increases and at a certain point there are steep dips in force, which then quickly increases again, until the LN is completely pulled free, and the force decreases rapidly.

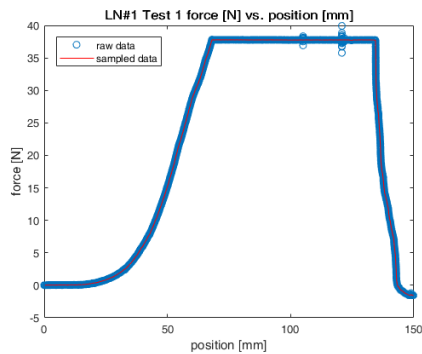


Figure B.4: This graph shows the force measurements while pulling *LN #1* from its surrounding tissue. The graph plateaus at position  $60\text{mm}$  due to the force exceeding the sensor's range of measurement. The maximum force measured was  $39.93\text{N}$ . This picture was created using the Matlab plot-function and subsequently saving the picture in .png format

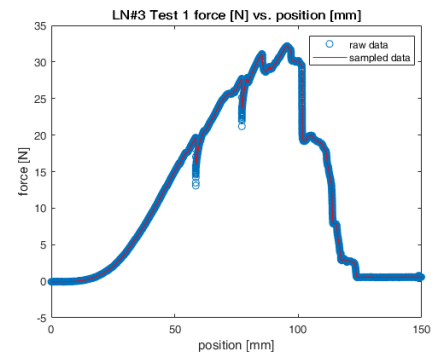


Figure B.5: This graph shows the force measurements of *LN #3* test 1. During this test the whole LN was pulled through the window of the top plate. However, this graph still holds important information, since the maximum exerted force on *LN #3* was  $32.25\text{N}$ . This picture was created using the Matlab-plot function and subsequently saving the picture in .png format

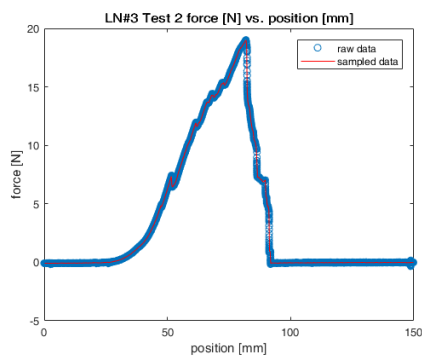


Figure B.6: This graph depicts the force measurements of test 2 of *LN #3*. It is noticeable that the maximum force measured is 41% lower than the maximum force measured in test 1, see [Figure B.5](#). The most likely explanation is that a considerable amount of tissue had already been torn during test 1, hence requiring less force to fully pull *LN #3* from its surrounding tissue during test 2. This picture was created using the Matlab plot-function and subsequently saving the picture in .png format

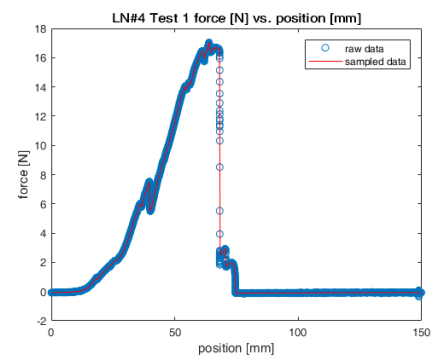


Figure B.7: This graph depicts the force measurements of *LN #4*. *LN #4* was a very small LN, see [Table B.1](#). It is believed that this is the reason for the relatively low force needed to pull this LN free when compared to more "standard sized" LNs like *LN #1*. A much smaller LN has a much smaller surface with less points of adhesion to its surrounding tissue (e.g., lymph ducts). This picture was created using the Matlab plot-function and subsequently saving the picture in .png format

Table B.1: This table shows the important aspects of the *RunTable*. The table includes the maximum force in Newton and Volt as evaluated using Matlab. As well as other measurements such as dimensions, weight and volume. *LN #1* corresponds to *Figure B.4*. *LN #3* corresponds to *Figure B.5*. *LN #3.2* corresponds to *Figure B.6* and *LN #4* corresponds to *Figure B.7*. All LNs except for *LN #1* were from female bodies. The sex of the donor of *LN #1* is unknown. All LNs were from the inguinal region and all bodies were embalmed using the *AnubiFix* method developed by dr. Kleinrensink

LN #	max Force [V]	long axis [cm]	short axis [cm]	weight [g]	volume [ml]	max Force [N]	comment/ remark
#1	0,207	1,8	0,6	0,58	0,6	39,93	LN was already quite cleared from the tissue. Sutures appeared to be around the LN. 4 sutures were used, 2-0 vicryl 2 knots let loose after the 150mm displacement two small strings of tissue were still attached. They were torn upon trying to reattach the LN to the stage.
#2	x	1,93	1,24	0,93	0,8	x	the LN was marked with 4 3-0 sutures an extra 0 multi suture was used to secure the 3-0 suture to the hook it looks like 2 LNs really close (what we saw on echo?) there was a problem with the 1st test, the complete tissue sample was pulled through the window, second test (teste 2,5) was done immediately after →worked out fine but no data was recorded by the apparatus
#3	-0,636	2,32	1,27	1,32	1,4	32,25	whole LN slipped through window
#3.2	-2,189					19,08	LNs #3 and #4 were obtained from the same tissue sample
#4	-2,425	0,62	0,56	0,06	0,1	17,08	



C

Literature Study

# A Systematic Review of Relevant Literature on Collecting Mechanisms with Potential Use for a Minimally Invasive Sentinel Lymph Node Biopsy Medical Device

BM51010 Literature Research  
in partial fulfilment of the requirements to obtain the degree of  
**Master of Science**  
in Biomedical Engineering  
at TU Delft

Louisa Rebekka Preis  
4229916

**Abstract**—Sentinel lymph node biopsy is the main staging tool to provide prognostic information for patients with early-stage melanoma or breast cancer. Over the last decade the number of sentinel lymph node biopsies has significantly increased. With a node positive result returned in only 20% of patients while the risk of experiencing morbidity being 10%, the importance of improving the procedure and improving upon this risk equation in favour of the patient is becoming more and more apparent. In order to do so, certain requirements need to be fulfilled such as *en bloc* excision of the sentinel lymph node and minimising the tissue damage experienced in order to be able to make the procedure possible under local instead of general anaesthesia. As a starting point of tackling this challenge, this systematic review has been contrived to find possible solutions for this problem, either in the form of an already existing device or a collection mechanism that can be adapted to meet the requirements. The most promising and important findings of the literature review are categorised into *mining* and *medicine* with the subgroups of *laparoscopic*, *patents* and *medical biopsy devices* with EU and/or FDA approval, namely the *NeoNavia® Biopsy System* and the *B.L.E.S.*. These findings will be introduced, analysed, and discussed in this article. The search revealed no ready-made device or mechanism meeting the requirements, however, the patent describing a ring-cutter as well as the working principle of an optomechanical biopsy tip and the B.L.E.S. bear promise upon further development with respect to minimally invasive sentinel lymph node biopsy. As well as a second patent that inspired a new concept for an excision mechanism that seems promising. It must be concluded that a lot more research needs to be done before a working prototype is achieved, but it is an achievable goal.

**Index Terms**—minimally invasive sentinel lymph node biopsy, medical device, collection mechanism

## I. INTRODUCTION

The intention of this article is to present a systematic review of collection mechanisms and devices found in scientific literature as well as other sources, with respect to a minimally invasive sentinel lymph node biopsy (MISLNB) medical device.

A sentinel lymph node biopsy (SLNB) is a staging procedure done for patients diagnosed with melanoma or breast cancer without clinically detected lymph nodes (LNs). Meaning that the LNs are not palpable and do not appear to be enlarged on imaging [11].

Research shows that for certain cancers, e.g., melanoma, the tumour first metastasises to the regional LNs [11], [25], [33]. More specifically, sentinel lymph nodes (SLNs), also known as the tumour draining LNs receive drainage from the primary tumour and therefore are the first to show metastasis, making determining the LN status one of the main prognostic tools for patients with cancer [9], [11], [25], [34], [50].

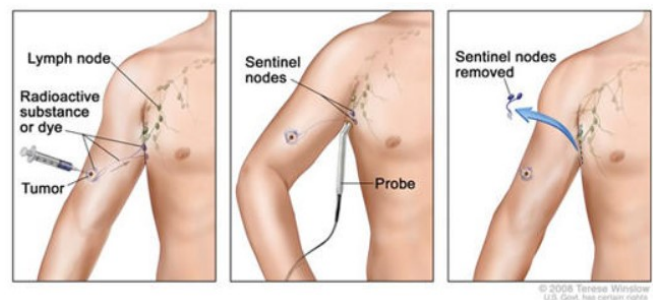


Fig. 1. This Figure depicts a SLNB procedure schematically. It can be seen how the patient is injected with  $^{99m}\text{Tc}$  and blue dye to identify and locate the SLNs. Then the SLNs are excised by a surgeon [65].

This is the reason that the majority of patients with early-stage melanoma or breast cancer is offered a SLNB.

The SLNB is performed as follows: in the morning of the procedure, a lymphoscintigraphy is performed, which entails a nuclear medicine physician injecting the patient with technetium 99 ( $^{99m}\text{Tc}$ ) in close proximity to the cancer, or

scar from the primary cancer resection [15], [17], [43].  $^{99m}\text{Tc}$  is a radioactive colloid that targets the receptor protein CD-206 which is found in high concentrations on the surface of macrophages, which in turn are found in abundance in LNs [43]. This causes the  $^{99m}\text{Tc}$  to accumulate in the SLN(s), see *Figure 1*. Subsequently, the nuclear medicine physician can mark the location of the SLN(s) on the patient's body for the surgeon. Depending on the patient, one or more SLNs are identified [25].

After the SLN(s) have been identified and their location marked on the patient's body, the patient is brought into the operating room (OR) and injected with blue dye in close proximity to the tumour or the scar from the primary cancer resection. The blue dye, similar to the  $^{99m}\text{Tc}$ , is absorbed by the surrounding lymph vessels, eventually colouring the SLN. The advantage is that blue dye can be seen with the naked eye by the surgeon and increases the probability of identifying all SLNs [36], [40]. Then the surgeon makes an incision of ca. 5 cm and locates the SLN(s) using a hand-held gamma probe and cuts the SLN(s) free from the surrounding tissue.

It is crucial that each SLN is excised *en bloc* and that the lymph node capsule stays intact, otherwise the nodal staging procedure can be impaired [13], [24]. During the whole procedure, the patient is under general anaesthesia. After the SLN(s) are excised, they are sent to the pathologist who performs the nodal staging [13]. A simplified version of the SLNB procedure can be seen in *Figure 1*.

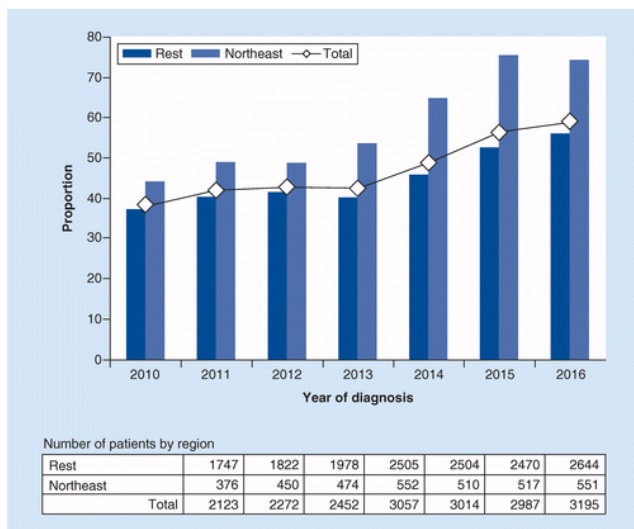


Fig. 2. This figure depicts the trend in the proportion of SLNBs performed in the Netherlands (Northeast vs. the Rest) between 2010 and 2016. Furthermore, the actual numbers can be seen in the lower half of the figure [14]

With the introduction of therapeutic options for patients with SLN metastasis (e.g., systemic adjuvant therapy), SLNB is not only a prognostic tool, but also has therapeutic consequences [4], [18], [20], [37].

If no metastases are detected, no further therapy is needed. Which has a huge impact on the quality of life of the patient. This reduces unnecessary treatments by 74% [11].

And is one of the reasons for SLNB gaining importance and more studies are being done on the benefits of patients with stage III cancer as well as other types of cancer (e.g., pelvic, prostate, colon, gastric and thyroid cancer) [22], [24], [39]. *Figure 2* shows the surge in SLNB performed on melanoma patients within the year of diagnosis from 40% in 2010 to 65% in 2016 [14].

However, this surge in popularity shines an even brighter light on the complications and morbidities accompanying SLNB which include: seroma/ hematoma, wound infection, delayed wound healing, scar formation and lymphoedema [15], [66].

Taking further into consideration that 80% of patients undergoing SLNB are node negative after nodal staging, meaning that there are no metastases detected in the SLNs, the risk-benefit relation needs to be evaluated very carefully for each patient [17], [48].

Hence, the question this review tries to answer is the following: *Is there a device or mechanism available that can easily be adapted to fit a minimally invasive sentinel lymph node biopsy medical device that fulfils the requirements of excising a SLN en bloc, with minimal tissue damage, requiring only a small incision and can be used under local anaesthesia?*

## II. METHOD

This section explains the acquisition of relevant scientific literature regarding answering the research question. The steps taken will be explained, as well as the relevant considerations.

A previous literature search done by the author to get familiar with the subject revealed that currently no device capable of excising LNs *en bloc* is on the market. Therefore, the author deemed it beneficial to search fields outside the medical one (e.g., mining, aerospace, and geology).

Before the first search was executed, a search strategy was composed, consisting of a list of databases, inclusion and exclusion criteria and search terms. The databases that were included are:

- Scopus
- Pubmed
- Web of Science

Google Scholar was intentionally excluded from the list of databases.

To maximise relevant findings on the databases, inclusion/exclusion criteria were assembled based on the knowledge of the author due to the aforementioned literature study to get familiar with the subject as well as discussions with other researchers from the medical field. The inclusion criteria are:

- accessible with TU Delft or Erasmus MC account
- language of publication either English, Dutch or German
- publications from the following fields:
  - mining (deep sea and ore)
  - aerospace
  - medicine (incl. veterinarian)
  - geology

- collection mechanism
- sampling mechanism
- sample collection
- minimally invasive tissue sampling or collection
- biopsy, sampling, or collection device
- probe, device, or instrument

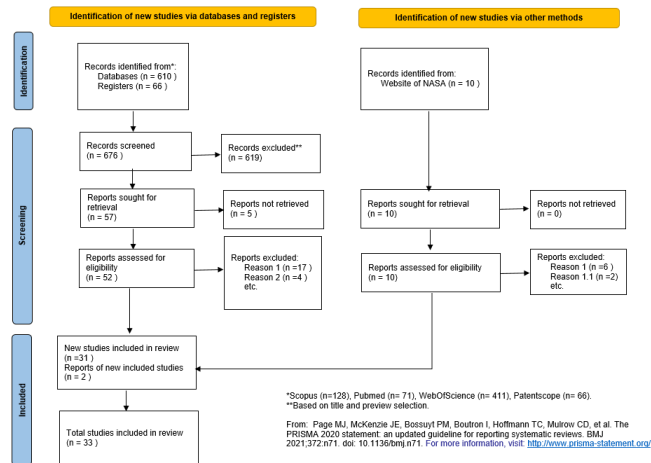


Fig. 3. This Figure shows the PRISMA flow-chart and summarises how the relevant literature was acquired. A total of 5 sources were searched, the databases *Scopus*, *Pubmed* and *Web of Science* for scientific literature, the registry *Patentscope* to search patents, as well as the website of *NASA*. *Reason 1* for exclusion was non-relevance to the literature search based on abstract evaluation. *Reason 1.1* indicates 2 NASA results that were about sampling microorganisms in water. *Reason 2* indicates the duplicates. The template for this flow-chart was made available on the website <http://www.prisma-statement.org/PRISMAStatement/FlowDiagram> and adjusted by the author.

All publications on polypectomy were excluded from the results because they poorly resemble the conditions experienced during SLNB. Publications were not filtered or excluded based on publication-date because the goal was to find a mechanism, which is timeless.

All review-relevant searches were carried out in January of 2022, a complete list can be found in Appendix A Table I. The searches were executed according to the PRISMA method [42].

A total of thirteen searches were executed on three databases and one registry. The databases were *Scopus*, *Pubmed* and *Web of Science*, see Table I.

The registry used was *Patentscope* because of its full text search capabilities and according to Jürgens et al. [31] it is the best registry for analysis searches. The registry *Derwnet* was neither with the TU Delft student account nor with the Erasmus MC account accessible.

In addition to the three databases and the registry, also NASA’s website (<https://www.nasa.gov/>) was searched.

The search-terms used were mainly Boolean (e.g., (*collecting OR excision*) AND (*device OR mechanism OR technique*) AND *aerospace*) and (*minimally AND invasive AND tissue AND sampling AND mechanism*)), see Table I.

The same search-terms were used across the databases; how-

ever, the filters were adjusted to their availability. A complete list of searches, search-terms, filters, and hits per database can be found in Appendix A Table I.

As can be seen in Figure 3, a total of 686 hits (across all databases, registries, and websites) were screened based on title and preview. A total of five scientific articles were not accessible with the accounts at hand (lpreis@tudelft.nl and l.preis@erasmusmc.nl). The remaining 62 articles were evaluated for relevance based on their abstract. While doing this, four duplicates were found. In the end 31 scientific articles and patents and two articles published on the NASA-website were considered relevant for answering the research question, see Table II.

### III. RESULTS

In this section the results of the reviewed literature found by the systematic literature search will be presented, for all relevant literature see Table II in the appendix. The results from all databases and registries are categorised into two topics *Mining* (III-A) and *Medicine* (III-B) and will be presented accordingly.

Figure 4 depicts the results and their relation to each other and the different areas. Detailed lists of the executed searches and included literature can be found in the appendix A (Table I and Table II respectively). The first topic presented is *Mining*.

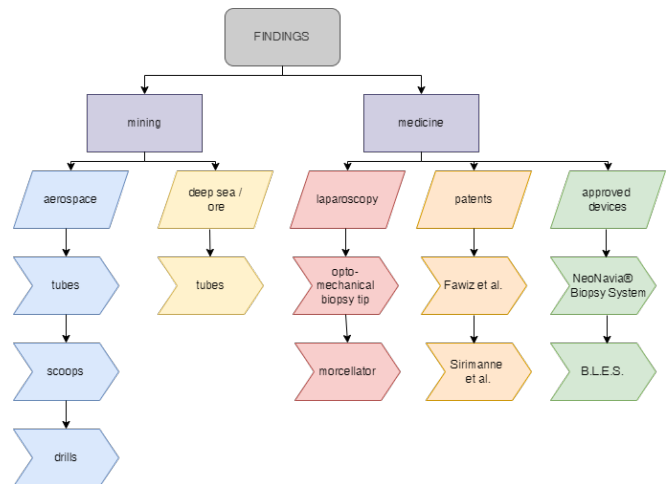


Fig. 4. This Figure shows a systematic overview of the findings and how they relate to the different areas and each other. It also represents the different findings presented in this article. This flow diagram was made by the author using diagrams.net (<https://app.diagrams.net/>) formerly known as draw.io

#### A. MINING

This topic is concerned with harvesting mechanisms of geological mining, with a special focus on deep-sea mining and applications in aerospace.

Zhang et al.’s [68] review on collecting technology for regolith sampling on moons and planets divides the technologies in two groups, *manual* and *robotic*. The manual technologies are operated by astronauts and resemble scoop-variations (e.g., scoop-and-tong, small scoop, bulk sample scoop), tongs,



tubes, and drills [68]. The robotic samplers are actuated drills with collecting bags [68].

Sampling on hard surfaces, such as the asteroid Ryugu's surface works as follows: A 5 g tantalum projectile is shot at a velocity of 300 m/s inside a sampler horn immediately after the horn has touched the surface. All the particles and pieces of asteroid that have come loose due to the impact of the projectile, are collected in the horn, as can be seen in Figure 5 [54]. This resembles some of the working principles described by Zhang et al. [68] as well as the working principle of deep-sea mining described by Zhao et al. where a cylindrical suction tube is brought close to a layer of ore in the deep sea and applies an upward force on the ore particles [69]. Halfar et al. [27] describes sampling micro plastics from sea water via suction tubes, similar to the ore mining described by Zhao et al. [69].

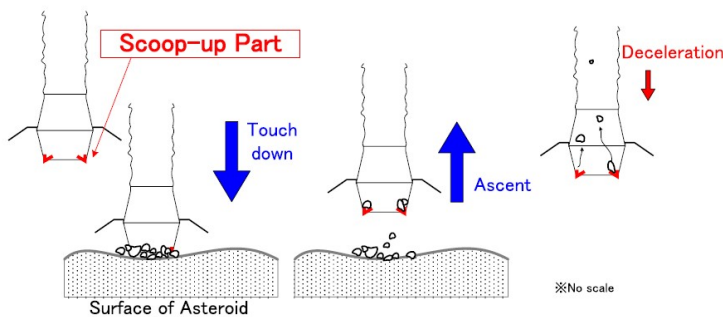


Fig. 5. This Figure schematically shows the working of the Hayabusa2 sample collecting mechanism as described by Sawada et al. [54]. As soon as the horn touches the surface of the asteroid, a projectile shoots inside the horn and hits the surface freeing particles. These particles are being scooped-up with the "scoop-up part". Then the horn is retracted and hence the samples collected [54].

Next to scoops, tubes are a common theme amongst sampling and collecting mechanisms in mining. Tang et al. [59] describes collecting samples from the lunar surface using a circular direct push sampling tube. The mechanism of the *lunar surface direct push sampling method* is pushing a hollow tube into the ground at high speed [59].

NASA's *Curiosity* Mars rover has a sampling mechanism, which works with a percussion drill that loosens the harder materials to be scooped up and stored [29]. The sample acquisition of the *Sample Analysis at Mars* utilises a scoop mechanism as well [38], [64].

Another scooping mechanism was described by Brinkmann et al. [8]. An actuator tilts a scoop bucket and glides the edge of the scoop bucket in a tilted position across the surface before returning the scoop bucket to its original position carrying material samples of various sizes.

In summary, the results concerning mining can be described as dominated by drills, tubes and scoops in different shapes and sizes, see Figure 4.

The next part will focus on the findings across different databases concerning the medical field.

## B. MEDICINE

In this section, the findings on sampling mechanisms used in the medical field will be presented sorted into three categories: *laparoscopic biopsy (III-B1)*, *Patents (III-B2)* and *approved biopsy devices (III-B3)*.

1) *laparoscopic biopsy*: In terms of laparoscopic biopsy, two especially interesting results were found: the *morcellator* and the *optomechanical biopsy tip*.

First the *morcellator*, a device used for laparoscopic hysterectomy [3], [28]. The working principle of the morcellator is shown in Figure 6. Figure 6(a) shows tissue initially being pulled inside the morcellator tube by grasping it with a laparoscopic grasper. A rotating cutting blade located at the distal end of the morcellator starts spinning and cutting the tissue into a long strip while simultaneously pulling the tissue into the morcellator tube, see Figure 6(b).

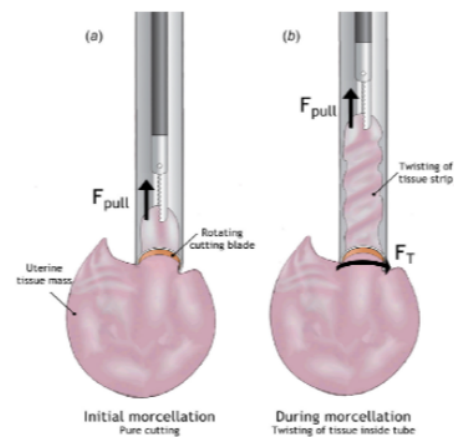


Fig. 6. This Figure depicts the working principle of a morcellator as currently in use and FDA approved [3]. It can be seen how the tissue of interest is grasped by the laparoscopic grasper and pulled inside the morcellator tube with force  $F_{pull}$ , (a). (b) depicts the twisting motion the tissue undergoes during morcellation (being pulled and cut with a rotating blade simultaneously).  $F_T$  indicates the torqued being applied to the tissue due to the rotation of the cutting blade. This picture was taken from [3] and modified using 3D paint (Microsoft, Redmond, Washington, United States).

The second mechanism is the *optomechanical biopsy tip*, a design combining three different biopsy mechanisms into one [30]. Namely: fine needle aspiration, core-needle biopsy, and punch biopsy. Enabling the user to biopsy various tissues with one device, see Figure 7(b). Another feature of the optomechanical biopsy tip are the fibre optics, making optical biopsies, or optical tissue differentiation possible, see Figure 7(a).

The sample collection mechanism is the following: the device is introduced and positioned in front of the tissue of interest. The cutter is spring loaded (purple spring in Figure 7). Upon actuation, the spring pushes Aristotle's lantern (depicted in yellow in Figure 7) into the tissue. Due to the narrowing

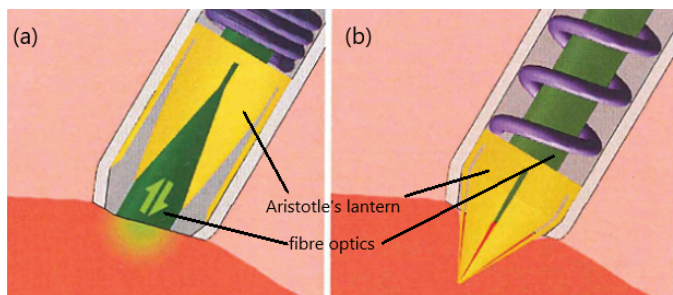


Fig. 7. This Figure depicts the optomechanical biopsy tip designed by Jelinek et al. [30]. (a) shows the fibre optics identifying the tissue they are in close proximity to or contact with. (b) shows the sea urchin inspired mechanical biopsy mechanism. By pushing Aristotle's lantern into the tissue, it closes and thereby cuts tissue which can be retrieved and evaluated. This picture was taken from the BITE Group site [61] and modified by the author using 3D paint (Microsoft, Redmond, Washington, United States).

of the outside tube at the distal end Aristotle's lantern closes and cuts at the same time, excising a conical piece of tissue [30].

2) *Patents*: This subsection is called patents because it describes two patents that were found that cannot be categorised more specifically. The first patent of interest was designed by Fawiz et al. [21].

Fawiz et al. [21] describes a medical device that is able to excise large volume tissue samples minimally invasive by inserting a larger-than-normal-cannula with a trocar-tipped needle to a position right in front of the lesion. Then a localisation wire is extended and pushed through the lesion. Next, the trocar-tipped needle is retracted, and the ring-shaped cutting member inserted, for a close up of the working see *Figures 8 and 9*.

*Figure 8* depicts a close up of the ring-shaped cutting member in its unfolded (left) and folded (right) position. It can be seen that the blade is wound up around the right rod. After insertion of the device in its folded position, the lesion is cut free by unrolling the blade from the rod. The edge of the ring-shaped cutting member is sharp and cuts the tissue. Because the cutting member can vary in size, bigger lesions can be cut as well as smaller lesions.

After the whole lesion has been enveloped by the cutting member and the mesh it is attached to, see *Figure 9*, a grasper can be inserted to additionally hold the excised lesion in place relative to the cutting member upon removal of the lesion and the device from the body [21]. A detailed depiction of the working of the cutting member after the localisation wire has been placed can be seen in *Figure 9*.

The second patent was designed by Sirimanne et al. [56]. This patent concerns a device and method for marking a cavity left by the biopsy of a breast lesion. The patent describes a device making the biopsy cavity location visible between one to five years after the biopsy has taken place. The goal of this device is to enable the physician to monitor the location of the lesion for new growths and re-growth. In case of insufficient

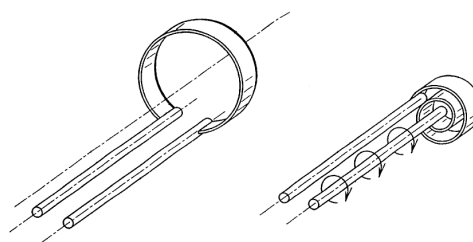


Fig. 8. This picture shows a close up of the ring-shaped cutting member of Patent US 6,471,709 B1. **Left** shows the ring-shaped cutting member in its unfolded position. **Right** shows the ring-shaped cutting member in its folded position. This position is used during insertion. The figure was taken from the Patent US 6,471,709 B1 [21] and altered by removing the numbers of the parts using 3D paint (Microsoft, Redmond, Washington, United States).

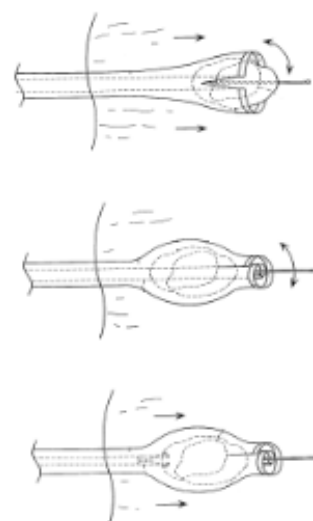


Fig. 9. This Figure depicts the detailed drawing of the working principle of the device after the lesion has been marked with a guide wire. It can be seen that the ring-shaped cutting member is attached to a mesh that is pulled over the lesion while the ring-shaped cutting member is cutting the lesion free from its surrounding tissue. The figure was taken from the Patent US 6,471,709 B1 [21] and altered by removing the numbers of the parts using 3D paint (Microsoft, Redmond, Washington, United States).

margins where re-excision is needed, the device clearly shows the location and orientation of the cavity, and a re-excision is more successful.

The working principle of this device is the following: after the lesion being biopsied, an absorbable gel or fibrin structure is placed in the cavity [56]. Then the radiopaque marker that is stored in a tube which can be used with standard biopsy devices like the Mammotome [56] has been brought in position (at the edge of the cavity). A plunger engages and pushes the folded marker into the absorbable material that fills the cavity. The marker is designed in different shapes, one of which is a spiral shape (as seen in *Figure 10*) [56]. The shape and size to

be used is determined by the physician. Upon the marker being pushed out of the tube by the plunger, the marker expands to up to 30 times its volume inside the cavity [56]. After one to five years, the marker is completely absorbed by the body.

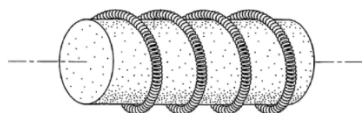


Fig. 10. This Figure depicts a spiral shaped radiopaque marker coiled around absorbable material to be inserted into a biopsy cavity in order for the location of the lesion to be detectable up to 5 years after removal. The size of the marker can be adjusted by the physician to adjust for preferred size. The figure was taken and adjusted from the patent US20100234726 [56] using 3D paint (Microsoft, Redmond, Washington, United States).

3) *approved biopsy devices*: This section presents two devices that have been approved to be traded on the extended Single Market in the Extended European Area (CE marking) and by the Food and Drug Administration (FDA) in the USA, respectively.

First, the *NeoNavia® Biopsy System*. This device is worth mentioning because it is the only device that was found that is designed and manufactured to biopsy LNs. It is approved in Europe and has filed a registration application for approval by the FDA (Food and Drug Administration) [44]. The NeoNavia® Biopsy System combines the working principle of the two standard needle biopsy methods, the core needle biopsy (CNB) and the vacuum assisted biopsy (VAB). CNB works by ejecting a needle (core needle) through a hollow tube into the lesion using a spring. VAB works by sucking tissue into the needle by applying vacuum and then cutting it.

The NeoNavia® Biopsy System combines those two working principles by consisting of an outer tube with a cutting edge and a trocar-tipped needle. Both are inserted together right up to the LN with ultrasound guidance. The trocar-tipped needle is then pulled back and the tube with the cutting edge is pushed into the LN via pneumatic pulses. Once the cutting tube is brought into position, the vacuum is applied, and a rotating movement simultaneously cuts the tissue and the NeoNavia® Biopsy System is ready to be pulled out of the body.

In order to recover the specimen, the trocar-tipped needle is pushed forward again and pushes the specimen out [55]. A schematic drawing of the working principle of the NeoNavia® Biopsy System is depicted in Figure 11.

The second approved biopsy device worth mentioning is the *B.L.E.S. (breast lesion excision system)* by *MEDTRONIC Inc.*. This device has been approved by the FDA [51]. It was formerly known as the *INTACT* (Intact Medical Corporation, USA) and recently as *B.L.E.S.* (Medtronic Inc., Ireland) [32].

The B.L.E.S. is a wire basket excision system. The apparatus consists of a vacuum-assisted probe receiver, five wires, an elastic radiofrequency (RF) ring and a pointed tip, see Figure 12. This rod-shaped probe is 6.6mmx11.4cm, which

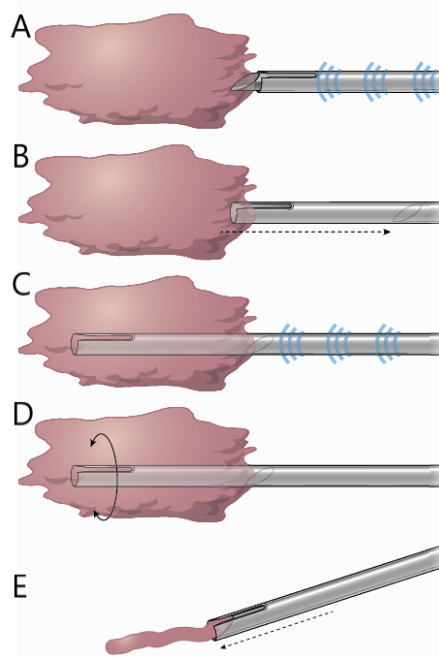


Fig. 11. This Figure depicts the working principle of the *NeoNavia® Biopsy System*. **A** depicts how the trocar-tipped needle (light grey) and the outer tube with cutting edge (dark grey) are inserted and positioned right in front of the LN. **B** shows the trocar-tipped needle being pulled back inside the outer tube with cutting edge. **C** shows the outer tube with cutting edge after being deployed into the LN via pneumatic pulses. **D** indicated the rotating movement of the outer tube with cutting edge in order to cut the specimen from the LN. **E** shows the device after it has been pulled out of the body. The trocar-tipped needle is being pushed back forward and the specimen is expelled from the device and ready for pathological examination [19]

is about the diameter of a G6 probe [32]. The B.L.E.S. works as follows: the wand (with retracted RF wires and protruding pointed tip) is inserted under ultrasound guidance until the lesion is reached. Then the pointed tip penetrates the lesion about 1mm in depth in order to fixate the lesion in place for more precise excision, limiting its movement upon deployment of the wires [32]. The lesion is also held in place with the US head used for guidance [32].

After penetrating the lesion with the pointed tip, the wires are deployed circumscribing the lesion. This is aided by RF cutting. Upon closure of the wire basket, the lesion is cut free from the surrounding tissue and the device with the lesion inside the basket can be retrieved. In order to free the specimen from the device, some wires have to be cut. Then the sample is ready for histopathological evaluation [32], [51].

The B.L.E.S. is available in different configurations with basket dimensions ranging from 12mm, 15mm to 20mm (14-16G) accommodating for different size tumour [32].

The B.L.E.S. is investigated for applications as a percutaneous lumpectomy device [32], [52]. However, MEDTRONIC Inc. has since retracted the device from the market and stopped producing and developing it.

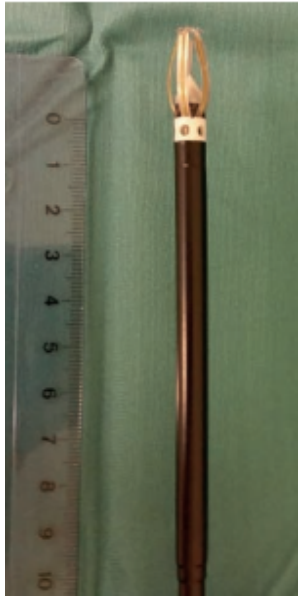


Fig. 12. This Figure depicts the B.L.E.S. (20mm) in its deployed status. The RF cutting wires as well as the pointed tip can clearly be seen [51]

#### IV. ANALYSIS

In this section the findings from section III *Results* will be analysed and evaluated. This includes a critical analysis of the working principle on applicability to the MISLNB medical device and whether a set of basic requirements is matched. The basic requirements that are taken into account in this section are:

- minimal tissue damage
- accommodates different LN sizes [41], [53]
- small incision (ca. 2.5cm) needed
- *en bloc* excisions or large volume excisions since LNs have to be excised as a whole for accurate pathological assessment, see Figure 13 [13], [47], [62]
- only local anaesthesia needed

One reason that local anaesthesia is an important requirement is that it will reduce the needed personnel. No anaesthesiologist and anaesthesia support staff will be needed, making an OR obsolete. This will also reduce the costs significantly [5]. Local anaesthesia also bears fewer risks of experiencing a stroke or myocardial infarction for the patient [5]. Another aspect is that it is being speculated that general anaesthesia can have a positive effect on cancer recurrence [5]. The reasoning is that metastases in transit that would normally be eradicated by the patient's immune system are not eliminated due to the administered drugs suppressing the immune system, hence making cancer recurrence more likely [5], [67]. However, more research needs to be done looking to prove or disprove this hypothesis. The order of mechanisms will be the same as in the previous section.

This section closes with an outlook on *Future Research IV-C* and the *Limitations IV-D* of this article.

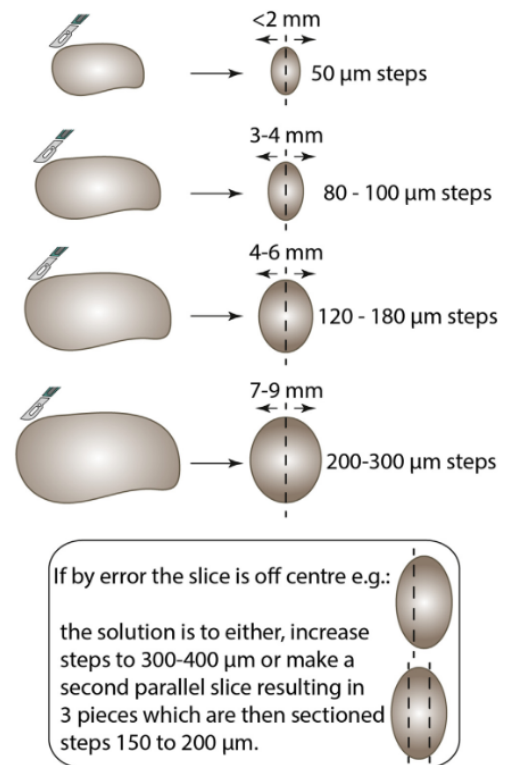


Fig. 13. This Figure depicts the steps taken during pathological evaluation of a LN. It also shows that it is important that the LN is excised *en bloc* [13]

#### A. MINING

The various collection mechanisms described by Zhang et al. [68] are used to collect samples in outer space. The described mechanisms are divided into manual or robotic driven mechanisms. The working principle of the collecting techniques is material being scooped up or picked up via a suction tube [68]. Additionally, a drill can be employed to loosen the surface before sample collection [68]. This can be seen as a preparatory step to collecting the samples.

The basic scoop and tube mechanisms can already be found in the medical field. A scooping mechanism is employed when sampling skin cells for pathological evaluation [1].

Also scraping will not allow the LN to be excised *en bloc*, thereby rendering this mechanism inappropriate for a MISLNB medical device.

In terms of suction tubes, these appear similar to vacuum assisted biopsies, where tissue is pulled into a tube by applying vacuum. Another application that already exists that utilises tubes is *puncture biopsy* [35], [49]. Here, suspicious skin is biopsied by pushing a round tube with a cutting edge with high velocity into the skin, thereby punching out a piece of skin for further evaluation [49]. These applications are all used externally. Applications for internal use are e.g., *Endoscopic Equipment* [12]. A suction tube is used

during polypectomy in order to ease the retrieval of the resected polyp [23]. As stated in section II (Method), articles on polypectomy were excluded due to the vastly different conditions encountered during polypectomy compared to SLNB due to the fact that polyps are only fastened to tissue (bowls) on one side instead of embedded in tissue and therefor van be snared, see *Figure 14*. This is not possible for SLNs. Hence, suction tubes are deemed inappropriate as a resection mechanism for a MISLNB medical device. Therefore, the review of Zhang et al. did not present any novel mechanisms that could be applied to a MISLNB medical device.

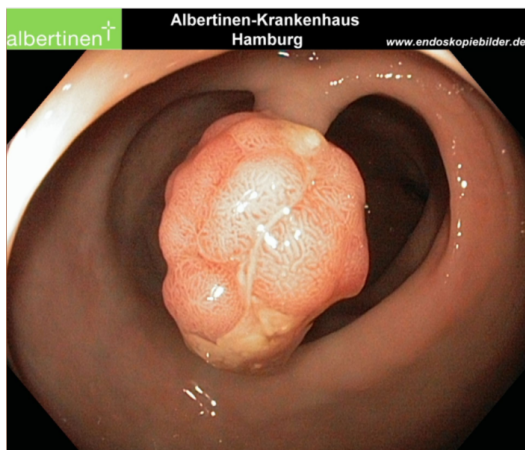


Fig. 14. This Figure shows a polyp before it is removed. It shows that the polyp is only attached to the bowl lining on one side, but most importantly, the polyp is surrounded by air. These are vastly different conditions to the excision of LNs [16]

Zhao et al. [69] and Halfar et al. [27] presented suction tubes in order to mine ore and collect microplastics from the ocean, respectively. Equally to the suction tubes discussed by Zhang et al. [68], such a principle is already applied in the medical field [12], [23], and hence does not present a novel mechanism for a MISLNB medical device.

Also, the Hayabusa2 sample collecting mechanism described by Sawada et al. [54] is an elaborated version of a collection tube. With the difference that first a projectile is shot through the tube to loosen the hard material. Shooting a projectile into the patient's body is not ethical. It will also not aide in excising a SLN *en bloc* and undamaged. Hence, this collecting mechanism neither fulfils the requirements nor represents a viable option for a MISLNB medical device.

Tang et al. described a push sampling mechanism to be used on the lunar surface [59]. This sample collecting mechanism resembles the punch biopsy [35], [49] and in addition it can be compared to core needle biopsies [55]. It is unlikely that a SLN can be removed pushing a tube into the human body. The damage the body would experience

would be unacceptable for a minimally invasive device. Next to the fact that the sizes in LNs vary between a few millimetres to a couple centimetres [53]. Another aspect making this method impossible is the varying location and orientation of the LNs [6].

The same has to be said for Jandura et al.'s [29] (NASA's *Curiosity* drill and scoop mechanism), Lin et al.'s [36] (*Sample Analysis at Mars (SAM)* using a scoop mechanism), Wei et al.'s [64] (*SAM* using a scoop mechanism), and Brinkmann et al.'s [8] (scoop mechanism) sample collecting mechanisms, who all present a variation of drills, scoops, and tubes.

It has to be concluded that reviewing the literature concerning mining has not revealed any feasible collecting mechanisms with possible application in a MISLNB medical device.

The next part of this section analyses the results concerning the medical field.

## B. MEDICINE

Now the results in the medical field will be discussed. The order is the same as in the result section and has nothing to do with importance.

First, the laparoscopic devices morcellator and optomechanical biopsy tip will be looked at.

In terms of laparoscopically removing LNs it has to be said that this is being done already [10], [45]. Search Nr. 7 (see Appendix A) obtained a scientific article about laparoscopic lymph node biopsy (LNB) in macaques [57]. What the laparoscopic LNBs have in common are that they are performed in the abdomen [10], [45], [57]. Laparoscopy has two sites of application, the abdomen, and the pelvic cavities [7], which means that the axillary as well as the inguinal regions cannot be operated on laparoscopically. The difficulty is that extra space within the abdomen and the pelvic cavities can be created by insufflation of these areas with gas ( $CO_2$ ) [7], which cannot be done in the axillary or inguinal regions because the gas will dissipate into other regions of the body and cause an emphysema [26].

Another aspect is that laparoscopies are usually performed under general anaesthesia, whereas the proposed MISLNB medical device has to be applicable under local anaesthesia only.

It needs to be added that the FDA is currently advising against using the morcellator in this configuration because the tissue has a habit of rupturing. This causes cancerous tissue to be flung around and be spread throughout the abdomen with the possibility of spreading the cancer in this manner [30].

In terms of collecting mechanism, both devices are intriguing. The *morcellator* first pulls tissue into the morcellation tube and then cuts the tissue with a rotating cutting blade [3]. The morcellator is not made to excise tissue of interest *en bloc*. It is designed to remove large lumps of tissue through

a laparoscopic port. Hence, the morcellator mechanism would have to be adjusted with respect to excising the LN undamaged and introducing the device into the body, in order to be able to use this mechanism for a MISLNB medical device.

An interesting aspect when looking at the optomechanical biopsy tip is the optical part. Although Jelinek et al. [30] does not go into detail about this part of the device, it is the authors believe that the optical biopsy could possibly be done utilising *diffused reflectance spectroscopy* as described by Swamy et al. [58]. This could aid the identification and navigation of the MISLNB medical device. However, optical biopsy methods lie outside the scope of this article.

Considering the optomechanical biopsy tip, the use of Aristotle's lantern sparked some interest. As is, the biopsy samples are too small to accommodate a whole LN. In order to excise a LN of average size (mean length of 16 mm for negative LNs [41]) the device mechanism will have to be scaled up. If it is possible to scale the mechanism up and it still works, this will mean that inserting the device in the axillar or inguinal region will cause a lot of damage to the tissue, because a cylinder of more than 2cm will have to be inserted to accommodate for larger LNs.

When looking at the patent discussed in section III (Results), designed by Fawiz et al. [21], the working of the device itself seems quite complex. A lot of different parts have to be used and the inserts have to be changed multiple times (trocar-tipped needle, the localisation wire, grasper, and ring-shaped cutting member). Based in the listed requirements, this mechanism is not suitable for a MISLNB medical device as is, because the localisation wire is pushed through the LN, thereby damaging the integrity of the LN. This device, however, has potential to be developed into a working mechanism compatible with the MISLNB medical device requirements. Furthermore, the patent, which was part of a cohort of patents seems to have been abandoned since.

When looking at the second patent designed by Sirimanne et al. [56], the relevance is not clear right away. Because for the SLNB medical device no marking mechanism is needed. However, this device sparked the idea to design an adjustable corkscrew mechanism that can be inserted into the body without much tissue damage and can be deployed once in position.

The mechanism would act like a corkscrew that cuts around the SLN without damaging it and rather cutting the adipose tissue surrounding the SLN. Such a mechanism would fulfil the requirements for the MISLNB medical device of excising the SLN *en bloc*. As described the device can expand inside the body to up to 30 times its size, which would minimise the tissue damage as well as only requiring a small incision [56].

Lastly, the *NeoNavia® Biopsy System* will be analysed. This device combines the CNB and VAB working principles. While on paper the idea of sampling the LNs only instead of having to excise the whole LNs sounds interesting because it would mean irradiating the morbidities for patients that would have been staged node negative and would mean only one operation for patients that would otherwise undergo first SLNB and then complete lymph node dissection [55].

This sounds too good to be true considering the evidence from a study by Oude Ophuis et al. [47] that has shown that ultrasound guided CNB is not feasible for accurate staging even though it was possible to identify the SLNs correctly. Verver et al. [62] has shown in a subsequent study that that even ultrasound guided fine needle aspiration cytology (FNAC) does not accurately sample LNs sufficiently enough for staging.

The author believes that nodal staging with needle biopsy has a major pitfall due to the fact that the metastases in the LNs from primary melanoma vary in their size, shape, and location a lot [13]. The LN can have one big metastasis, or several smaller ones, micro satellites and so on, see *Figure 15* [13].

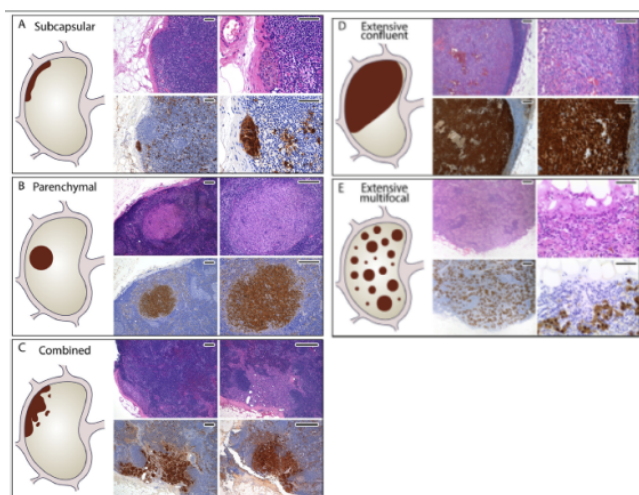


Fig. 15. This Figure depicts the vastly varying topography of metastatic deposits in SLNs, schematically drawn on the left and as found in tissue during nodal staging on the right. **A** shows subcapsular metastasis; **B** shows parenchymal metastasis; **C** shows a combination of subcapsular and parenchymal metastases; **D** shows extensive confluent metastases and **E** shows extensive multifocal metastases. It was adjusted from a publication of Cook et al. [13]

As of yet, these metastases cannot be identified reliably with ultrasound imaging [11], [46], [63]. Research is being done into using computer tomography (CT) and magnetic resonance imaging (MRI) to perform nodal staging, but these imaging techniques cannot detect metastases reliably [24]. Which leads to the physician basically blindly biopsying a LN because the physician does not know of presence, shape, or location of the metastases. Which, in the author's opinion makes it hard to conclude that a LN is negative, when there is a possibility of the LN metastases simply being missed

due to its shape and location inside the LN. Looking at *Figure 15* the author considers it highly unlikely that a physician is able to biopsy exactly where the metastasis lies for cases **A-C**. **D & E** represent a more evolved metastasis that started out as **A** or **B**, respectively. Cases **D** and **E** might not appear as clinically negative nodes, which would omit the choice of SLNB.

There currently is a trial registered (ClinicalTrials.gov Identifier: NCT03975855 [60]) for the evaluation of this device on breast cancer patients. However, as of the writing of this article (22.01.2022), the results have not been published. Therefore, it is still to be seen if the NeoNavia® Biopsy System is able to sample sufficiently enough for conclusive nodal staging.

The B.L.E.S device appears to be a ready-made device capable of large-volume excisions [2], [32], [52]. It definitely fulfils the requirements of small incision (8-10mm wide [32]), local anaesthesia and minimum tissue damage, however, there are some aspects that need to be considered. For example: the B.L.E.S. is designed and used for breast lesions. Meaning it only has to cut breast tissue (mainly adipose tissue). LNs are embedded in adipose tissue, but are close to blood vessels, muscle tissue and bones. This might present a problem with the deployment of the basket, as has been reported happening with more dense breast tissue [32].

Another problem is the pointed tip that penetrating the lesion in order to fixate and prevent partial excision [32]. This is not acceptable when excising SLNs. The SLNs have to be intact, otherwise the pathological evaluation is impaired.

Also, the B.L.E.S. wire baskets can be changed to accommodate for varying lesion sizes; however, they are relatively rigid their volume. It needs to be investigated whether the B.L.E.S. would be able to circumscribe a SLN. This investigation is not possible due to the discontinuation of the B.L.E.S. by MEDTRONIC Inc. as well as the worldwide recall of the B.L.E.S.. A search of the Manufacturer and User Facility Device Experience (M.A.U.D.E.) database has not revealed why the B.L.E.S. is being recalled. Due to the inability to further investigate this product, it cannot be concluded that this is a ready-made mechanism for a MISLNB medical device.

This concludes the analysis of the most important results that were obtained by the systematic search of available information pertaining to a MISLNB medical device.

### C. Future Research

Next, an outlook on future research as well as the limitations of this article will be presented. There is still a lot of research to be done before a MISLNB medical device design is finished.

As this article has shown, there is currently no device or mechanism that can readily be adapted to fit a MISLNB medical device adhering to the requirements.

The patent by Fawiz et al. as well as Aristotle's lantern seem to be two concepts that need to be further investigated in order to determine their ability to fulfil the mentioned requirements (IV). A first step would be a thorough search

about the status of ring-cutter patent by Fawiz et al. [21]. There might already be a medical device on the market that was not picked up by the author's search.

Also, the patent by Sirimanne et al. inspired an idea for an excision mechanism that needs to be worked out further and be conceptualised.

Next the mechanisms would have to be designed to theoretically fulfil the requirements and prototypes will need to be build and tested.

Other registries such as *Espacenet* and *Depatisnet* should be combed through to find more inspiration on possible mechanisms concepts in case the current concepts do not work.

The material properties of the LNs need to be researched. Knowing these, might facilitate the design process and save costs when building prototypes. Unfortunately, as of writing this article, next to nothing is known about the Young's modulus, impedance, or reflectance of LNs. These are all properties that give valuable input to a designer.

Another aspect that will have to be investigated is imaging and navigation. As of now, lymphoscintigraphy is used to identify, image, and navigate to SLNs. Due to its use of radioactivity, it is wishful to investigate other lanes. In order to reap the most economic benefits it is beneficial to completely omit the use of radioactive colloids, because of the necessity of the involvement of the department of nuclear medicine. One solution could be a pre-procedural 3D echo imaging with an in-procedure artificial intelligence assisted US guided insertion of the device. This are just preliminary ideas that need to be researched further.

At a later stage in the design process, it will be of value to perform surveys on what surgeons and patients wish for with this product. For now, this is not relevant because first the working mechanism of the device has to be ascertained. The knowledge and experience of patients and surgeons will give valuable input that should be considered when it comes to design aspects such as actuation of device, shape, and form. Aspects of patient experience can potentially have an influence on the design as well. For instance, do the patients prefer to sit or lie when the biopsy is done. And what do the surgeons who will use this device think about this. It is however important to involve surgeons from the beginning because of the extra point of view the engineer gets. They know what they want and what is possible, and what may not be due to anatomy. This is why regular meetings with the surgeons is to be wished for in order to stay on a reasonable path with the development of the product.

### D. Limitations

In terms of limitations concerning this article, one is that only one registry was searched. With the knowledge of now, a solely registry-based literature review might reveal more relevant findings pertaining to answering the research question.

Also, the registry was searched with Boolean search terms and not on INID codes. A search on INID codes should have delivered more search results

Another limitation is the broadness of the search. By keeping the search terms broad, more specific solutions might have been missed, or designs might have slipped through the cracks due to the sheer number of results.

This might be the reason that medical devices such as the breast lesion excision system (B.L.E.S.) [52] or the punch biopsy mechanisms [35] were not picked up by the searches. Due to the B.L.E.S. being a large volume biopsy device that was investigated as a percutaneous lumpectomy device, it was included in the results and analysis sections. The B.L.E.S. will furthermore be taken into and evaluated in the design process.

The author does not claim that this literature study includes all the sample collection mechanisms that have been thought of.

## V. DISCUSSION

This section answers the research question and discusses the results and subsequent analysis from sections III (Results) and IV (Analysis) with respect to a MISLNB medical device.

The research question has to be negated. There is currently no device or mechanism already in use that can easily be adapted to fit a MISLNB medical device.

This study reviewed a lot of different scientific articles concerned with different fields. It explained the importance of a MISLNB medical device and showed the methodology applied for the systematic searches across several databases and registries. The most promising and intriguing collecting mechanisms were chosen and presented in section III (Results) and subsequently analysed in section IV (Analysis). The analysis was done based on requirements the MISLNB medical device has to fulfil in order to solve the problem at hand: being able to excise SLNs *en bloc* while reducing morbidities experienced by the patients.

Thereby reducing the risk of experiencing morbidities significantly and making the procedure as a whole more attractive to patients and physicians because of advantages such as: local anaesthesia only, out-house patients, faster recovery, no complete operating room team needed, easier planning for the hospital

Although the research question had to be negated based on the results and their analysis, several promising concepts were brought to light. By radically adapting and possibly combining the ring-cutter [21] with electronic devices such as the DRS [58], the author believes that a working MISLNB medical device fulfilling all requirements can be achieved.

The author sees great potential in the optomechanical biopsy tip. But due to the reasons mentioned in the analysis section, the author believes that adapting this mechanism to suit the MISLNB medical device will be much more challenging and less rewarding since the great advantage the designs by Fawiz

et al. and Sirimanne et al. have is their ability to be folded, see Figure 8. Making the damage to the tissue minimal while inserting the device, and only deploying the device once in position. The designs can also accommodate LNs of different sizes. Making it them the most viable option in the authors opinion.

Considering this, it is the author's opinion that a MISLNB medical device is possible. But developing this device is not straight forward since no mechanism or device is currently available to readily be applied.

## VI. ACKNOWLEDGEMENTS

This literature research was written as part of the Master of Science program for Biomedical Engineering with a specialisation in Medical Devices as devised by Delft University of Technology. The MISLNB medical device project was conceived by dr. Dirk Grünhagen (Erasmus Medical Center Cancer Institute) and is a collaboration between the Erasmus Medical Center Cancer Institute (EMC) and Delft University of Technology (TUD).

This literature research was performed under the supervision of dr. ir. J. J. van den Dobbelsteen (TUD) and E. E. A. P. Mulder (EMC), whom I am grateful for their support and the opportunity to partake in this fascinating project.

Many thanks also to A. Schurink who offered a critical viewpoint pertaining to the search strategy as well as the inclusion and exclusion criteria.

## REFERENCES

- [1] P. C. Alguire and B. M. Mathes. Skin biopsy techniques for the internist. *Journal of general internal medicine*, 13(1):46–54, 1998.
- [2] S. D. Allen, A. Nerurkar, and G. U. Q. Della Rovere. The breast lesion excision system (bles): a novel technique in the diagnostic and therapeutic management of small indeterminate breast lesions? *European radiology*, 21(5):919–924, 2011.
- [3] E. Arkenbout, L. van den Haak, M. Penning, E. Rog, A. Vierwind, L. van Cappelle, F. Jansen, and J. de Winter. A laparoscopic morcellator redesign to constrain tissue using integrated gripping teeth. *Journal of Medical Devices*, 11(1), 2017.
- [4] P. A. Ascierto, M. Del Vecchio, M. Mandalá, H. Gogas, A. M. Arance, S. Dalle, C. L. Cowey, M. Schenker, J.-J. Grob, V. Chiarion-Sileni, et al. Adjuvant nivolumab versus ipilimumab in resected stage iiib–c and stage iv melanoma (checkmate 238): 4-year results from a multicentre, double-blind, randomised, controlled, phase 3 trial. *The Lancet Oncology*, 21(11):1465–1477, 2020.
- [5] A. Bodenham and S. Howell. General anaesthesia vs local anaesthesia: an ongoing story, 2009.
- [6] N. Bontumasi, J. A. Jacobson, E. Caoili, C. Brandon, S. M. Kim, and D. Jamadar. Inguinal lymph nodes: size, number, and other characteristics in asymptomatic patients by ct. *Surgical and Radiologic Anatomy*, 36(10):1051–1055, 2014.
- [7] L. Bouré. General principles of laparoscopy. *Veterinary Clinics: Food Animal Practice*, 21(1):227–249, 2005.
- [8] W. Brinkmann, F. Cordes, T. M. Roehr, L. Christensen, T. Stark, R. U. Sonsalla, R. Szczuka, N. A. Mulsow, F. Bernhard, and D. Kuehn. Modular payload-items for payload-assembly and system enhancement for future planetary missions. In *2018 IEEE aerospace conference*, pages 1–12. IEEE, 2018.
- [9] S. Cabrera, V. Bebia, S. Franco-Camps, C. Forcada, D. Villasboas-Rosciolesi, I. Navales, A. Pérez-Benavente, and A. Gil-Moreno. Technetium-99m-indocyanine green versus technetium-99m-methylene blue for sentinel lymph node biopsy in early-stage endometrial cancer. *International Journal of Gynecologic Cancer*, 30(3), 2020.



- [10] M. Casaccia, R. Fornaro, F. S. Papadia, T. Testa, M. Mascherini, A. Ibatici, C. Ghiggi, S. Bregante, and F. De Cian. Single-port vs. conventional multi-port laparoscopic lymph node biopsy. *JSL: Journal of the Society of Laparoscopic & Robotic Surgeons*, 24(4), 2020.
- [11] J. M. Chang, J. W. Leung, L. Moy, S. M. Ha, and W. K. Moon. Axillary nodal evaluation in breast cancer: state of the art. *Radiology*, 295(3):500–515, 2020.
- [12] S. Choi and K. El-Hayek. Endoscopic equipment—from simple to advanced. *Surgical Clinics*, 100(6):993–1019, 2020.
- [13] M. G. Cook, D. Massi, A. Szumera-Ciećkiewicz, J. Van den Oord, W. Blokk, L. C. van Kempen, T. Balamurugan, F. Bosisio, S. Koljenović, F. Portelli, et al. An updated european organisation for research and treatment of cancer (eortc) protocol for pathological evaluation of sentinel lymph nodes for melanoma. *European Journal of Cancer*, 114:1–7, 2019.
- [14] E. A. Deckers, M. W. Louwman, S. Kruijff, and H. J. Hoekstra. Increase of sentinel lymph node melanoma staging in the netherlands; still room and need for further improvement. *Melanoma management*, 7(1):MMT38, 2020.
- [15] A. F. Delgado, S. Zommorodi, and A. F. Delgado. Sentinel lymph node biopsy and complete lymph node dissection for melanoma. *Current oncology reports*, 21(6):1–7, 2019.
- [16] P. Deyhle, F. Largiader, S. Jenny, and I. Fumagalli. A method for endoscopic electroresection of sessile colonic polyps. *Endoscopy*, 5(01):38–40, 1973.
- [17] N. U. Dogan, S. Dogan, G. Favero, C. Köhler, and P. Dursun. The basics of sentinel lymph node biopsy: anatomical and pathophysiological considerations and clinical aspects. *Journal of oncology*, 2019, 2019.
- [18] R. Dummer, A. Hauschild, M. Santinami, V. Atkinson, M. Mandalà, J. M. Kirkwood, V. Chiarion Sileni, J. Larkin, M. Nyakas, C. Dutriaux, et al. Five-year analysis of adjuvant dabrafenib plus trametinib in stage iii melanoma. *New England Journal of Medicine*, 383(12):1139–1148, 2020.
- [19] N. DynamicsAB. Needle types.
- [20] A. M. Eggermont, C. U. Blank, M. Mandalà, G. V. Long, V. G. Atkinson, S. Dalle, A. M. Haydon, A. Meshcheryakov, A. Khattak, M. S. Carlino, et al. Adjuvant pembrolizumab versus placebo in resected stage iii melanoma (eortc 1325-mg/keynote-054): distant metastasis-free survival results from a double-blind, randomised, controlled, phase 3 trial. *The Lancet Oncology*, 22(5):643–654, 2021.
- [21] N. V. Fawiz, D. L. Sirimanne, G. D. Hermann, D. S. Sutton, and T. A. Howell. Expandable ring percutaneous tissue removal device. <https://patentimages.storage.googleapis.com/aa/24/f9/f21625df78b3a7/US6471709.pdf>, US 6,471,709 B1, Oct. 2002.
- [22] M. Frumovitz and A. Buda. Encouraging worldwide adoption of sentinel lymph node biopsies for gynecologic malignancies. *International Journal of Gynecological Cancer*, 30(3):281–282, 2020.
- [23] C. J. Fyock and P. V. Draganov. Colonoscopic polypectomy and associated techniques. *World Journal of Gastroenterology: WJG*, 16(29):3630, 2010.
- [24] S. Ganeshalingam and D.-M. Koh. Nodal staging. *Cancer Imaging*, 9(1):104, 2009.
- [25] M. Gherghe, C. Bordea, and A. Blidaru. Sentinel lymph node biopsy (slnb) vs. axillary lymph node dissection (alnd) in the current surgical treatment of early stage breast cancer. *Journal of medicine and life*, 8(2):176, 2015.
- [26] B. Haggemueller, T. Breining, C. Kloth, S. A. Schmidt, M. Huber, J. B. Hagemann, S. Traub, and D. Voegelé. Lethal course due to an infectious soft tissue emphysema. *Der Radiologe*, 61(8):748–751, 2021.
- [27] J. Halfar, K. Brožová, K. Čabanová, S. Heviánková, A. Kašpárková, and E. Olšovská. Disparities in methods used to determine microplastics in the aquatic environment: a review of legislation, sampling process and instrumental analysis. *International Journal of Environmental Research and Public Health*, 18(14):7608, 2021.
- [28] A. Isakov, K. M. Murdaugh, W. C. Burke, S. Zimmerman, E. Roche, D. Holland, J. I. Einarsson, and C. J. Walsh. A new laparoscopic morcellator using an actuated wire mesh and bag. *Journal of Medical Devices*, 8(1), 2014.
- [29] L. Jandura. Mars science laboratory sample acquisition, sample processing and handling: subsystem design and test challenges. In *Proceedings of the 40th aerospace mechanisms symposium*, pages 233–248. NASA Kennedy Space Center FL, 2010.
- [30] F. Jelínek, G. Smit, and P. Breedveld. Bioinspired spring-loaded biopsy harvester—experimental prototype design and feasibility tests. *Journal of Medical Devices*, 8(1), 2014.
- [31] B. Jürgens and V. Herrero-Solana. Espacenet, patentscope and depatisnet: A comparison approach. *World Patent Information*, 42:4–12, 2015.
- [32] H. M. Karakas and G. Yildirim. Minimally invasive excision of breast masses under ultrasound guidance: A single center’s five-year experience on the breast lesion excision system. *The Breast Journal*, 2022, 2022.
- [33] E. Z. Keung and J. E. Gershenwald. The eighth edition american joint committee on cancer (ajcc) melanoma staging system: implications for melanoma treatment and care. *Expert review of anticancer therapy*, 18(8):775–784, 2018.
- [34] T. Kim, A. E. Giuliano, and G. H. Lyman. Lymphatic mapping and sentinel lymph node biopsy in early-stage breast carcinoma: a metaanalysis. *Cancer*, 106(1):4–16, 2006.
- [35] T. Lapa. The tangential punch biopsy. *Dermatology Online Journal*, 25(12):14, 2019.
- [36] K. M. Lin, T. H. Patel, A. Ray, M. Ota, L. Jacobs, B. Kuvshinoff, M. Chung, M. Watson, and D. M. Ota. Intradermal radioisotope is superior to peritumoral blue dye or radioisotope in identifying breast cancer sentinel nodes. *Journal of the American College of Surgeons*, 199(4):561–566, 2004.
- [37] G. V. Long, A. Hauschild, M. Santinami, V. Atkinson, M. Mandalà, V. Chiarion-Sileni, J. Larkin, M. Nyakas, C. Dutriaux, A. Haydon, et al. Adjuvant dabrafenib plus trametinib in stage iii braf-mutated melanoma. *New England Journal of Medicine*, 377(19):1813–1823, 2017.
- [38] P. R. Mahaffy, C. R. Webster, M. Cabane, P. G. Conrad, P. Coll, S. K. Atreya, R. Arvey, M. Barciniak, M. Benna, L. Bleacher, et al. The sample analysis at mars investigation and instrument suite. *Space Science Reviews*, 170(1):401–478, 2012.
- [39] C. Mathelin, S. Salvador, D. Huss, and J.-L. Guyonnet. Precise localization of sentinel lymph nodes and estimation of their depth using a prototype intraoperative mini  $\gamma$ -camera in patients with breast cancer. *Journal of Nuclear Medicine*, 48(4):623–629, 2007.
- [40] K. M. McMasters, D. S. Reintgen, M. I. Ross, J. E. Gershenwald, M. J. Edwards, A. Sober, N. Fenske, F. Glass, C. M. Balch, and D. G. Coit. Sentinel lymph node biopsy for melanoma: controversy despite widespread agreement. *Journal of Clinical Oncology*, 19(11):2851–2855, 2001.
- [41] J. Merkow, A. Paniccia, E. Jones, T. Jones, M. Hodges, R. Stovall, N. Koulalakis, C. Gajdos, K. Lewis, W. Robinson, et al. Association of sentinel lymph node diameter with melanoma metastasis. *The American Journal of Surgery*, 212(2):315–320, 2016.
- [42] D. Moher, A. Liberati, J. Tetzlaff, D. G. Altman, and P. Group. Preferred reporting items for systematic reviews and meta-analyses: the prisma statement. *PLoS medicine*, 6(7):e1000097, 2009.
- [43] V. M. Moncayo, J. N. Aarsvold, and N. P. Alazraki. Lymphoscintigraphy and sentinel nodes. *Journal of Nuclear Medicine*, 56(6):901–907, 2015.
- [44] NeoDynamics. Neodynamics has filed for registration of neonavia® in the us, Mar 2022.
- [45] A. Nevler, G. Har-Zahav, A. Abraham, G. Schiby, O. Zmora, M. Shabtai, M. Gutman, and D. Rosin. Laparoscopic lymph node biopsy: Efficacy and advantages. *The Israel Medical Association Journal: IMAJ*, 19(4):231–233, 2017.
- [46] D. Olmedo, M. Brotons-Seguí, C. Del Toro, M. Gonzalez, C. Requena, V. Traves, A. Pla, I. Bolumar, D. Moreno-Ramírez, and E. Nagore. Valor de la ecografía ganglionar previa a la biopsia del ganglio centinela en 384 pacientes con melanoma: análisis de coste-efectividad. *Actas Dermo-Sifilográficas (English Edition)*, 108(10):931–938, 2017.
- [47] C. M. O. Ophuis, L. B. Koppert, C. De Monyé, C. H. van Beurden, S. Koljenović, A. C. van Akkooi, C. Verhoef, and D. J. Grünhagen. Gamma probe and ultrasound guided fine needle aspiration cytology of the sentinel node (gulf) trial—overview of the literature, pilot and study protocol. *BMC cancer*, 17(1):1–9, 2017.
- [48] C. M. O. Ophuis, A. C. van Akkooi, P. Rutkowski, C. A. Voit, J. Stepniak, N. S. Erler, A. M. Eggermont, M. W. Wouters, D. J. Grünhagen, and C. K. Verhoef. Effects of time interval between primary melanoma excision and sentinel node biopsy on positivity rate and survival. *European Journal of Cancer*, 67:164–173, 2016.
- [49] C. Ottomann et al. Resection force analysis of 1 and 2 mm punch biopsies combined with rotation on temperature-controlled cadaver skin use for the acquisition of full skin islets for skin transplantation. *Int J Biotech & Bioeng*, 3(5):109–114, 2017.
- [50] F. Petrelli, V. Lonati, and S. Barni. Axillary dissection compared to sentinel node biopsy for the treatment of pathologically node-negative breast cancer: a meta-analysis of four randomized trials with long-term follow up. *Oncology reviews*, 6(2), 2012.

- [51] W. Sanderink. *Detection and minimally invasive treatment of small breast cancers*. PhD thesis, [SI: sn], 2021.
- [52] W. Sanderink, L. Strobbe, P. Bult, M. Schlooz-Vries, S. Lardenoije, D. Venderink, I. Sechopoulos, N. Karssemeijer, W. Vreuls, and R. Mann. Minimally invasive breast cancer excision using the breast lesion excision system under ultrasound guidance. *Breast Cancer Research and Treatment*, 184(1):37–43, 2020.
- [53] M. Savazzi, S. Abedi, N. Ištuk, N. Joachimowicz, H. Roussel, E. Porter, M. O'Halloran, J. R. Costa, C. A. Fernandes, J. M. Felício, et al. Development of an anthropomorphic phantom of the axillary region for microwave imaging assessment. *Sensors*, 20(17):4968, 2020.
- [54] H. Sawada, R. Okazaki, S. Tachibana, K. Sakamoto, Y. Takano, C. Okamoto, H. Yano, Y. Miura, M. Abe, S. Hasegawa, et al. Hayabusa2 sampler: Collection of asteroidal surface material. *Space Science Reviews*, 208(1):81–106, 2017.
- [55] K.-U. Schässburger, S. Paepke, A. Saracco, E. Azavedo, C. Ekström, and H. Wiksell. High velocity pulse biopsy device enables controllable and precise needle insertion and high yield tissue acquisition. *Physica Medica*, 46:25–31, 2018.
- [56] D. L. Sirimanne, D. Fawiz, Natalie V., and Sutton. Device and method for safe location and marking of a biopsy cavity. [https://patentscope.wipo.int/search/en/detail.jsf?docId=US43358722&\\_cid=P21-KY04HS-00209-1](https://patentscope.wipo.int/search/en/detail.jsf?docId=US43358722&_cid=P21-KY04HS-00209-1), US 20100234726, May 2010.
- [57] J. Smedley, R. Macalister, S. Wangari, M. Gathuka, J. Ahrens, N. Iwayama, D. May, D. Bratt, M. O'Connor, P. Munson, et al. Laparoscopic technique for serial collection of para-colonic, left colic, and inferior mesenteric lymph nodes in macaques. *PLoS One*, 11(6):e0157535, 2016.
- [58] A. Swamy, J. W. Spliethoff, G. Burström, D. Babic, C. Reich, J. Groen, E. Edström, A. Elmi-Terander, J. M. Racadio, J. Dankelman, et al. Diffuse reflectance spectroscopy for breach detection during pedicle screw placement: a first in vivo investigation in a porcine model. *BioMedical Engineering OnLine*, 19(1):1–12, 2020.
- [59] D. Tang, X. Gao, D. Zhao, S. Jiang, and Z. Deng. Analyses of sampling disturbance of the lunar surface in direct push sampling method. *IEEE Access*, 6:48656–48663, 2018.
- [60] M. Thill. Evaluation of neonavia® biopsy system in axillary lymph nodes (pulse). <https://clinicaltrials.gov/ct2/show/NCT03975855>, 2019. ClinicalTrials.gov Identifier: NCT03975855.
- [61] B. G. TuDelft. Biopsy harvester – high-speed tissue cutting. <https://www.bitegroup.nl/interventional-devices/biopsy-harvester/biopsy-harvester/>, Jan 2013.
- [62] D. Verver, C. M. O. Ophuis, L. B. Koppert, C. De Monyé, C. H. Van Deurzen, S. Koljenović, A. Bruining, B. Van Der Hiel, S. Ter Meulen, A. C. Van Akkooi, et al. Gamma probe and ultrasound-guided fine needle aspiration cytology of the sentinel node (gulf) trial. *European journal of nuclear medicine and molecular imaging*, 45(11):1926–1933, 2018.
- [63] C. A. Voit, C. M. O. Ophuis, J. Ulrich, A. C. van Akkooi, and A. M. Eggermont. Ultrasound of the sentinel node in melanoma patients: echo-free island is a discriminatory morphologic feature for node positivity. *Melanoma research*, 26(3):267–271, 2016.
- [64] J. Wei, A. Wang, J. L. Lambert, D. Wettergreen, N. Cabrol, K. Warren-Rhodes, and K. Zacny. Autonomous soil analysis by the mars micro-beam raman spectrometer (mmrs) on-board a rover in the atacama desert: a terrestrial test for planetary exploration. *Journal of Raman Spectroscopy*, 46(10):810–821, 2015.
- [65] T. Winstow. Sentinel lymph node biopsy - national cancer institute. <https://www.cancer.gov/about-cancer/diagnosis-staging/staging/sentinel-node-biopsy-fact-sheet>, June 2019. (Accessed on 12/16/2021).
- [66] S. L. Wong, M. B. Faries, E. B. Kennedy, S. S. Agarwala, T. J. Akhurst, C. Ariyan, C. M. Balch, B. S. Berman, A. Cochran, K. A. Delman, et al. Sentinel lymph node biopsy and management of regional lymph nodes in melanoma: American society of clinical oncology and society of surgical oncology clinical practice guideline update. *Annals of surgical oncology*, 25(2):356–377, 2018.
- [67] P. Y. Wuethrich, S.-F. Hsu Schmitz, T. M. Kessler, G. N. Thalmann, U. E. Studer, F. Stueber, and F. C. Burkhard. Potential influence of the anesthetic technique used during open radical prostatectomy on prostate cancer-related outcome: a retrospective study. *The Journal of the American Society of Anesthesiologists*, 113(3):570–576, 2010.
- [68] T. Zhang, B. Wang, H. Wei, Y. Zhang, C. Chao, K. Xu, X. Ding, X. Hou, and Z. Zhao. Review on planetary regolith-sampling technology. *Progress in Aerospace Sciences*, 127:100760, 2021.
- [69] G. Zhao, L. Xiao, T. Peng, and M. Zhang. Experimental research on hydraulic collecting spherical particles in deep sea mining. *Energies*, 11(8):1938, 2018.

APPENDIX  
SEARCHES

Here, a list of the executed searches performed in January 2022 can be found. The table below lists the search-terms, applied filters and hits per database per search. All the filters were set to either "include" or "limit to" depending on the database settings.

TABLE I

THIS TABLE LISTS THE EXACT SEARCH-TERMS USED BY THE AUTHOR IN JANUARY 2022. THE SEARCHED DATABASE CAN BE SEEN IN THE SECOND COLUMN. THE SEARCH-TERM CAN BE FOUND IN THE THIRD. IN THE FOURTH COLUMN THE APPLIED FILTERS CAN BE SEEN. THE FILTER-OPTION DIFFERED PER DATABASE AND SOMETIMES EVEN PER SEARCH. IN THE FURTHEST COLUMN TO THE RIGHT THE AMOUNT OF SEARCH-HITS CAN BE SEEN. THESE HITS WERE THEN EVALUATED BY THE AUTHOR BASED ON TITLE AND PREVIEW VISIBLE.

#	DATABASE / REGISTRY	SEARCH-TERM	FILTERS	HITS
1	Pubmed	(collecting OR excision) AND (device OR mechanism) AND probe AND geology	/	6
2		minimally invasive tissue sampling mechanism	-free full text -full text	57
3		minimally invasive tissue sampling mechanism	-free full text -full text -books & documents -clinical trial -meta-analysis -randomized controlled trial -review -systematic review	8
4	Scopus	(collecting OR sampling) AND (device OR mechanism OR technique) AND aerospace	-engineering -medicine and multidisciplinary	37
5		(collecting OR sampling) AND (device OR mechanism OR technique) AND aerospace	-open access -engineering -articles -reviews	22
6		(collecting OR sampling) AND (device OR mechanism) AND mining	-open access -articles -reviews -engineering	52
7		(minimally AND invasive AND tissue AND sampling AND mechanism)	-open access -articles -reviews -chapters	17
8	Web of Science	minimally invasive tissue sampling mechanism	-biomedical engineering -instruments instrumentation	43
9		((collecting OR sampling) AND (device OR mechanism OR technique) AND aerospace)	-review articles	283
10		((collecting OR sampling) AND (device OR mechanism OR technique) AND mining)	-review articles -biochemical research methods -environmental sciences	85
11	Patentscope	lymph node biopsy device	N/A	35
12		minimally invasive tissue sampling device	N/A	31
13	NASA	sampling instrument	N/A	10

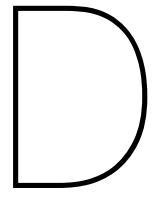
LIST OF ALL RELEVANT PAPERS

The following table lists all the 33 relevant results that were found during the systematic search in the databases *Scopus*, *Pubmed*, *Web of Science* as well as the registry *Patentscope*.

TABLE II

THIS TABLE INCLUDES ALL THE PAPERS THAT WERE FOUND RELEVANT BY THE AUTHOR. HOWEVER, NOT ALL WERE CONSIDERED RELEVANT ENOUGH TO BE MENTIONED IN DETAIL IN THIS ARTICLE.

#	TITLE	AUTHOR	REMARK
1	Modular Payload-Items for Payload-assembly and System Enhancement for Future Planetary Missions	W. Brinkmann et al.	aerospace
2	Hayabusa2 extended mission: New voyage to rendezvous with a small asteroid rotating with a short period	H. Sawada et al.	aerospace
3	Analysis of Sampling Disturbance of the Lunar Surface in Direct Push Sampling Method	D. Tang et al.	aerospace
4	Experimental Research on Hydraulic Collecting Spherical Particles in Deep Sea Mining	G. Zhao et al.	deep sea mining
5	METHOD AND INSTRUMENT FOR MINIMALLY INVASIVE SENTINEL LYMPH NODE LOCATION AND BIOPSY	R. Essner et al.	US 20060106306 - B2
6	DEVICE AND METHOD FOR SAFE LOCATION AND MARKING OF A BIOPSY CAVITY	D. L. Sirimanne et al.	US 201000234726 -B2
7	EXPANDABLE RING PERCUTANEOUS TISSUE REMOVAL DEVICE	N. V. Fawiz et al.	US 6471709 - B1
8	ENERGY-BASED LYMPH NODE DISSECTION DEVICE	A. B. Ross et al.	US 20160089119 - A1
9	Energy devices safety and impact on video-assisted thoracoscopic lung lobectomy postoperative course: monopolar electrocautery versus ultrasonic dissector	M. Cattoni et al.	
10	BIOPSY DEVICE	L. P. Cervi	US 20030171766 - B1
11	SENTINEL NODE LOCATION AND BIOPSY	F. H. Burbank et al.	US 20010002250 - B2
12	DIGESTIVE TRACT EXTRACAVITARY COMPLETE LYMPH NODE BIOPSY DEVICE AND BIOPSY SYSTEM	X. Yang et al.	CN 209285581 - U
13	INTRAUTERINE INTACT LYMPH NODE BIOPSY DEVICE, BIOPSY SYSTEM AND USE METHOD THEREOF	X. Yang et al.	CN 109124693 - A
14	MINIMALLY INVASIVE LIVING BODY SAMPLING DEVICE FOR BREAST NODULES	W. Wang	CN 112572149 - A
15	DEVICE FOR MINIMALLY INVASIVE INTERNAL TISSUE REMOVAL	C. W. Cicenas et al.	EP 1839582 - B1 EP 1832235 - B1 CN 101032419 - B US 20070239064 - B2
16	CERVICAL SAMPLING FORCEPS	X. Qiangsheng et al.	CN 208988967 - U
17	SAFE MULTIFUNCTIONAL PERCUTANEOUS PUNCTURE DEVICE FOR ABDOMINAL CAVITY DIAGNOSIS AND TREATMENT	L. Yuan	CN 111227876 - A
18	BIOPSY NEEDLE	Y. Duan et al.	CN 107260230 - A
19	High velocity pulse biopsy device enables controllable and precise needle insertion and high yield tissue acquisition	K.-U. Schässburgera et al.	needle biopsy
20	Virtobot 2.0: the future of automated surface documentation and CT-guided needle placement in forensic medicine	L. C. Ebert et al.	forensic needle biopsy, us-guided
21	Development of an MRI-Compatible Needle Driver for In-Bore Prostate Biopsy	M. Li et al.	needle biopsy for prostate tumour
22	Laparoscopic Technique for Serial Collection of Para-Colonic Left Colic, and Inferior Mesenteric Lymph Nodes in Macaques	J. Smedley et al.	laparoscopic SLNB
23	Evaluation of Pathological Findings of COVID-19 by Minimally Invasive Autopsies: A Single Tertiary Care Center Experience from India	V. Vishwajeet et al.	post mortem core needle biopsy
24	PIPES: Piezoelectric Instrument for Precision Exploration Sampling	J. Xu	collecting tube for microorganisms
25	Rover Arm Delivers Rock Powder Sample	T. Greicius	percussion sampling
26	NASA - Mars Soil Sample Delivered for Analysis Inside Rover	NASA	scoop for soil collection
27	The Next Step in NASA's Hunt for Life: Scientist Begins Developing Instrument for Finding Extraterrestrial Bacteria	L. Keesey	water sample acquisition
28	A Laparoscopic Morcellator Redesign to Constrain Tissue Using Integrated Gripping Teeth	E. A. Arkenbout et al.	laparoscopic morcellator
29	Bioinspired Spring-Loaded Biopsy Harvester- Experimental Prototype Design and Feasibility Test	F. Jelinek et al.	laparoscopic optomechanical biopsy tip
30	A new Laparoscopic Morcellator Using an Actuated Wire Mech and Bag	A. Isakov et al.	laparoscopic morcellator net
31	Review on planetary regolith-sampling technology	T. Zhang et al.	aerospace
32	The Sample Analysis at Mars Investigation and Instrument Suite	P. R. Mahaffy et al.	SAM, mars sample analysis demonstrates 6 sampling devices for water sampling:
33	In Situ Soil Water Extraction: A Review	L. Weihermüller et al.	- porous cups -porous plates - capillary wicks - pan lysimeters - resin boxes - lysimeters



## Blade Test Run Tables

Figure D.1: screenshot from the actual excel RunTable. RunTable of 0.04mm tests. This figure is a screen-capture of the actual RunTable made in Microsoft Excel (Microsoft, Redmond, Washington, United States)

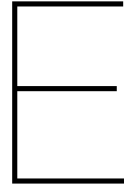
	#*	thickness [mm]	MODE		max FORCE		Remark
			insertion	cutting	[V]	[N]	
CUTTING	1	0.04		x	-4.494	3.483	*video
	1.2	0.04		x	-4.506	7.333	the tip at the far end came loose a bit. Needed
	2	0.04		x	-4.517	7.435	
	3	0.04		x	-4.520	7.381	
	4	0.04		x	-4.521	7.946	*blade detached -- > new one
	5	0.04		x	-4.523	7.090	
	6	0.04		x	-4.513	7.692	
	7	0.04		x	-4.513	8.549	
	8	0.04		x	-4.512	7.505	*incomplete cut *incomplete cut --
	9	0.04		x	-4.519	7.234	> termination of
INSERTION	1	0.04	x		-4.440	2.865	
	2	0.04	x		-4.465	3.149	
	3	0.04	x		-4.428	2.603	
	4	0.04	x		-4.441	2.354	*a bit far to the
	5	0.04	x		-4.489	2.354	
	6	0.04	x		-4.483	2.997	
	7	0.04	x		-4.439	2.659	
	8	0.04	x		-4.469	2.940	
	9	0.04	x		-4.435	2.531	
	10	0.04	x		-4.457	2.753	

Figure D.2: screenshot from the actual excel RunTable. RunTable of 0.05mm tests. This figure is a screen-capture of the actual RunTable made in Microsoft Excel (Microsoft, Redmond, Washington, United States)

	#*	thickness [mm]	MODE		FORCE		Remark
			insertion	cutting	[V]	[N]	
CUTTING	1	0.05		x	-4.504	9.200	*video
	2			x	-4.514	9.645	
	3	0.05		x	-4.512	9.806	
	4	0.05		x	-4.492	8.810	
	5	0.05		x	-4.514	8.531	
	6	0.05		x	-4.512	8.652	*incomplete cut
	7	0.05		x	-4.513	5.779	*complete cut
	8	0.05		x	-4.513	6.277	
	9	0.05		x	-4.514	9.993	*cut through dried bubbles
	10			x	-4.511	9.629	*cut through dried bubbles
INSERTION	1	0.05	x		-4.477	2.254	
	2	0.05	x		-4.486	2.158	
	3	0.05	x		-4.464	2.171	
	4	0.05	x		-4.460	2.198	
	5	0.05	x		-4.466	2.166	
	6	0.05	x		-4.491	2.356	
	7	0.05	x		-4.472	2.091	
	8	0.05	x		-4.488	2.131	
	9	0.05	x		-4.467	1.936	
	10	0.05	x		-4.462	1.965	







# Test Protocol for Prototype 1

## E.0.1. Goal

The goal of this test is two-fold: 1) the test is to be a proof-of-principal concerning the designed working principle of a medical device; 2) to measure the insertion force of the spring in extended and folded configuration.

## E.0.2. Requirements

To do the tests, previously fabricated phantoms are needed. For the fabrication see the document “Phantom Fabrication Prototype 1 testing”, F.

Prototype 1 consists of two poles, two caps, 10 blades (five of  $0.04mm$  thickness and five of  $0.05mm$  thickness).

The *device holder* is needed to execute this protocol.

## E.0.3. Important

The driving/ steering mechanism of the design is not being implemented. For the time being, the desktop prototype will be actuated with two hands. The same is true for the first proper prototype. The plan is to implement an actuation mechanism once the proof-of-principal tests have been passed.

## E.1. Proof-of-Principal

### Why

This test is important because it will determine whether cutting LNs from adipose tissue using this mechanism is possible.

The test will be executed on tissue phantoms first and later, in case of positive results, on human tissue.

For now, the actuation mechanism that enables the user to steer the mechanism with one hand is not implemented. This has no influence on the mechanism itself. This way there is more room for manoeuvring the device before decreasing the DoFs (degrees of freedom) later. Crucial findings might be done with respect to how the actuation mechanism will have to act for optimum results.

### How

The phantoms are taken out of the refrigerator about 30 minutes before the test can commence.

For this test, no force sensor is needed.

The phantom is placed in the cupcake-tray for fastening. Then the device is deployed. The device is actuated with both hands. And the working principle is tested.

There are two different spring thicknesses (other dimensions, length and height are the same):

- 0.04mm
- 0.05mm

The rods are 2mm in diameter and 60mm in length with a small slit at the top to insert the ring-cutter-leaf-spring-blade.

### Preparation

Execute the following steps:

1. record which phantom is used, to identify the ALN's size later
2. make sure the phantom has reached room temperature (≈30 minutes outside the refrigerator)

### E.1.1. Execution

For execution of this test, follow these steps:

1. place the phantom on a flat, sturdy surface
2. optional: position a camera to record the test

the next steps are done by hand:

1. wind the blade around one pole to bring the device into "insertion" mode
2. insert the device next to the ALN
3. begin unwinding the blade by rotating the pole the blade is wrapped around
4. simultaneously, move the other pole around the ALN in a spiral motion
5. when the blade is fully unwound, the device should have circumferenced the ALN
6. retrieve the device
7. note whether the test was a success and whether the ALN was retrieved by retrieving the device in the *RunTable*

### E.1.2. Clean-up

1. throw the phantom and ALN out
2. wash the device
3. store the dry device

## E.2. Cutting force

### Why

It is important to measure the cutting force of the device because this is important in validating the concept in terms of leaf spring thickness as well as one of the determining factors for the importance of implementing a cauterisation mechanism.

Therefore, the cutting force has implications for the design and the use of the device and the feasibility of the design.

### How

First, a calibration test is run to determine the sensor calibration.

Next, a piece of gelatine is laid on a towel underneath the sensor. Next, the rods are fastened to the hook in the stage. Then the test is run.

This is done for the device in extended, aka ("cutting mode").

### Materials

- device
- device holder
- plastic cloth
- phantom with ALN
- something to adjust the height of the phantom with respect to the device
- linear stage + laptop + Matlab code
- personal laptop with *RunTable*

Prior to starting this test, the phantoms should be taken out of the refrigerator  $\approx 30$  minutes before testing. So that they are at room temperature when testing begins.

### E.2.1. Experimental Set-up

#### Preparation

Execute the following steps:

1. insert and fasten the device in the *device holder* in 'cutting' mode (the blade making a circle fully unwrapped from the pole)
2. trace the circumference of the device in the *device holder*
3. fasten the *device holder* with the device to the sensor using a M3 bolt
4. mark the device when first inserted into the *device holder*, this mark will be used for the ensuing tests as a marker on how far the device has to be inserted
5. run a test to see where the phantom needs to be in order to be almost completely cut
6. make sure the phantom is positioned to only be cut by the blade and not by the poles too

#### Calibration linear stage

Before every experiment, make sure the correct block is on the sensor, then the linear stage needs to be calibrated.

Execute the following steps for calibration:

1. move the linear stage 'home position' to 'initial position'
2. adjust the name the data will be saved to read '0g calibration'
3. make sure the *device holder* with the device fastened to it is attached to the stage
4. run the '0g calibration' test with setting: down 150mm @ 1mm/s

### E.2.2. Execution

Execute these steps in order to execute the test:

1. make sure the stage is in 'initial position' by clicking on it, now the stage is in starting position
2. make sure 'record 1' reads: 'down 150mm @ 1mm/s'
3. adjust the name the data will be saved under to include the mode the prototype is tested in and the blade thickness
4. now click "run". The linear stage will move downwards cutting the phantom. Do not touch anything before the run is completed. Otherwise, the measurements will be distorted.
5. Make sure to save this data correctly indicating which run it was and write additional comments in the *RunTable*.
6. Save all data (.mat file, videos, and photos)

### E.2.3. Clean-up

1. throw the used phantom out
2. disconnect the laptop
3. turn off the stage and unplug
4. make sure to transfer the recorded data to a USB drive or similar memory device
5. store the dry device

## E.3. Insertion force

### Why

It is important to measure the insertion force of the device because this is important in validating the concept in terms of leaf spring thickness as well as one of the determining factors for the importance of the implementation of a cauterisation mechanism.

Therefore, the insertion force has implications for the design and the use of the device and the feasibility of the design.

### How

First, a calibration test is run to determine the sensor calibration.

Roll up the device into insertion mode and draw its circumference on a piece of paper (device needs to be taped in order to keep mode).

Next, a piece of gelatine is laid on a towel underneath the sensor. Next, the rods are fastened to the hook in the stage. Then the test is run.

### Materials

- device
- device holder
- plastic cloth
- phantom with ALN
- something to adjust the height of the phantom with respect to the device
- linear stage + laptop + Matlab code
- personal laptop with *RunTable*

Prior to starting this test, the phantoms should be taken out of the refrigerator  $\approx 30$  minutes before testing. So that they are at room temperature when testing begins.

### E.3.1. Experimental Det-up

#### Preparation

Execute the following steps:

1. insert and fasten the device in the *device holder* in 'insertion' mode (the blade making a circle fully unwrapped from the pole)
2. trace the circumference of the device in the *device holder*
3. fasten the *device holder* with the device to the sensor using a M3 bolt
4. mark the device when first inserted into the *device holder*, this mark will be used for the ensuing tests as a marker on how far the device has to be inserted
5. run a test to see where the phantom needs to be in order to be almost completely cut

### Calibration linear stage

Before every experiment, make sure the correct block is on the sensor, then the linear stage needs to be calibrated.

Execute the following steps for calibration:

1. move the linear stage 'home position' to 'initial position'
2. adjust the name the data will be saved to read '0g calibration'
3. make sure the *device holder* with the device fastened to it is attached to the stage
4. run the '0g calibration' test with setting: down 150mm @ 1mm/s

### E.3.2. Execution

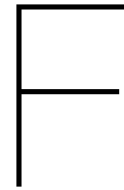
Execute these steps in order to execute the test:

1. make sure the stage is in 'initial position' by clicking on it, now the stage is in starting position
2. make sure 'record 1' reads: 'down 150mm @ 1mm/s'
3. adjust the name the data will be saved under to include the mode the prototype is tested in and the blade thickness
4. now click "run". The linear stage will move downwards cutting the phantom. Do not touch anything before the run is completed. Otherwise, the measurements will be distorted.
5. Make sure to save this data correctly indicating which run it was and write additional comments in the *RunTable*.
6. Save all data (.mat file, videos, and photos)

### E.3.3. Clean-up

1. throw the used phantom out
2. disconnect the laptop
3. turn off the stage and unplug
4. make sure to transfer the recorded data to a USB drive or similar memory device
5. store the dry device





# Phantom Fabrication Prototype 1 testing

## F.1. Disclaimer

A mistake was made in the fabrication of the second batch of phantoms fabricated for the tensile tests. The weight percent was calculated wrong. The weight percent ended up being 14.5wt% gelatine instead of 17wt%. This error was noticed when preparing this batch and corrected.

This error propagated through the *prototypeV0.1* tests.

This error should not have grave consequences because:

- For the tensile test it was mainly for proof of concept and getting familiar with the stage and code reasons that phantoms were used. Therefore, the overall results should not be affected.
- The *prototypeV0.1* tests can be affected. However, these tests will be redone with *prototypeV0.1*. The choice of excluding the 0.07mm spring should still be valid because the material will be stiffer now and it is expected that more force will be needed. Excluding the 0.1mm spring was unrelated to force tests. The 0.1mm spring was too stiff to be rolled around the rod.

### Goal

The goal is to fabricate phantoms that mimic adipose tissue with embedded lymph nodes. The adipose tissue is 17wt% gelatine [25] and the LNs are represented by raisins and cranberries. The phantoms are to be used for force tests and proof of principle tests to validate the current LN detachment mechanism, the ring-cutter.

### Calculations

- a cup is assumed to have a volume of  $\approx 100\text{cm}^3$
- to achieve 17wt% (aka 17g of gelatine per cup for 12 cups the following is needed:
  - 204g of gelatine
  - 996g of water
- the wt% was checked with the following formula:  $\text{gelatinewt\%} = \frac{\text{gelatine}[g]}{(\text{gelatine}+\text{water})[g]}$  [9]

### Preparation

Prior to mixing the gelatine, the artificial lymph nodes (ALNs) need to be prepared:

1. The ALNs (raisins and cranberries) need to be measured and assigned to a cup colour, see *Figure F.1*.
2. A thread needs to be out through the ALNs for fastening them to the skewer later in order to suspend them in the middle of the gelatine cup cake.

Note: Not all phantoms have to include an ALN! This depends on the intended purpose of the phantom.

## F.2. Mixing the gelatine

To mix the phantom, follow the following steps:

1. Prepare the artificial LNs by attaching a string to them
2. Measure 204g of gelatine
3. Mix the gelatine with 330g of water (20°C) and let soak for 10 minutes (this step is needed, because when mixing gelatine with hot water directly, the outside will soak up water too quickly [31].)
4. Heat the rest of the water, 666g, to about 72°C (hot water not boiling, 72°C was the hottest temperature we could achieve) and add it to the soaked gelatine. Stir continuously till uniformity is reached.
5. Place the artificial LNs suspended in the cupcake cups using a skewer
6. Pour the gelatine into the cups
7. Let it cool to room temperature
8. Put the cupcake cups in the refrigerator in the refrigerator for at least 24 hours
9. Let the phantom warm to room temperature ( $\approx 30$  minutes)
10. Testing can begin!



Figure F.1: This figure shows the phantoms made in the cupcake forms. These phantoms have already cooled for 24h in the fridge at 6°C. After warming up to room temperature, they are ready to be used





# Tensile Test Protocol

The goal of this tensile test is to get an (ballpark) idea of the force needed to free LNs from the surrounding tissue.

Before commencing anything, start up a personal laptop and open this document as well as the excel file "RunTable".

## G.1. Materials

- measuring tube (conical tube)
- ruler (to be found in the LN research box)
- scale (to be found in the LN research box)
- calliper
- scalpel
- plastic cloth for moisture absorption
- tissue with marked LNs
  - LNs marked with 0-Vicryl, multi (see *Figure G.1*)
  - stitching material to be found in the LN research box
- tissue holder bottom and top plate (to be found in the LN research box)
- Bolts and nuts to secure tissue holder
- linear stage + laptop + Matlab code
  - linear stag: EGSL-BS-45-200-3P, Festo BV, Delft, The Netherlands
  - sensor: LSB200-FSH00104, FUTEK Advanced Sensor Technology Inc., Irvine, CA, USA
- hook holder attached to linear stage + hook
- cleaning materials
- gloves and lab coat
- laptop with "RunTable" to add data and comments

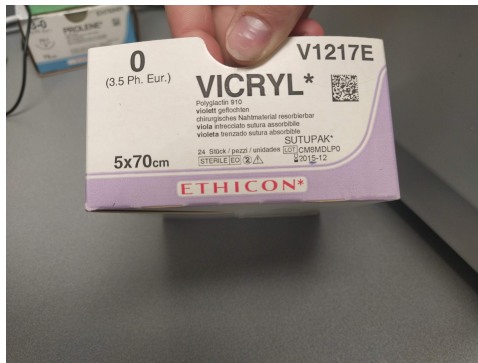


Figure G.1: Flower one.

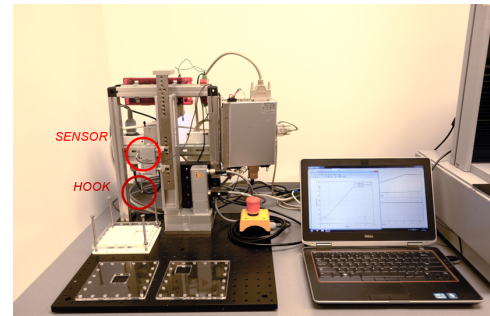


Figure G.2: Flower two.

## G.2. Experimental Set-Up

### G.2.1. Calibration linear stage

Before every experiment, make sure the correct block (for tissue attachment) is on the sensor, then the linear stage needs to be calibrated with the block attached.

In order to calibrate, execute the following steps:

Step 1: Make sure the linear stage goes from home position to initial position, to  $150\text{mm}$  @  $20\text{mm/s}$  down.

Step 2: Name the next run "cali-0g". Make a run with  $0\text{g}$  attached at  $150\text{mm}$  @  $1\text{mm/s}$ .

Step 3: The average value of the amount of Newton obtained by this measure is used later on for the analysis of the results. This makes sure that the offset of the linear stage is correct.

#### Preparation

Step 1: Make sure the tissue holder, all instruments, and the tensile test stage are gathered and clean.

- get all items from the LN research box
- check the accuracy of the weighing scale by placing the  $50\text{g}$  weight on it and noting if any offset is present. If an offset is detected, weigh the same  $50\text{g}$  5 times and calculate the average offset. Write it in the "RunTable"

Step 2: Prepare the measuring tube with water, the ruler for the dimensions, the calliper for the thickness and the scale for the weighing.

Step 3: Obtain the sample of adipose tissue with embedded and marked LNs from the dissecting room. Place it on an absorbent cloth to soak up all excess preservation fluid.

Step 4: Place the sample in the tissue holder and place the corresponding top plate on the tissue. Make sure the sutures protrude through the window in the top plate. If necessary, lock the top plate in place with an extra nut.

- Bolts of different lengths can be found in the LN research box. They can accommodate for different tissue thicknesses. Additional nuts can also be found in the LN research box. Extra nuts can be used to adjust for tissue thickness.
- If the tissue sample is  $< 10\text{mm}$  in thickness, put absorbent cloth under the tissue to fill the void. The tissue should NOT be lying loosely in the tissue holder after the tissue holder has been assembled.

Step 5: Start the linear stage and run the Matlab interface to starting position. Record 2 should read: "down  $150\text{mm}$  @  $20\text{mm/s}$ ".

## G.3. Execution

Step 1: Make sure the tissue holder is fastened, see [Figure G.2](#).

Step 2: Make sure the following Matlab settings are set up to execute the correct movement (velocity, distance) to pull the LNs from the tissue:

1. click on "Go home", this lets the stage move upwards
2. make sure the initial position is set to "5mm", then click "Go to initial position"
3. make sure Record 1 reads: "up 1mm @ 30mm/s" Record 2 reads: "down 150mm @ 1mm/s". Then click run
4. the stage is now in starting position. These steps need to be repeated before every test!
  - connect the stitches that mar the LN to the hook on the linear stage, see *Figure G.2*, by lying a knot around the hook and then lying two subsequent knots around the sutures (right under the hook) to secure the suture material tightly around the hook so it cannot slip off.
  - **IMPORTANT** leave slack in the sutures, to avoid initial behaviour distorting the measurement!
5. Set Record 1 to "up 150mm @ 1mm/s"
6. Adjust the name the measurements will be saved under
7. Click "run". The linear stage pulls on the LN till the LN is completely freed from the adipose tissue or failure occurs. Don't touch anything before the run is completed.
8. Make sure to save this data correctly indicating which run it was and write additional comments in the RunTable.
9. Save all data (video, Matlab .m files, and photos) securely

Step 3: Remove the sutures and adipose tissue from the LN.

Step 4: Measure the clean LN for:

- Weight
  - Take offset already acquired into consideration
  - Weigh the LN 5 times and calculate the average weight
  - Lastly, subtract the average offset from the average LN weight
- Dimensions: measure the long and short axis at the widest point of the LN, respectively
- Volume: use a water-displacement test, depending on LN size use:
  - a small 14ml conical tube filled with water till the 10ml indicator mark
  - a larger 40ml conical tube filled with water till the 30ml indicator mark

Step 5: Note the measurements in the RunTable and interesting occurrences during testing in the "Remark" section.

Step 6: If multiple LNs are to be tested, repeat the steps.

## G.4. Clean-Up

Step 1: The adipose tissue is disposed in the correct way via the dissecting room. This has to be communicated with Yvonne or Lucas (in advance).

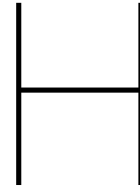
Step 2: The LNs are preserved for future testing. Should the LNs not be suitable for further use, dispose of it in the same manner as the adipose tissue in step 1.

Step 3: Used instrumentation (forceps, scalpel etc.) are put in a tray for cleaning (at dissecting room).

Step 4: CLEAN EVERYTHING thoroughly with disinfectant and place everything back (box with name on is situated under the table) Laptop goes into the 3rd drawer from the top, with charger.

- **Wipe down the working area, tissue holder and tissue attachment block and hook with alcohol!**





## MatLab Code

```
1 %% MatLab code for Prototype Testing
2 % 11-03-2022 by Louisa Preis
3
4 %The purpose of this program is to convert the measured Volts into Newtons
5 %The tests were done in order to determine the thickness of the
6 %ring-cutter-leaf-spring-blade
7 %Tests were done in "insertion mode" and "cutting mode"
8 % clc;
9 % clear all;
10 %% The formula looks as follows:  $F[N] = A \cdot F[V] + B - C$ 
11 %In order to determine the factors A and B, the Force[N] is known.
12
13 %Determining A
14     %A is the weight factor. A can be determined by looking at the changes
15     in
16     %measured Volt when the weight is changed. so 1N = 0.1179V
17 A = -8.48176; %[N/Volt] (negative sign because compression force is now
18     positive, before, tension was positive (because we pulled on a LN now
19     we push into tissue)!)
20
21 %Determining B
22     %B is the offset that is omnipresent. B is defined as the value that
23     is
24     %measured when NO weight is put on the sensor, or the measured Newton
25     %should be 0. Therefore, all voltage measured is the offset of the
26     %system, hence B
27 B_V = -4.529880361098510; %[Volt] = the average force [V] of a 0
28     _calibration test (av_F_V)
29 B = B_V * A; % = abs(B_V * A)
30 %C = 2.4248; % this is the extra offset of unknown origin, which can be
31     determined by
32     % doing a 0g test before every testing session. Then take the
33     % average value (N) supplied by the matlab code, and viola
34 %W = uigetfile({'*.mat'}, 'Pick one or more files ...', 'MultiSelect', 'on');
35 F_V = capture.force_V;
36 F_N = A * F_V - B; % - B because of the negative sign of the volt measurements!
37 av_F_V = mean(F_V);
```

```

34 s = capture.time_s;
35
36 max_F_N = max(F_N);
37 min_F_N = min(F_N);
38 av_F_N = mean(F_N);
39 max_F_V = max(F_V);
40
41 %% these values are the average values from calibration tests
42 % The captured data was read into MatLab and the 1st 32 lines of code were
43 % run. The average force av_F_V was then set as the corresponding F_N_X.
44 F_N_0 = -4.7239;
45 F_N_50 = -4.6649;
46 F_N_100 = -4.6062; % = 1N
47 F_N_150 = -4.5462;
48 F_N_200 = -4.4875; % = 2N
49 F_N_250 = -4.4287;
50 F_N_300 = -4.3703; % = 3N
51
52 %% calculating the change in V per 50g steps
53 diff_50_0 = F_N_50-F_N_0;
54 diff_100_50 = F_N_100-F_N_50;
55 diff_150_100 = F_N_150-F_N_100;
56 diff_150_200 = F_N_200-F_N_150;
57 diff_250_200 = F_N_250 - F_N_200;
58 diff_300_250 = F_N_300-F_N_250;
59
60 % average change in V for 50g step
61 D_50 = [diff_50_0, diff_100_50, diff_150_100, diff_150_200, diff_250_200,
        diff_300_250 ];
62 step_50g = mean(D_50);
63
64
65 F_step = [F_N_0, F_N_50, F_N_100, F_N_150, F_N_200, F_N_250, F_N_300];
66 w= [0, 50, 100, 150, 200, 250, 300];
67 figure
68 plot(w,F_step)
69 title('Newton vs. Volt')
70 xlabel('force [N]')
71 ylabel('force [V]')
72
73 %% Calculating the change in V per 100g= 1N steps
74
75 diff_100_0 = F_N_100-F_N_0;
76 diff_200_100 = F_N_200-F_N_100;
77 diff_300_200 = F_N_300-F_N_200;
78
79 D_100 = [diff_100_0, diff_200_100, diff_300_200];
80 step_100g = mean(D_100);
81
82
83 %% Plotting figures
84
85 v = F_N;
86 t = 1:numel(v);
87
88

```

```
89
90 figure
91 plot(s, F_V);
92 xlabel('time [s]');
93 ylabel('force [V]');
94 title('time [s] vs. force [V]');
95
96 % figure
97 % plot(s,F_N, 'b');
98 % hold on
99 % plot(s(500:500:end),v(500:500:end), 'r' );
100
101 % xlabel('time [s]');
102 % ylabel('force [N]');
103 % legend('raw data', 'sampled data');
104 % title('test5 cranberry 1 20210924 time[s] vs. force [N]');
105
106 %% plot position vs. Force_N
107
108 p = capture.position_mm;
109 P = linspace(0,150,306800);
110
111 figure
112 plot(P(200000:end),F_N(200000:end));
113 hold on;
114 %plot(p(500:500:end),v(500:500:end), 'r' );
115 %set(gca, 'XDir', 'reverse')
116 xlabel('position [mm]');
117 axis ([90 150 -1 4]);
118 ylabel('force [N]');
119 title('0.05mm inertia Test 10 Prototype V1');
120 %legend('raw data', 'sampled data');
121
122 % figure
123 % plot(-p(:,1), F_N(:,2));
```







# Medical Device Regulation & Documentation

The MDR has been mentioned a few times in this thesis and gets a chapter in the appendix because the author deems it an important aspect of researching and designing a medical device. Instead of looking at the MDR as the necessary evil, which it definitely is, it can also be seen as a universal structure that helps with planning the steps that can and need to be taken when designing a (safe) medical device of any kind. This is how the author of this thesis chooses to look at the MDR.

The MDR also highlights some aspects that can easily be forgotten, such as failure safety. Next to this, the author of this thesis wants to use the documentation of the design choices to help guide the next Master student working on this project to have clear insight into what was done and how. So that the next student can identify what was missed, needs improvement or the next step that needs to be taken. By setting up the *design history files* (DHF), see *Figure 1.1*, the author also hopes to give the project as a whole some structure and that next students can fill-in, add, and remove aspects as deemed necessary. Therefore, the DHFs are supposed to be the building blocks for future students. Furthermore, should the device be fully developed at some point, the documentation for an application can be assembled more easily, because the design choices have been documented.

## I.1. Intended Purpose

The *intended purpose* is of interest to a designer for two reasons: 1) it sets some boundaries for the design giving the process some guidance, and 2) it helps determining the classification of the device, which will be of value when applying for *CE-marking*. However, this does not mean that the classification might not change at a later step when for instance electronics are incorporated. *Annex VIII, Chapter III* of the MDR 2017/745 lists the classification rules [16]. The aspects of interest when classifying a medical device are the duration of use and whether the device is invasive or active.

Thus, the *intended purpose* of the *Preis Device* is the removal of already identified SLNs one by one by inserting the device through an incision in the skin. The removal is done by mechanically cutting the SLNs free. The duration of the excision of SLNs with this device does not exceed a duration of *60minute*.

Applying *Annex VIII, Chapter III* the intended purpose can be translated into the classification of a Class IIa medical device according to the MDR 2017/745 [16].

Because:

1. the duration is *< 60minutes* the device classifies as *transient*
2. the device is *surgically invasive* because it "penetrates inside the body through the surface of the body" [Annex VIII, Chapter I, 2.2]
3. the device is not a *reusable surgical instrument* because it is not intended to be cleaned, sterilised and reused on another patient

4. the device is not classified as an *active device intended for diagnosis* because active devices administer energy. At this point, the device only uses mechanical forces to excise the SLNs.

If in a later design a cauterisation module is added to the device, it has to be investigated if the administered energy to the body is potentially hazardous, which would change the classification of the MISLNB medical device to Class IIb.

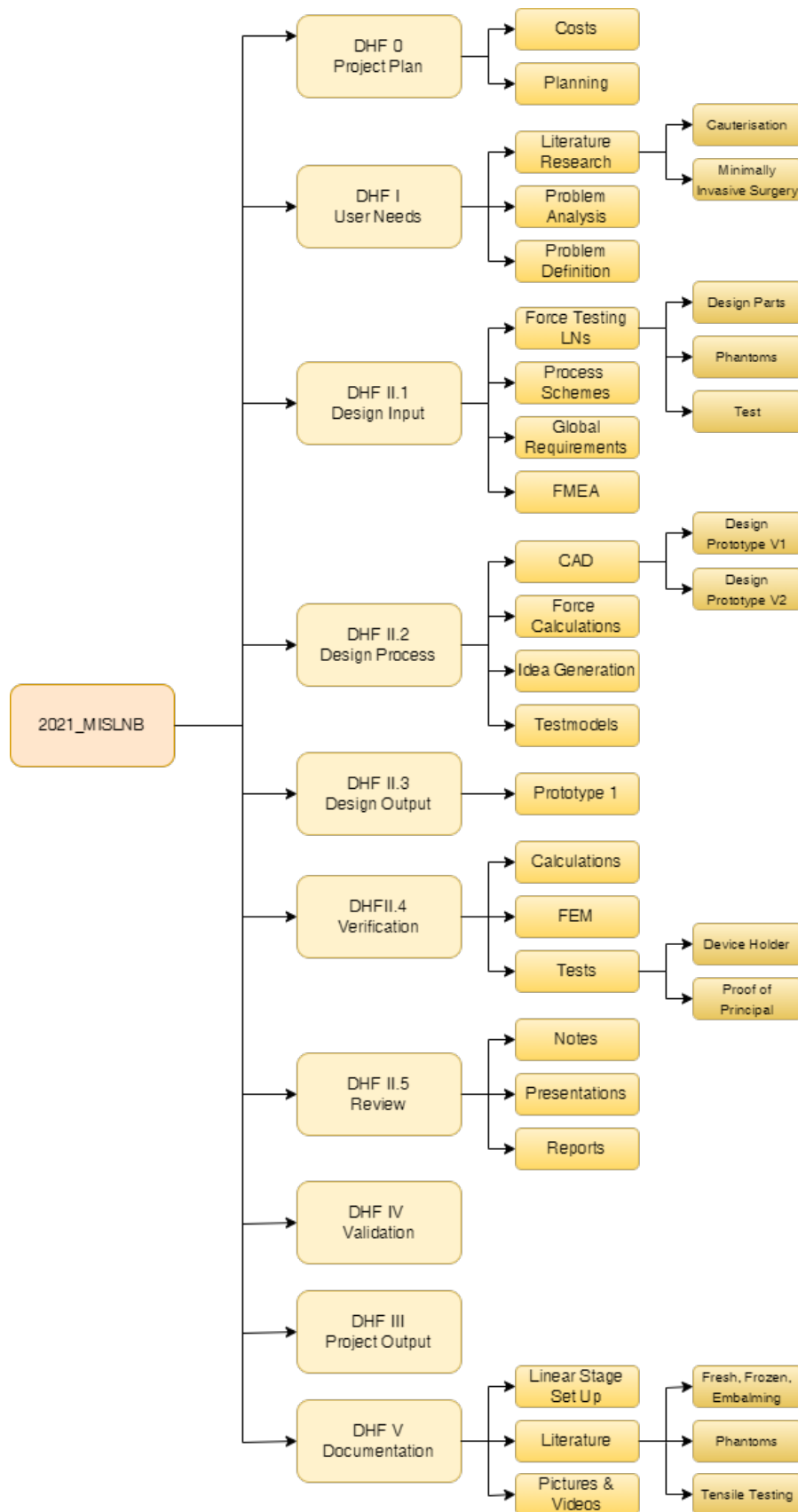


Figure I.1: This shows the structure of the MISLNB filing system. This system is supposed to give the next student a scaffold to lean on and improve or alter. Another purpose for this filing system is for applying for *CE marking* upon finishing of designing this device. In the meantime, it will help also the Erasmus MC should they want to manufacture and use the device under article 5 of the MDR. This file tree is not depicted in its entirety, but the most important folders are shown. This is also supposed to serve as a map to navigate through the files





## How was the Project conceived?

This chapter of the appendix is included to give the next student and any reader an overview of the project's history and the parties and departments involved. First, it will be presented how the project came about in *section J.1 Idea for the project*, then the project's organisation and involved departments will be presented, in *section J.2 Project Organisation*, without whom this thesis would not have been possible.

### J.1. Idea for project

The idea for this project came from dr. Dirk Grünhagen, an oncology surgeon at the Erasmus Medical Center Cancer Institute (Erasmus MC) in Rotterdam. Dr. Grünhagen is tackling MISLNB from various angles. With the GULF trials, his team of researcher proved that SLNs can be identified using ultrasound with sufficient accuracy to make the use of radioactive colloids obsolete, easing the burden for the patients [45, 46]. In a subsequent study it was explored whether fine needle aspiration (FNAC) can be used to accurately stage the SLNs, this was however disproven [59]. Therefore, a MISLNB medical device capable of excising SLNs *en bloc* is the next logical step when trying to transform SLNB surgery into a minimally invasive procedure.

He presented this clinical problem to dr. John van den Dobbelsteen from the Technical University Delft (TUD) and together they set up the MISLNB project. Therefore, this is a joint venture between the EMC and the TUD. Being able to use relevant facilities at Erasmus MC and TU Delft that are ready to go and willing to help is of great value when developing a medical device. Dr. Grünhagen, dr. van den Dobbelsteen and dr. Mulder were available for answering questions when they arose, and with their combined knowledge and expertise, they would offer insight when crucial decisions needed to be taken. This streamlined the design process and taught the author a great amount of knowledge as well as appreciation for the respective fields.

### J.2. Project Organisation

The big picture organisation of the project was constructed together with dr. Grünhagen, dr. van den Dobbelsteen, dr. Mulder and dhr. Schurink. This helped mapping the needs and wishes from the medical point of view (physicians and patients), which are important since the physician is one of the stakeholders. Dr. John van den Dobbelsteen and dhr. Schurink gave valuable insight into the technical decisions that needed to be taken. The day-to-day planning was the responsibility of the author. Various departments of the EMC and TUD were involved in this project and are depicted in comprehensive *Figure J.1*

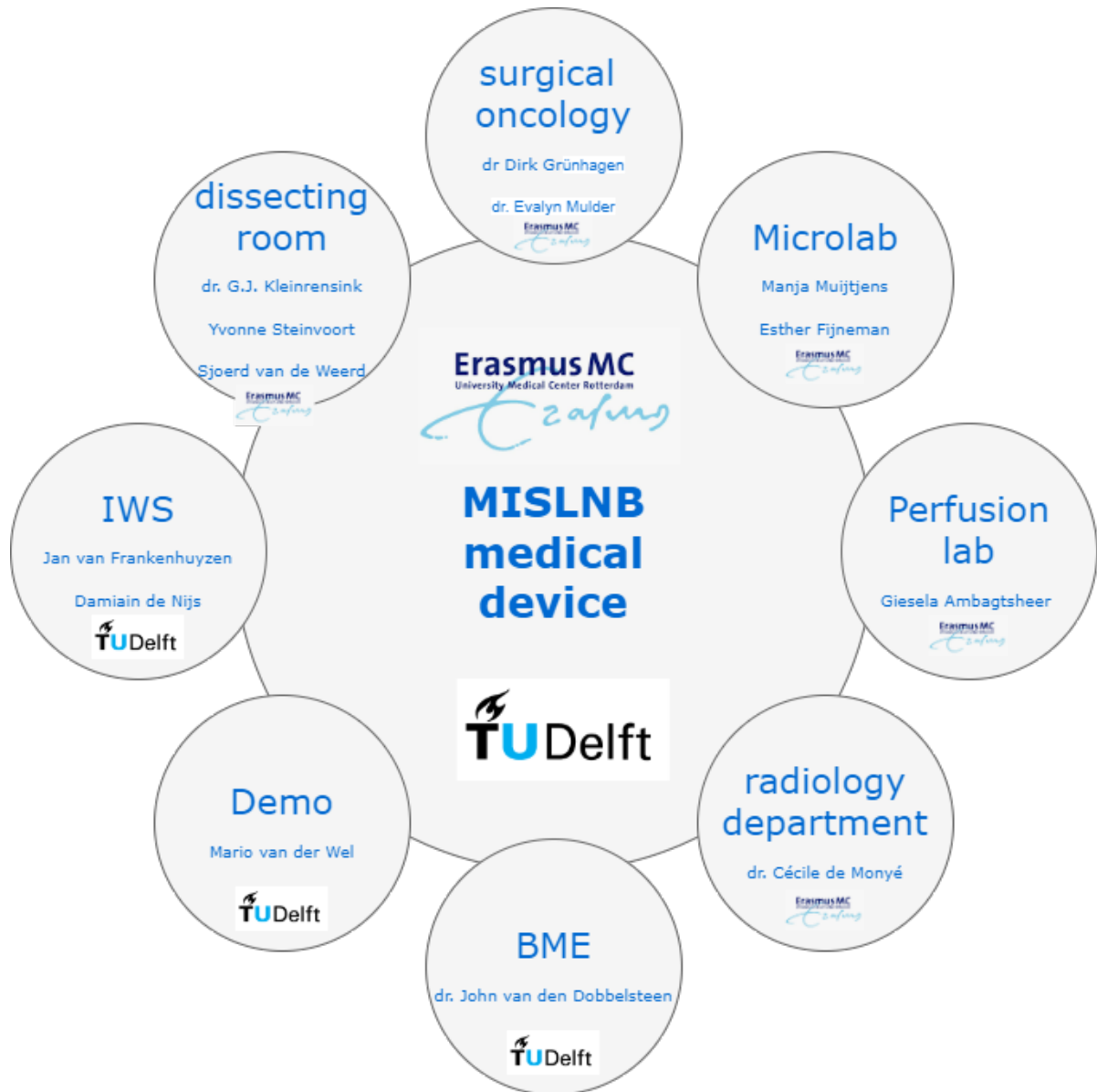
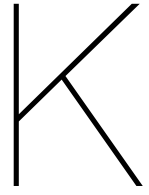


Figure J.1: This graph shows that the relation between Volts and Newton measured with the experimental set-up is indeed linear. This picture was created using the Matlab plot function and subsequently saving the picture in .png format.



# ACE Grant Proposal

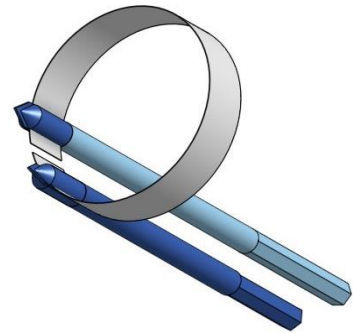
# Minimally Invasive Sentinel Lymph Node Biopsy Medical Device

Joint Venture Erasmus MC and TU Delft

**Principal investigator:** Dr. D.J. Grünhagen  
Oncological surgeon  
[d.grunhagen@erasmusmc.nl](mailto:d.grunhagen@erasmusmc.nl)

**Co-principal investigator 1:** Dr. J.J. van den Dobbelsteen  
Associate Professor at TU Delft  
[J.J.vandenDobbelsteen@tudelft.nl](mailto:J.J.vandenDobbelsteen@tudelft.nl)

**Co-principal investigator 2:** Dr. A.A.M. van der Veldt  
Medical Oncologist  
[a.vanderveldt@erasmusmc.nl](mailto:a.vanderveldt@erasmusmc.nl)



Prototype L.R. Preis (Master student TU Delft)

**Problem description:** The incidence and mortality of melanoma, a form of skin cancer, is increasing rapidly, from 2.860 in 2001 to 7.530 in 2021.<sup>1,2</sup> Evaluation of a melanoma suspected cutaneous lesion generally starts with a diagnostic excision. Sentinel lymph node biopsy (SLNB) is recommended in patients with stage T1b melanoma or higher, which entails >40% of all newly diagnosed patients.<sup>2</sup> Traditionally, SLNB is a key step in disease staging and prognostic stratification according to the American Joint Committee on Cancer (AJCC) classification.<sup>3-6</sup> Rationale behind the SLNB is the premise that metastases do not progress randomly, but occur in a stepwise fashion. Thus, if the sentinel lymph node (SLN) is not invaded then there should be no distant metastases. Since the introduction of adjuvant systemic therapy for patients with surgically resected stage III melanoma, SLNB is performed to identify candidates with SLN metastasis who are eligible for adjuvant treatment.<sup>7-9</sup> As a result, the proportion of patients who underwent SLNB increased from 23% in 2003 to 64% in 2018, in the Netherlands.<sup>10</sup> The majority (70-85%) of SLNs from patients with melanoma are histologically *negative* (i.e., without metastasis),<sup>11-14</sup> with even higher rates in thin melanomas.<sup>15</sup> The procedure needs to be performed under general anaesthesia. In addition, this diagnostic tool causes radiation burden (Technetium 99m is used to identify the SLN preoperatively) and blue discoloration of the skin (patent blue is injected to visualize the SLN preoperatively), which can be long-lasting.<sup>16,17</sup> Postoperative complications, such as seroma, wound infection, scar formation, and lymphedema, occur in approximately 10% of patients.<sup>16,18,19</sup> For nodal staging by the pathologist, it is critical that the SLNs are excised *in toto*.<sup>20</sup> Nodal staging is the main prognostic tool for melanoma patients and determines whether the patient is eligible for adjuvant immunotherapy.<sup>21</sup> Being able to excise SLNs minimally invasive makes it possible to perform this procedure under local anaesthesia and will significantly lower the risk of patients experiencing morbidities. This may, especially in light of the adjuvant therapeutic options (currently only for stage III, but stage II will follow soon), reducing the impact on patients, while reducing the strain on operating room capacity and day care beds.

**Research question:** Is it possible to design a **Minimally Invasive Sentinel Lymph Node Biopsy (MISLNB)** medical device that lowers the risks of experiencing morbidities for the patients and perform SLNB under local anaesthesia only?

**Relevance & Collaboration:** This project is of the utmost relevance because of the surge in SLNB performed on patients with melanoma from 40% in 2010 to 65% in 2016<sup>20</sup>. Which is amplified by the increased incidence in melanoma diagnosis<sup>1</sup>. Patients with other types of cancer can also benefit from



a minimally invasive SLNB medical device<sup>22</sup>. Realising this project is only possible with the collaboration between TU Delft and Erasmus MC. Without the expertise and experience of the departments of Surgical & Medical Oncology, the technical student that is needed to design this device will not be able to solve this problem. Therefore, this project is the perfect convergence between technology and medicine. The technical student will get crucial first-hand experience working closely with medical professionals which is not possible in a solely TU Delft based setting.

**Impact:** The impact of this project is significant, both medically and technologically. Currently, there is no device available that can excise the LN *in toto*. The challenges that need to be overcome will give the technology of large-volume excision a boost. Moreover, the impact of this project on the burden on both patients and health care resources is enormous: with the increasing number of patients eligible for an SLNB (and the consequences regarding adjuvant treatment, if *positive*), morbidity can be reduced while helping to solve the scarcity of operating room availability (i.e., during COVID-19 pandemic), as this procedure can be performed outside the operating room.

**Implementation plan:** Building on promising early results, we are currently in the iteration phase (see *Figure 1*). There is still a lot of work to be done, requiring TU Delft Master Students and funding (for materials and further development of the device). The students will have to test on (human) tissue, incorporating the results into (optimizing) the design. A start has already been made on setting up documentation towards CE certification. The Erasmus MC medical technology department will play a crucial role too. Especially with regard to sterilisation and production.

We look for students from different backgrounds, who work together simultaneously and very closely. Student profiles should vary. One must have a background in electrical engineering to implement electrical components, one must have a background in systems and control, while also a student with a mechanical engineering background is required for the operating mechanism of the device. Ideally, electric components and an actuation mechanism can be implemented in the following year. These need to be designed working closely with surgeons in order to implement their vision as well as experience in handling handheld devices. A student with an industrial design background will also be a valuable addition, especially regarding patient needs and the ergonomic design of the device.

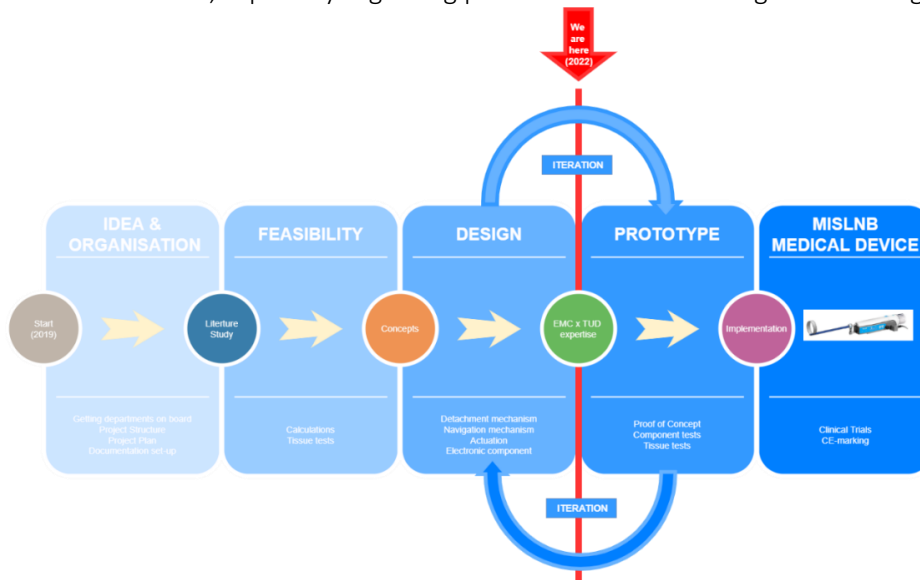


Figure 1: This figure depicts the global project plan from idea to finish. It also indicates in which phase the project is (see red arrow)

Realistically, it will take another three to four years before a complete prototype is realized. Receiving this grant will help realize the next feasibility test on human tissue using the *Stone Excision Basket*<sup>23</sup> as a potential SLN retrieval mechanism. These results will be useful when applying for additional funding (e.g., ZonMW, TTW, KWF). This grant therefore gives this promising project the necessary impetus and even accelerates its development. The ultimate goal is to reduce the burden on (the increasing number of) patients eligible for SLNB.

## References

- [1] Sabrina N Pavri et al. "Malignant melanoma: beyond the basics". In: Plastic and reconstructive surgery 138.2 (2016), 330e–340e.
- [2] Nederlandse Kankerregistratie (NKR). IKNL. <https://iknl.nl/nkr-cijfers>. Accessed Jan 12, 2022.
- [3] Morton DL, Thompson JF, Cochran AJ, et al. Final Trial Report of Sentinel-Node Biopsy versus Nodal Observation in Melanoma. *N Engl J Med*. 2014;370(7):599-609. doi:10.1056/NEJMoa1310460
- [4] Balch CM, Soong SJ, Gershenwald JE, et al. Prognostic factors analysis of 17,600 melanoma patients: validation of the American Joint Committee on Cancer melanoma staging system. *J Clin Oncol*. Aug 15 2001;19(16):3622-34.
- [5] Balch CM, Gershenwald JE. Clinical value of the sentinel-node biopsy in primary cutaneous melanoma. *N Engl J Med*. Feb 13 2014;370(7):663-4.
- [6] Morton DL, Wen DR, Wong JH, et al. Technical details of intraoperative lymphatic mapping for early stage melanoma. *Arch Surg*. Apr 1992;127(4):392-9.
- [7] Weber J, Mandala M, Del Vecchio M, et al. Adjuvant Nivolumab versus Ipilimumab in Resected Stage III or IV Melanoma. *N Engl J Med*. Nov 9 2017;377(19):1824-1835.
- [8] Eggermont AMM, Blank CU, Mandala M, et al. Adjuvant Pembrolizumab versus Placebo in Resected Stage III Melanoma. *N Engl J Med*. May 10 2018;378(19):1789-1801.
- [9] Long GV, Hauschild A, Santinami M, et al. Adjuvant Dabrafenib plus Trametinib in Stage III BRAF-Mutated Melanoma. *N Engl J Med*. Nov 9 2017;377(19):1813-1823.
- [10] Leeneman B, Schreuder K, Uyl-de Groot CA, et al. Stage-specific trends in incidence and survival of cutaneous melanoma in the Netherlands (2003-2018): A nationwide population-based study. *Eur J Cancer*. Sep 2021;154:111-119.
- [11] Oude Ophuis CM, van Akkooi AC, Rutkowski P, et al. Effects of time interval between primary melanoma excision and sentinel node biopsy on positivity rate and survival. *Eur J Cancer* 2016; 67: 164-73.
- [12] Parrett BM, Accortt NA, Li R, et al. The effect of delay time between primary melanoma biopsy and sentinel lymph node dissection on sentinel node status, recurrence, and survival. *Melanoma Res* 2012; 22(5): 386-91.
- [13] van Akkooi AC, de Wilt JH, Verhoef C, et al. High positive sentinel node identification rate by EORTC melanoma group protocol. Prognostic indicators of metastatic patterns after sentinel node biopsy in melanoma. *Eur J Cancer* 2006; 42(3): 372-80.
- [14] Morton DL, Thompson JF, Cochran AJ, et al. Final Trial Report of Sentinel-Node Biopsy versus Nodal Observation in Melanoma. *N Engl J Med* 2014; 370(7): 599-609.
- [15] Isaksson K, Nielsen K, Mikiver R, et al. Sentinel lymph node biopsy in patients with thin melanomas: Frequency and predictors of metastasis based on analysis of two large international cohorts. *Journal of Surgical Oncology* 2018; 118(4): 599-605.
- [16] Moody JA, Ali RF, Carbone AC, Singh S, Hardwicke JT. Complications of sentinel lymph node biopsy for melanoma – A systematic review of the literature. *Eur J Surg Oncol* 2016; 43(2): 270-7.
- [17] Gumus M, Gumus H, Jones SE, Jones PA, Sever AR, Weeks J. How long will I be blue? Prolonged skin staining following sentinel lymph node biopsy using intradermal patent blue dye. *Breast Care (Basel)* 2013; 8(3): 199-202.
- [18] Lucci A, McCall LM, Beitsch PD, et al. Surgical complications associated with sentinel lymph node dissection (SLND) plus axillary lymph node dissection compared with SLND alone in the American College of Surgeons Oncology Group Trial Z0011. *J Clin Oncol* 2007; 25(24): 3657-63.
- [19] Faries MB, Thompson JF, Cochran AJ, et al. Completion Dissection or Observation for Sentinel-Node Metastasis in Melanoma. *N Engl J Med* 2017; 376(23): 2211-22.
- [20] Eric A Deckers et al. "Increase of sentinel lymph node melanoma staging in The Netherlands; still room and need for further improvement". In: Melanoma management 7.1 (2020), MMT38.
- [21] Paolo A Ascierto et al. "Adjuvant nivolumab versus ipilimumab in resected stage IIIB–C and stage IV melanoma (CheckMate 238): 4-year results from a multicentre, double-blind, randomised, controlled, phase 3 trial". In: The Lancet Oncology 21.11 (2020), pp. 1465–1477.
- [22] Michael Frumovitz and Alessandro Buda. "Encouraging worldwide adoption of sentinel lymph node biopsies for gynecologic malignancies". In: International Journal of Gynecological Cancer 30.3 (2020), pp. 281–282.
- [23] Jiuhong Med. Disposable Foreign Body Removal Diamond Shape Basket. <https://jiuhongmed.en.made-in-china.com/productimage/RXjQThcuhNkG-2f1j00eFrtVpqrJokU/China-Disposable-Foreign-Body-Removal-Diamond-Shape-Basket.html>.

# Nomenclature

ALN	artificial lymph node
CAD	computer aided design
CLND	complete lymph node dissection
CNB	core needle biopsy
DHF	design history file
Erasmus MC	Erasmus Medical Center
FEM	finite element method
FNAC	fine needle aspiration cytology
LA	long axis
LMPA	low melting point alloy
LN	lymph node
MDR	medical device regulation
MISLNB	minimally invasive sentinel lymph node biopsy
OR	operating theatre
SA	short axis
SLN	sentinel lymph node
TU Delft	Technical University Delft